الجمهورية الجزائرية الديمقراطية الشعبية
RÉPUBLIQUE ALGÉRIENNE DÉMOCRATIQUE ET POPULAIRE
وزارة التعليم العالي و البحث العلمي
Ministère de l'Enseignement Supérieur et de la Recherche Scientifique

المدرسة الوطنية المتعددة التقنيات
ÉCOLE NATIONALE POLYTECHNIQUE

المدرسة الوطنية المتعددة التقنيات
Ecole Nationale Polytechnique

قسم الآلية
DÉPARTEMENT
AUTOMATIQUE

Graduation project's report in fulfillment of the requirements for the degree of State Engineer in Control Systems

Design and Implementation of a Neuromuscular Controller on the E-Walk Hip Orthosis for Partial Assistance During the Gait Cycle

Author:
Sara Messara

Presented and defended on September 13th, 2023 , in front of the members of the Jury:

President	Abdelhafid	Hellal	Prof.	ENP	Algeria
Examiner	Hakim	Achour	MCB	ENP	Algeria
Supervisor	Omar	Stihi	MAA	ENP	Algeria
Supervisor	Mohamed	Bouri	MCA	EPFL	Switzerland
Supervisor	Auke	Ijspeert	Prof.	EPFL	Switzerland

الجمهورية الجزائرية الديمقراطية الشعبية
RÉPUBLIQUE ALGÉRIENNE DÉMOCRATIQUE ET POPULAIRE
وزارة التعليم العالي و البحث العلمي
Ministère de l'Enseignement Supérieur et de la Recherche Scientifique

المدرسة الوطنية المتعددة التقنيات
ÉCOLE NATIONALE POLYTECHNIQUE

المدرسة الوطنية المتعددة التقنيات
Ecole Nationale Polytechnique

قسم الآلية
DÉPARTEMENT
AUTOMATIQUE

Graduation project's report in fulfillment of the requirements for the degree of State Engineer in Control Systems

Design and Implementation of a Neuromuscular Controller on the E-Walk Hip Orthosis for Partial Assistance During the Gait Cycle

Author:
Sara Messara

Presented and defended on September 13th, 2023 , in front of the members of the Jury:

President	Abdelhafid	Hellal	Prof.	ENP	Algeria
Examiner	Hakim	Achour	MCB	ENP	Algeria
Supervisor	Omar	Stihi	MAA	ENP	Algeria
Supervisor	Mohamed	Bouri	MCA	EPFL	Switzerland
Supervisor	Auke	Ijspeert	Prof.	EPFL	Switzerland

الجمهورية الجزائرية الديمقراطية الشعبية
RÉPUBLIQUE ALGÉRIENNE DÉMOCRATIQUE ET POPULAIRE
وزارة التعليم العالي و البحث العلمي
Ministère de l'Enseignement Supérieur et de la Recherche Scientifique

المدرسة الوطنية المتعددة التقنيات
ÉCOLE NATIONALE POLYTECHNIQUE

المدرسة الوطنية المتعددة التقنيات
Ecole Nationale Polytechnique

قسم الآلية
DÉPARTEMENT
AUTOMATIQUE

Mémoire de projet de fin d'études pour l'obtention du diplôme d'Ingénieur d'État en Automatique

Conception et Implémentation d'un Contrôleur Neuromusculair sur l'Orthèse de Hanche E-Walk pour l'Assistance Partielle à la Marche

Auteure :
Sara MESSARA

Présentée et défendue le 13 Septembre 2023, devant les membres du jury :

Président	Abdelhafid	HELLAL	Prof.	ENP	Algérie
Examinateur	Hakim	ACHOUR	MCB	ENP	Algérie
Promoteur	Omar	STIHI	MAA	ENP	Algérie
Promoteur	Mohamed	BOURI	MCA	EPFL	Suisse
Promoteur	Auke	IJSPEERT	Prof.	EPFL	Suisse

ENP 2023

ملخص

من بين المجموعة الكبيرة من الأجهزة الروبوتية القابلة للارتداء، استهدفت عدة أبحاث تطوير أجهزة تقويم الأطراف السفلية وعلى وجه التحديد المساعدة في دورة المشي حيث يعتبر المشي أحد أهم أنشطة الحياة اليومية . يندرج جوهر هذا المشروع في هذه إشكالية اذ انه يهدف الى انجاز وحدة تحكم جديدة من أجل تقديم مساعدة جزئية للورك أثناء المشي. تنتمي هذه الطريقة إلى فئة ما يسمى بوحدات التحكم البيوميميكية. تم تنفيذ العمل النظري وكذلك تطوير البرمجيات على ثلاثة مستويات؛ يقترح المستوى العلوي طبقة تزامن تعتمد على أجهزة الحالة المتهية والتي تهدف إلى مزامنة حالة وحدة التحكم مع المراحل المختلفة لدورة المشي. يقدم المستوى الأدنى أولاً، نموذجًا محسنًا للعضلات الهيكلية لتقدير الحالة الذي يهدف إلى تجسيد فسيولوجية العضلات البشرية، وثانيًا، وحدة تحكم في ردود الفعل التي تحاكي أوامر الجهاز العصبي أثناء دورة المشي من حيث تحفيز العضلات. الهدف النهائي هو توفير مساعدة كافية خلال المشي، قريبة من العزم البيولوجي ومناسبة لتقليل الجهد عند المشي. سيتم تطبيق وحدة التحكم لأول مرة على جهاز تقويم الورك للمساعدة الجزئية؛ جهاز تقويم $E-Walk$ التابع لمخبر $REHAssist$. تدعم النتائج التي تم الحصول عليها بشكل جيد فعالية هذا النهج للتحكم ، مما يمهد الطريق لتطبيقات جديدة تمامًا وأسئلة بحث مستقبلية إضافة الى مساهمات ملحوظة في الأدبيات.

كلمات مفتاحية ـ مقوم آلي للورك، دورة المشي، المساعدة الجزئية، آلة ذات حالات متهية، النموذج العصبي العضلي، المنعكس العصبي

Résumé

Les recherches scientifiques ont été très prolifiques en matière de conception et contrôle des orthèses des membres inférieurs, plus particulièrement celles visant l'assistance à la marche étant donné que la locomotion est une activités centrales pour les êtres vivants. Le sujet de ce mémoire de fin d'étude s'inscrit dans cette problématique avec comme objectif l'élaboration d'un nouveau contrôleur bio-inspiré dédié à une orthèse de hanche d'assistance partielle à la marche. Les travaux théoriques ainsi que les développements logiciels réalisés interviennent sur 3 niveaux ; Le premier propose une couche de synchronisation basée sur des machines à états finis qui vise à synchroniser l'état du contrôleur avec l'évolution du marcheur. Le deusième niveau apporte une amélioration du modèle d'estimation de l'état des muscles squelettiques. Le troisième et dernier niveau propose un contrôleur par retour d'état qui imite les commandes du système nerveux pendant la marche en terme de stimulation musculaire. L'objectif final est de fournir une assistance en couple adéquate, proche du profil du couple biologique pour la réduction de l'effort pendant la marche. Le contrôleur sera implémenté pour la toute première fois sur l'orthèse E-Walk V1 du groupe RE-HAssit dédiée à l'assistance partielle de la hanche. Les résultats obtenus soutiennent l'efficacité de cette approche de contrôle, ouvrant la voie à de nouvelles applications et questions scientifiques à investiguer et apportant des contributions notables à la littérature.

Mots-clefs : *Orthèse robotique, assistance partielle, machine à états finis, modèle neuromusculaire, reflexe positive, retour d'état*

Abstract

Among the large spectrum of wearable robotic devices, research have been highly prolific in investigating the control of lower limbs orthoses and most specifically the assistance of the gait cycle as walking is considered one of the most important activity of daily living (ADL). The core of this internship inserts within the described quest as it bears the promise of a new mid-level controller dedicated to a hip orthosis in order to provide partial assistance during the gait cycle. This new assistance method belongs to the category of so-called bio-inspired controllers. The theoretical work as well as the software development carried out intervene at 3 levels; The upper level of the mid-level proposes a synchronization layer based on finite state machines (FSM) which aims to synchronize the state of the controller with the evolution of the walker according to the different phases of the gait cycle. The lower level offers firstly, an improved skeletal muscle model for state estimation that aims to capture the physiology of human muscles, and secondly, a state feedback controller that mimics commands of the nervous system during the gait cycle in terms of muscle stimulation. The final objective is to provide adequate torque assistance, close to the biological torque profile and that reduces the effort when walking. The controller will be implemented for the very first time on a partial assistance hip orthosis; The E-Walk V1 orthosis of the REHAssist research group. The obtained results support well the effectiveness of this control approach, paving the way for entirely new applications and future research questions and adding notable contributions to the literature.

keywords: *Hip orthosis, gait cycle, partial assistance, finite state machine, neuromuscular model, positive reflexes, state feedback*

Acknowledgement

First and foremost, El Hamdou'Li'Lah for giving me the strength, the courage and the acuity to survive a year paved with challenges and to be successful in this research project.

I would like to thank Mr. Mohamed Bouri; Mohamed you didn't just give me an opportunity to learn, grow and excel, you also gave me a chance to show my mettle and most importantly, to practice what I love and when you love, you don't count. During my time in the REHAssit family, I didn't count my working hours, because I loved what I was doing. Each milestone, each tripping, each disillusionment and each accomplishment was building me more and surrounding me with an infinite feeling of fulfillment. Thank you Auke for you humility and kindness, for sharing your vision and advice. Thank you Ali Reza and Andrea for your patience, for being the most supportive and stringent supervisors at the same time. I would also like to thank Mr. Omar Stihi and all my ENP teachers for their unfading support in difficult times and for their three years of valuable teaching and training. I am also infinitely grateful to my mother and father for pushing me to never give up and for believing in my ability to overcome the near impossible. A final thanks goes to all my colleagues at the REHAssist research group, among which I tightened eternal friendships and for their precious help during experiments.

Dedication

In the memory of my grandpa who passed away during this apprenticeship,
to my parents for making all this happening,
sister and brothers for our confidences,
grandma, my example in life, for her strength,
to my beloved one for his tender support,
to my old friends and those who newly became ones along this journey.

Contents

List of Tables

List of Figures

Acronyms

BLEEK Berkeley Lower Extremity Exoskeleton

DARPA Defense Advanced Research Projects Agency

EHPA Exoskeletons for Human Performance Augmentation

LOPES LOwer-extremity Powered ExoSkeleton

SCI Spinal Cord Injury

ALEX Active Leg EXoskeleton

CES Consumer Technology Association

ADL Activity of Daily Living

TUPLEE Technische Universität Berlin Powered Lower Extremity Exoskeleton

BBB Beagle Bone Black

SEA Serial Elastic Element

FSR Force Sensing Resistors

EEG Electroencephalography

PD Proportional-Derivative

PID Proportional-Integral-Derivative

AFO Adaptive Frequency Oscillator

GEMS Gait Enhancing and Motivation System

HMI Human Machine Interface

EMG Electromyography

MAD Median Absolute Deviation

KEA Knee Extension Assist

FSM Finite State Machine

CoP Center of Pressure

LuT Look up Table

CoT Coast of Transport

MR Metabolic Rate

MTU Muscle Tendon Unit

CPG Central Pattern Generator

DoF Degree of Freedom

FBD Free Body Diagram

RRMS Relative Root Mean Square Error

WiFi Wireless Fidelity

RTC Real Time Clock

NMC Neuromuscular Controller

Synch Synchronisation

Ref Reference

DC Direct Current

GRF Ground Reaction Force

IMU Inertial Measurement Unit

UART Universal Asynchronous Receiver Transmitter

I2C Inter-Integrated Circuit

IDE Integrated Development Environment

HAL Hardware Abstraction Layer

Avg Average

PFS Preferred Stride Frequency

FDHO Force Driven Harmonic Oscillator

TCP Transmission Communication Protocol

CAN Controller Area Network

SPI Serial Peripheral Interface

NTP Network Time Protocol

RT Real Time

FES Functional Electrostimulation

PSAO Particularly-Shaped Adaptive Oscillator

Introduction

Presentation of BioRob and REHAssist Host Laboratories

The Biorobotics Laboratory (BioRob) is part of the Institute of bioengineering in the School of Engineering at the EPFL (also co-affiliated to the Institute of Mechanical Engineering). The research orientation of the laboratory are the computational aspects of locomotion control, sensorimotor coordination, and learning in animals and in robots. The interests of the laboratory lay at the intersection of robotics, computational neuroscience, biomechanics, nonlinear dynamical systems, and machine learning. The current research fields of the laboratory could be grouped into five categories enumerated as follow: Neuromechanical simulations of locomotion and movement control, amphibious robotics, modular robotics, quadruped robotics and rehabilitation technologies which are the field of research of the REHAssist group.

The research group Rehabilitation and Assistive Robotics (REHAssist) headed up by Dr. Mohamed Bouri is affiliated to the Laboratory of Biorobotics (BioRob) and the Laboratory of Translational Neural Engineering (TNE). REHAssist benefits from the close collaboration with the two entities while maintaining decentralisation and independence in defining its research quests and managing projects. It occupies this way an enviable position by being the hyphen between the two fields of human bioengineering and robotics. Rehabilitation and motor learning are the main driving topics of REHAssist. This mainly concerns the following research areas:

— Development of devices to assist locomotion and for rehabilitation;

— Control strategies for assistance, mobilization and management of balance;

— Closed loop functional electro-stimulation (Functional Electrostimulation (FES)) and sensory substitution;

— Haptics for sensory-motor rehabilitation and surgery.

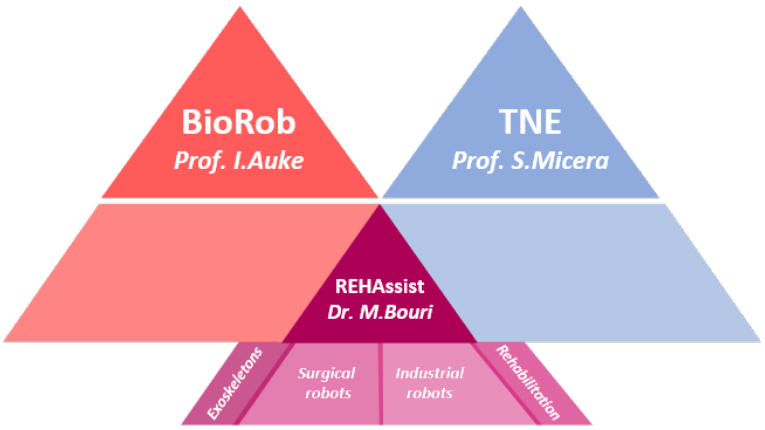

Figure 1 – Laboratory affiliation and subjects

Context and Motivations

The rise of wearable robotic devices was driven by their valuable contribution to improve people's condition during their activities of daily living (ADL), by either restoring lost motor functions, improving partially disabled motor functions via rehabilitation or contributing to the accomplishment of Activity of Daily Living (ADL)s in a less effortful way by reducing the metabolic demand of energy. The ascending enthusiasm toward these devices has pushed the science to jump over the closed bulwark of laboratories to eventually pervade daily use without experts supervision.

Among robotic devices, orthoses have been greatly explored and developed. Their success is drained from their contribution to automatise the task of partial mobilisation either for rehabilitation matters to partially disabled people or to a broader range of users via assistance (or resistance) of healthy subjects in the finality of effort reduction (or augmentation, respectively).

In the large spectrum of assistive orthoses, research have been highly prolific in assistive strategies targeting the hip and ankle joints. This is due to the fact that these two joints occupy 42% of the metabolic energy expenditure of walking for each, against only 16% for the knee joint [1].

The core of this thesis inserts within this research question and comes with the promise of an improved neuromuscular model during the gait cycle. The ultimate output would be the design of a bio-inspired controller that would be implemented for the very first time on an assistive hip orthosis dedicated to healthy subjects. The contributions of the present work is expected to bring notable added value to the literature.

As it will be expended more in details in the literature review chapter, the taxon-

omy as well as the control angles of attack are very layered. For the taxonomy, what will retain our attention are partial assistance portable hip orthoses. In this category, many works have been contributed to the control strategies and the reduction of the cost of transport, the best performance so far in portable devices brings a net reduction of 14% Coast of Transport (CoT) [2]. Since the none portable devices are less constrained regarding the hardware, the achieved CoT reduction with such devices was more important reaching 24% CoT saving for a hip assistance exosuit [3] and up to 50% for a full leg emulator [4].

Regarding control strategies, our main focuse is the mid-level controller, layered itself into two levels; Gait synchronisation and the control layer. The first layer establishes the evolution phase of the gait. Despite the frequent use of FSM in the literature, the reviewed works showed low number of states given by two states when the legs are considered separately and up to four states when the legs are coupled which adds more rigidity to phase identification. We believe that the full potential of state machines is not fully exploited and deserve to be pushed further as the FSM is highly suitable for gait decomposition since it captures well the changes of the neural system's behavior in the different gait subphases as intuited by neuromuscular gait simulations [5].

For the control layer, offline computation remains the most worked with to date using the Look up Table (LuT) or fitted curves such as the ones based on human in the loop optimisation [6] [4]. Online methods are less employed and system modeling and state feedback even less. Despite its great potential, the NMC that is a model proposed first by Geyer and Herr in 2010 [7] has not witnessed any serious improvement and has been restricted in terms of implementation only to full mobilization or partial assistance for pathological subjects. In this thesis, we will contribute to the improvement of this model and try to demonstrate its applicability to partial assistive devices control. We will then attempt the very first implementation of our neuromuscular controller on an assistive hip orthosis.

The REHAssit has designed two hip assistive orthoses; The Hibso and the E-Walk V1. The controller developed during the scope of this thesis is intended to be implemented on the E-Walk. At the moment of writing this report, there are two implemented controllers on this orthosis, one simple controller based on the amount of leg weight bearing and the second based on an offline torque computation with phase synchronisation.

Overview of the Thesis' Objectives and Scope

The core of this thesis is to propose a novel mid-level controller dedicated to a hip orthosis device in order to provide partial assistance during the gait cycle. This new assistance method belongs to the category of bio-inspired controllers. The achieved theoretical and software work intervenes at 3 levels of control; The higher level of the mid-level controller proposes a synchronisation layer based on FSMs that intents to synchronise the behavior of the controller to match the evolution of the walker in the various stages of the gait. The lower level proposes first an improved model of the skeletal muscles for the state estimation that aims to capture the physiology of the human muscles and ultimately a positive state feedback controller will mimics the commands of the nervous system during the gait cycle in terms of muscles stimulation. The final objective is to provide an adequate assistive torque commands close to the biological torque profile for effort reduction during walking. The controller will be implemented for the very first time on an assistive hip orthosis; The E-Walk V1 orthosis of the REHAssist EPFL research group. The obtained results support well the effectiveness of this control approach paving the way to a brand new applications and future quest and adding notable contributions to the literature of assistive robotic devices. The provisional as well as the effective project's Gantt charts can be found in the appendix A.5 and A.6, respectively.

This report is structured as follow: The next chapter presents an overall understanding of the biological functioning of the neuromuscular system and a literature review of wearable robotic devices and their control. The second chapter exposes the theoretical foundations of our proposed controller. The third chapter tackles the software development and hardware implementation, followed by the experimentation and validation step. We dedicate the last chapter to the potential future works before concluding on the outcomes.

Chapter 1

Literature Review

This chapter presents an overall understanding of the biological functioning of the neuromuscular system and a literature review of wearable robotic devices as well as their control.

1.1 Human Locomotion

1.1.1 Human Skeletal Muscles and Neural System

There are three types of muscles in the body; Smooth muscles, cardiac and skeletal muscles. The myriad of motor functions of the human body is performed by the conjunction of the neural system and the skeletal muscles. The skeletal muscles are attached to the bones, they have a non-linear elastic behavior of varying impedance depending on the stretch and contraction condition. They generate an active force only at the contraction that induces the motion of the limb in one unique direction. In order to cover the inverse direction of motion, the muscles always work in pairs and the other muscle is called the antagonist muscle.

The skeletal muscles are biological actuators [8]. Their active element (responsible of contraction) is the Sarcomere and is composed of Myosin and Actin filaments oriented in one direction called the pennation angle. The muscles are organised into motor units composed each of a motor neuron and the set of fibers it enervates. The motor neurons are the messenger that transmit the synaptic [1] inputs coming from the neural system to the Sarcomeres.

The skeletal muscles are attached to the bones through the tendons. They are elastic elements with varying stiffness depending on the physical condition, activity and stretching length [9]. A scheme depicting muscles composition can be found in the appendix A.1.

In the active working region, the muscle is subject to two types of contractions; The isometric contraction results in force generation at contraction state without change in the length of the muscle (static, null velocity of the muscle), this occurs for examples when grabbing an object or in a gravity compensation position of the limb. Reversely, the isotonic contraction results in force generation at varying contraction lengths of the muscle (dynamic, none null velocity of the joint), it can be concentric if the muscle is shortening (active) otherwise eccentric (passive).

The passive reaction of the muscle happens whenever there is a hyper contraction of the antagonist muscle resulting in a hyper extension of the muscle. In this case, the muscle becomes stiff and its rigidity brakes exponentially (regarding the length)

1. electrical stimulation

the motion [10] to prevent damaging the soft tissues and tendons.

The elastic behavior of the muscle comes from the biological nature of fibers, the elasticity of the tendons and the parallel tissues (antagonist muscle).

The other face of the dice is the neural signals. The nervous system is the complex biological controller of all the body including the motor functions by commanding its various elements through neural electrical stimulation generated from the external and internal sensory information of the body. It is composed of two main blocs; The central nervous system is active in the voluntary movement, where the stimulation is generated at the brain level under the consciousness of the human then transit by the spinal cord before being transmitted through the neural network to the target element. Reversely, the Reflex Arcs intervene in the involuntary movements, the stimulation is decentralized and generated directly at the Spinal Cord level relying only on the sensory inputs without consciousness of the human [11].

In an activity such as the gait cycle, both control scheme intervene in the synchronisation of the muscles as it will be explained in the next section [12] [13].

There exist in the literature two main models of the neuromuscular system; *Ekeberg model* and *Hill type muscles*.

The Ekeberg model represents the muscle by a 2^{nd} order mechanical (mass-damper-elastic) system and the neural system by a Central Pattern Generator (CPG) [14] that is an endogenous neural activation pattern for cyclic locomotion activities validated for animals such as the Salamander [15]. As such, this model is more often used to simulate animals motor functions rather then the human's.

The Hill type model [16] captures the physiology of the muscle by an arrangement of compliant elastic passive elements, an active element and a dynamic model for the neural stimulation and muscle activation. We call this complex the Muscle Tendon Unit (MTU). This model is often used by biologists and biophysicists to simulate the human muscles [5]

In the scope of this thesis, we opt for the Hill type model with additional contributed simplifications. The model is depicted more in details in the next chapter.

1.1.2 The Gait Cycle

The gait is the pseudo-cyclic pattern drawn from the activity of walking. When disregarding sideways disturbances, the gait is a stable limit cycle from the control system point of view. Nevertheless, the limit of the cycle is hardly ever perfectly the same given the stochastic disturbances induced by the human and the environment. The intra-subject variability in steady stages of walking will remain fairly low such

as each person has a characteristic unique walking pattern [17].

For gait progress estimation, a convention is to normalize the evolution by a percentage instead of time where the 0% is relative to a characteristic event in the gait (most commonly the Heel Strike or the Toe off) and the 100% corresponds to the reproduction of the same event.

From the biological and the control point of view, the gait cycle engages complex mechanisms, ranging from trunk balance, neuromuscular synchronisation and joints kinematics and kinetics considerations.

From the geometric point of view, the gait takes place in the sagittal plane along the anteroposterior axis (also know as dorsoventral axis) involving flexion-extension of the lower limbs. The leg is composed of rotary joints called synovial joints that must synchronise to produce walking. Each joint has an inherent DoF and set of antagonist pairs of muscles to perform the movements. We shall depict the former as follows [18]:

— Ankle joint: Links the shank segment to the foot. It is a hinge joint of 2 DoF composed in reality of two articulations; Tibiotalar allowing dorsiflexion-plantarflexion and the Subtalar perfomring the eversion-invesion in the coronal (frontal) plane [19]. Some sources make a distinction between the ankle and tarsal joint, they thus consider the ankle to be a 1 DoF-hinge joint responsible of sagittal rotations only [18].

— Knee joint: Links the thigh to the shank segment. It is a hinge joint of 1 DoF allowing flexion-extension in the sagittal plane.

— Hip joint: The hip joint links the trunk segment to the thigh, it is a ball and socket joint having 3 DoF allowing 3 types of motions that are: the flexion-extension in the sagittal plane, the abduction-adduction in the coronal plane and the medial-external rotation in the trasversal plane. We will focus more on the hip flexion-extension.

In normal gait patterns there is also the participation of the upper limbs such as the pelvis joints and the arms whose main objective is to achieve balance. For maintaining balance pelvis motion and subtalar motion happens with a low magnitude in the coronal plane thus the restriction of the gait only to the sagittal plane when dealing with flexion-extension assistance and not balance.

There are several aspects inherent to the characterization, the most important ones are listed bellow [20]:

— Joints kinematics and kinetics: The kinematics concerns the angles and velocity portraits of the various leg joints. Kinetics deal with the external forces applied

on the joints. There are 3 major forces considered, the Ground Reaction Force (GRF) occurring at ground contact, the gravity and the biological torque.

— Stride/step length: The stride represents one cycle of the gait. Its start is generally concurrent with the heel strike and the end is the heel strike of the same leg. Reversely, the step is half of a stride, it starts likewise and ends at the heel strike of the contralateral (second) leg.

— Cadence: The measure of the number of steps per minute.

The gait cycle has two major phases; The stance phase and the swing phase. The stance phase is the period of leg's ground contact and occupies on average 60% of the gait cycle. Reversely, the swing is the period where the leg have no ground contact (40% of the cycle). Each phase is divided into stages. The beginning of the cycle (in regard to the ipsilateral leg) is often taken to be the heel strike (HS). The first stage of the stance is the early stance (0%-15%). This initial contact is followed by the loading response for weight acceptance. This phase ends with the contra-lateral leg leaving the ground, announcing the beginning of the mid-stance (15%-50%) also called the single support phase. This phase ends when the contra-lateral hits the ground, followed by the pre-swing (50%-60%) where the leg starts the push-off (or propulsion) to prepare the swing. The swing starts at the toe-off and is followed by the landing preparation (85%-100%) beginning when the leg starts pushing backward and ends with the heel strike of a new cycle [21] [17]. The scheme of the cycle is left in the appendix A.2.

1.1.3 Characteristics of the Hip Joint During the Gait

Since the scope of the present thesis restrict to the hip joint flexion-extension, it is depicted more in details. Hip flexion lifts the thigh forward whereas the extension pulls it backward the sagittal plane. The hip has two major extensors; The Gluteus Maximus (GLU) and the Hamstring (HAM) and two major flexors; The Iliopsoas (ILPS) and the Rectus Femoris (RF) [22].

At the early stance, the hip is in a flexed position, hip extensors are thus stimulated and a negative extension torque is applied, it is also the phase where there is weight acceptance by the leg leading to a peak of extension at around 12%. During the mid-stance, the foot keeps pushing backward preparing for an extension angle, the extensors are then hyper-contracted and the antagonist muscles are hyper-stretched, the latter are stimulated by a stretch reflex and the extensors are inhibited. At the pre-swing, the hip undertakes the propulsion from the ground, the flexors are stimulated thus the torque rises to a peak of flexion at late 50%. It is now the flexors that

become hyper-contracted and their antagonists hyper-stretched, thus a stretch reflex is activated on the latter inhibiting the former and causing the torque to decrease until it becomes negative at the landing preparation in forecast of the heel strike [17].

1.2 Wearable Robotic Devices

1.2.1 Definitions

The interest in conceiving wearable robotic devices has emerged since late twentieth century (20^{th}) [23] as a sprawling multidisciplinary research and application field laying in the entanglement of mechanics, system control, electronics, perception, computer science and bio-engineering. Being a spin-off from robotics, it heaps up as such all the challenges inherited from the later with an additional thorny difficulty deriving from the everlasting cognitive and physical close interaction with the human. Indeed, wearable robotic devices are by definition, powered anthropomorphic [2] powered equipment addressed to perform specific human motor activities by either working collaboratively with the targeted limbs of the body or by replacing them to a certain extent [24]. This definition entails a broad range of possible classifications intended to be depicted in the next subsection. Wearable robotic devices are commonly but falsely referred to as exoskeletons, whereas in reality exoskeletons constitute narrowly a subset. Another common false belief concerns the wearability that need be distinguished carefully from the portability of the device.

1.2.2 Taxonomy

Classification paradigms and criteria diverge greatly between authors. We rigorously enumerate all the possible classification axes of the wearable devices found in the literature. Of uttermost priority is found the function which leads to 3 possible classification: Exoskeletons for parallel full mobilization, prosthesis for serial replacement of lost limbs and orthosis for partial mobilisation. Then is found the motor activity, the scope and body part, the mechanics and the portability. The rigorous referenced description of each axis can be found in the attached appendix A.3. Taking this into account, it is now possible to classify the contribution of the present master thesis that will focus exclusively on the control of a lower limb rigid hip orthosis to provide assistance during the gait cycle. As reviewed earlier gait assistance strategies are one of the most challenging yet prolific research quests, given the fact that

2. Mimicking the human

walking is one of the most important ADL.

1.3 State of the Art

1.3.1 Mechatronics and Design

Pioneer theoretical works appeared during the sixties (1960s) with the United States Department of Defence bearing military application intents [25]. Later on, there have been attempts to shift into practice but stumbled because of hardware limitations, as it is the case for the Hardiman project driven by General Electric Research and Cornell University for load carriage enhancement (1966-1971) [24]. It is only in 1990 that the concept of human augmentation was first formalized by H.Kazerooni with the parallel power transfer structure as it is known in nowadays. He was also the first reaching the milestone of a fully autonomous load-bearing exoskeleton with the so called Berkeley Lower Extremity Exoskeleton (BLEEK) under the Defense Advanced Research Projects Agency (DARPA) project Exoskeletons for Human Performance Augmentation (EHPA) [26]. Since then, many enhancing devices saw birth such as the full body exoskeleton Sarcos [27] for load carrying, the full body Nurse-Assistant [28] for patients carrying. Nowadays, many of these devices reached the necessary maturity to be commercialized such as the Cray X power suit (2021) for upper body that allows up to 30 Kg support per lifting [29].

Coming to the mobilization and rehabilitation devices, the main focus will be on lower limb devices given the scope of the present thesis. As for augmentation, the building blocks for applications in rehabilitation and mobilization were carved during the sixties (1960s) by Vukobratovic and his associates at the Mihailo Pupin Institute in Belgrade [30]. Their work proposed a hydraulically actuated hip-knee orthosis to assist walking for patients with levels of lower limbs paralysis. Many lower limbs devices have since been developed targeting either the partial or full motorization of the leg joints (hip, knee and ankle). One pioneer in physical therapy is the LOPES othosis [16] which is a treadmill non-portable orthosis with eight (8) deported actuators; Two translations for the pelvis, two rotations for the hip joint and one rotation for the knee joint. The device was dedicated to gait rehabilitation for patients with ambulatory disabilities. Active Leg EXoskeleton (ALEX) I and ALEX II followed the same design pattern with a different control paradigm [31]. Likewise, the Symbitron orthosis came with the alternative of portability and modularity. It bears 8 rotary actuators: Two for the hip, one for the knee and one for the ankle and was dedicated to the mobilization of Spinal Cord Injury (SCI) patients [32]. Out-

side the therapeutic environment, numerous powered orthosis saw birth; One of the leading projects was ATLAS [33] for the lower limbs motorization of quadriplegic children. $ReWalk^{tm}$, that is FDA approved [34], includes a boarder range of patients with complete cervical and thoracic SCI and is actuated at the hip-knee with a passive actuator at the ankle [35] while Knee Extension Assist (KEA) orthosis addressed knee assistance for stand-to-sit and sit-to-stand tasks [36]. At the 2019 annual trade Consumer Technology Association (CES), Samsung stamped its print in the field by releasing Gait Enhancing and Motivation System (GEMS), an easy fitting, lightweight (2.4 Kg), modular hip assistance and resistance device with important transport coast reductions for healthy users and those suffering from ambulatory weaknesses [2].

As presented above, albeit the shy start of wearable robotic devices, it began since the early twenty-first (21^{st}) century attracting researchers of several fields ranging from engineering to biology as it demonstrated high added value in improving the well being of people either for augmentation purposes or for physio-therapeutic, assistance and mobilization matters. It is at this moment in time one of the most prolific and active robotics domain with no less then one hundred and fifty (150) related publications for the single period of 2015-2021 [37].

1.3.2 Gait Assistance Control Strategies

The wild jungle of control strategies addressing wearable robotic systems for gait assistance or mobilization is an organised chaos. They first appear highly entangling and fuzzy but they eventually nest into a very much organised and layered genealogy depicted in figure 1.1.

In practice, it is quite challenging to decouple the effect of the assistive control strategy from the mechanical design of the orthosis. In some cases, the contribution of a good control strategy could be diminished because of the hindering induced by the device (e.g., none fitting, bulkiness, heaviness). In other cases, the effectiveness of the control strategy could be overestimated because of high performance of the orthosis especially when applying high torques magnitude [38].

First, and unlike other systems, controlling a wearable robotic device does not require only a controller but a control strategy. The control strategy entails 3 control layers, that are modular but remains in close interaction such as to determine the overall behavior of the device. Second, the control need to handle the everlasting interaction with the human.

The first layer represents the high level controller, it grants the identification of the task carried out by the user by detecting the changes in the user intention. The sim-

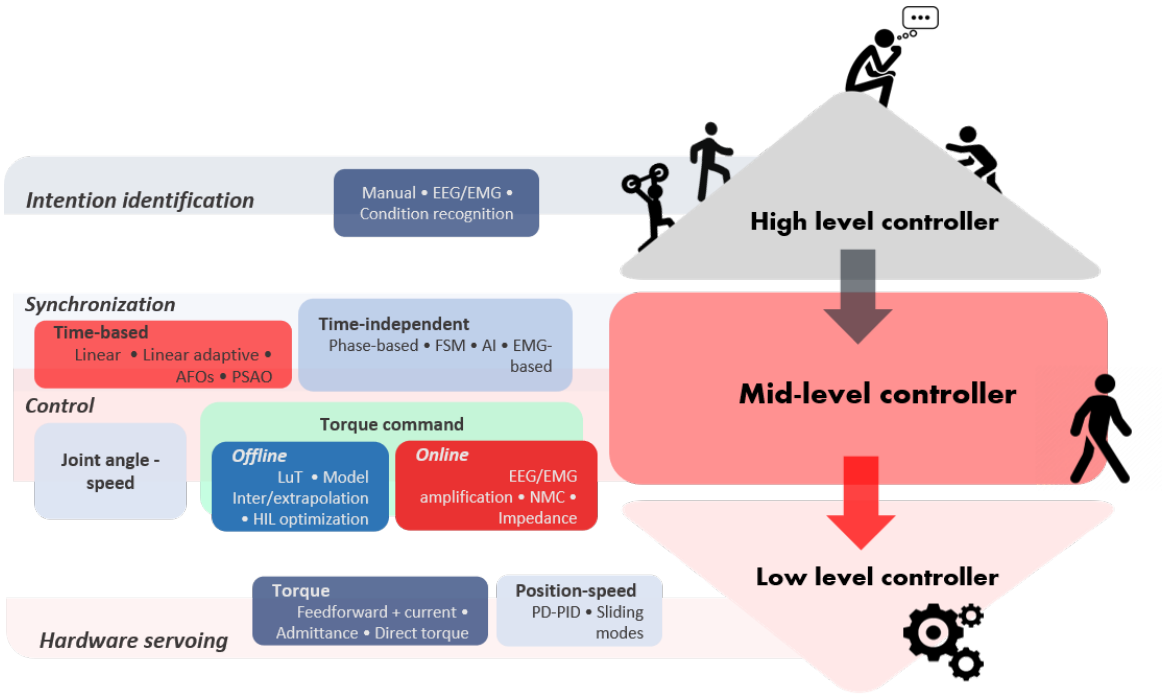

Figure 1.1 – Control levels of wearable robotic devices

plest yet still very used approaches is the explicit input from the user using human-machine interfaces [37]. Neuroscience-based techniques are also actively being investigated where Electroencephalography (EEG) signal of the user's brain are measured and analysed to predict his intention. As this might seems tightly close to science fiction, it is already being experimented as presented by [39]. Other techniques for movement and terrain recognition mostly based on AI (Artificial Intelligence) can also be found in [37]. This type of controller is not mandatory since most rehabilitation and assistive orthosis specialize to one unique task. However, some simple high level controller could be beneficial even for single task assistance, e.g., for gait assistance it is useful to detect the static standing phases of the user in order to provide assistance while walking only [40].

The mid level controller acts as a dynamic set-point generator. It delivers the final or intermediate reference value to be tracked by the actuators and defines as such the reference input of the low level controller. It implements in a whole the assistance logic as well as the way the device should react to the user's current evolution stage while completing the motor task as well as the change of motion mode broadcasted by the high level controller. This has been said, it is clear that the mid level control is the most important layer. First because it is the interface between the high and low control layers. Second, it defines single-handedly the assistance algorithm for each

task and thus the actuation/device response. The main search questions sourced in the control of wearable robots are directly related to the mid control layer given its inherent importance and challenges. Since the scope of the present thesis tackle the implementation of a mid-level controller, an overview of current control techniques is presented later on.

The low level controller is hardware dependent and deals with the control of the actuators while ensuring stability [37]. This level is mostly generic to all robotic systems as most actuators are constituted of Direct Current (DC) motors with transmission systems (e.g., gear boxes, screw balls, Bowden cables) or pneumatic pistons, it will thus be skimmed briefly as it is not inherent to wearable robotics only. Well known control system techniques are employed typically the Proportional-Derivative (PD) and Proportional-Integral-Derivative (PID) for position and velocity control, respectively [41]. Some attempts for Sliding Modes implementation have also been explored to bring more compliance [42]. For the torque control, when the device does not provide feedback on the torque, one way is to control the torque through the regulation of the current, the simplest controller is then the open loop feedforward controller with an inner closed loop on the current. The other alternative, is to control the force via the speed, this is done by an admittance controller followed by a closed-loop on the speed. When the device does not include a torque sensor, a closed loop is applied on the torque and enables precise regulation directly on the actuators or via a Serial Elastic Element (SEA) for more compliance [37].

1.3.3 Phase Synchronisation Layer

The role of this sub-layer is to map the current gait state of the wearer to its corresponding one from the side of the controller [37]. From the literature review, we propose a classification into two main categories; The time-based and time-independent approaches.

The time-based approaches target the synchronisation of the elapsed time since a reference event in the gait cycle and maps the user's current evolution state to its percentage of the gait cycle. The overwhelming majority of authors in the literature are found to take this event to be the heel strike given its unequivocal detection using simple techniques such as the measurement of the GRF using either accelerometers integrated to an Inertial Measurement Unit (IMU) or less commonly, force plate sensors on the treadmills or by detecting the first contact with the ground surface by the means of Force Sensing Resistors (FSR) placed at the level of the foot insoles. Other reference events might be the Toe-off that happens at the end of the heel strike, the

joint kinematics (for instance the detection of the peak of the joint angle, muscles activation using Electromyography (EMG) or the event could be directly triggered by the user using a Human Machine Interface (HMI) [37]. At each event detection, the time or gait percentage is reset to zero then increased linearly (knowing the cadence or linear speed and step length) in an open loop until the next event detection [35]. A slight improvement of this method is to dynamically estimate the cadence based on the precedent stride or step time as in [43]. Adaptive Frequency Oscillator (AFO)s from sensory data are also highly suitable to determine dynamically the step frequency given the pseudo-periodicity (or periodicity) of the gait cycle. However, it does not inform about the current evolution in the cycle and must be synchronized with an external event (e.g., heel strike). Most famous AFOs are those using sinusoidal harmonic [44], other studies replaced the first harmonic with the averaged natural profile of the subject resulting in Particularly-Shaped Adaptive Oscillator (PSAO) [2].

The major inherent flaw of time-based synchronization techniques is that they are built upon the assumption that the gait cycle is perfectly periodic or pseudo-periodic. This assumption is perfectly valid when walking on treadmill where the user is constrained to a constant linear speed making him less likely to abruptly change gait characteristics such as step length and cadence beyond the initial transient period. Nevertheless, this assumption fails for ground walking where the user is unconstrained thus free to walk unsteadily and undertake abrupt changes in his intentions such as sudden stopping, leading leg switching and variable kinematic characteristics (cadence and step length). Such use case will lead to complete dyssynchronization for early cited methods (linear time increment, period anterior estimation) and will induce longer transient times and convergence issues for AFOs.

The time independent approaches do not rely explicitly on the time variable. The phase-based uses the phase shift between, generally, 2 state variables given the fact that the gait could be simplified and represented by a second (2^{nd}) order system. The phase is then converted into percentage of of gait cycle. Angle-speed profiles of the joint are found to be the most recurrent in the literature as they are relatively easier to measure using motor feedback whose motion must shadow synergically the joint's or more accurately via motion tracking systems such as the VICON [45]. They can also be estimated using inverse kinematics of the leg.

The advantage of this method is that since it is detached from time and state variables magnitudes, it adapts instantaneously to the change of cadence and step sizes. However, the wearer must maintain walking, stopping suddenly for instance will induce a sliding from the phase portrait leading to an unknown working region. It also requires extra mechanism to prevent the effects of bouncing that might lead to

a retraction in the percentage estimation.

Another popular method is the FSM. FSMs are of particular convenience for this use case considering that the gait cycle, as presented in the former section, is biologically subdivided into finite states where each state defines a continuous monotonous motor neuron behavior from the body, using FSM facilitates the use of hybrid control strategies suitable for each phase. Unlike the previous synchronization methods, the FSM do not provide the exact percentage of the gait cycle but a more or less gross localisation on one phase of the gait. The number of states in the literature differs ranging from two to four states maximum. The two states FSM are the stance/swing. In such FSM , the triggering events are the heel strike/toe off. Dzeladini and colleagues used this 2-state subdivision for the implementation of a neuromuscular controller [46] . Yan and colleagues [40] also proposed a 3-states FSM where the transition triggering relies on the FSRs as well as the position of the Center of Pressure (CoP). The largest FSM found in the literature is a 4 states FSM contributed by Bokman et al. [47] and used on a hip assistive orthosis. However, they coupled the state machine of the 2 legs, this means that they couple as well the motion of the legs. Their state transitions are based on two zero-crossing events for each leg that are: Zero hip velocity at the end of the swing and zero angle difference between the two legs. The majors issue of this approach is the coupling of the two legs, as this might work fine for healthy subjects with symmetrical gait and constrained on treadmill. Nevertheless, it cannot generalize to a broader range of targets, such as people with muscular weaknesses and those recovering from stroke. Also the proposed triggering events does not provide an absolute control of the states, for example the entering of the swing for the ipsilateral leg is assumed to coincide with the contralateral leg speed zero-crossing, whereas there is an important time backlash between this two events. This alters highly the intended synchronisation and thus the preciseness of the assistance torque. Other similar works could also be found either with reduced number of states (2 to 3) as in [45], [48], [49] or with a maximum of 4 states but coupled as in [50].

Other approaches bases on machine learning (ML) propose non-parametric architectures that map the sensory inputs (FSRs, Encoder, EMG) directly to the assistance torque without prior synchronization as presented in [51]. Despite their good results, these optimization methods are purely numerical meaning prone to noise, they also require powerful electronic hardware to process the bulky calculations induced by the ML architectures. Other works based on the detection of the electrical stimulation of the muscles using EMG signals are also less frequently found as in [52]. Such methods are restricted to experimental environments and could be invasive if the

monitored muscles are not reachable using external EMG.

Increasing the number of states implies increasing the number of detected events. As this is tightly related to the available sensory inputs, it can be leveraged by searching characteristic key transition events in the gait cycle bearing in mind that it must remain robust enough. Despite the huge potential of FSM in the use case of walking assistance, they are found to be shyly exploited in the literature with a poor number of states compared to the biological phases of the gait or used with less appropriate triggers. The work of the present thesis will propose 3 novel FSMs with augmented number of states and improved triggers that we will demonstrate the effectiveness and accuracy for control synchronization.

1.3.4 Control Layer

This layer intakes the phase estimation of the synchronisation sub-layer and generates consequently the adequate control reference to servo the actuators. The variety of approaches found in the literature belongs to two main groups; Position/velocity control *vs*. force/torque control. The position/velocity control is generally performed in the joint space by imposing the kinematics of the joint at each phase of the gait. The imposed profiles are tuned from healthy subjects' recorded kinematics. This approach is mainly used in full mobilization where the wearer is passive [41] but can also be found in partial assistance [53]. In case of rehabilitation and assistance, this approach is less frequent since the user has a none null motor activity thus he becomes an active agent in the control loop. This interaction rises the need to a more compliant control approach whereas the position control is stiff [54].

The other approach is the force/torque control which happens to be the most popular for rehabilitation and assistance devices. The reason behind this is that this approach fulfill the compliance that allows the control of the proportion of power delivered to the actuators which is safer when dealing in close interaction with the human. As the core of this thesis is the design of a torque controller, an overview of the existing methods is presented.

The profile based method is one of the most used in the literature given its simplicity. The command torque is pre-computed off-line, stored in LuT and by knowing the stage of the gait, the right value is retrieved at each time step. The off-line profile is tuned differently in the literature, one common method is the direct tuning from biological torque profile normalized by the weight of the person as in [55]. In some other references, they rely first on the biological torque profile then hand tune the characteristic timing and magnitudes depending on the subject's preferences, that is the

case for Samsung's GEMS orthosis, where the authors attempted to reduce the negative work which induced shifting in characteristic times of the profile [56]. The other alternative over LuTs in off-line torque computation is the model based approach. The model is either obtained by interpolation of LuT values using Fourier transforms or polynomial functions or obtained via optimisation as it has been performed by Collins et al. [6] [4] where a spline curve has been optimized on the criterion of CoT minimization. These approaches performs well in the context where the gait conditions are not changed such as the speed and the incline, the optimization of Collins at al. [6].

The other way round is the online computation of the torque profile. One method is based on the amplification of the muscular force by monitoring the brain or muscular activity using EEG and EMG signals respectively [57]. As mentioned previously, this method is unsuitable for outdoor uses outside experimental environment and could be invasive. Another method in the literature is the use of real time state estimators. It could be direct state estimators based on inverse kinematics and kinetics or body weight distribution on the legs [37] as it could be much more complex models. In this category is found the neuromuscular controller which belongs to the branch of the bio-inspired controllers. Such controllers mimic the biological control and physiology of the neural and muscular system of animals to achieve the control of electro-mechanical systems. The Biorob laboratory for instance is well known for successfully achieving the control of a Salamander robot using a bio-inspired controller that models the CPG of the neural system of animals [15]. The very first famous application in the filed of human gait simulation is the neuromuscular model of Geyer and Herr's that made use of the Hill type muscle model and positive force feed-back for 7 virtual muscles of the leg [7]. Their controller presented only a simulation algorithm for normal human gait cycle on MATLAB and had a 2-states FSM with hybrid virtual muscles stimulation. It has been later adopted in other studies mainly for full mobilizations of people suffering from SCI (Spinal Cord Injury) contributed by Dzeladini et al. [58] or in prosthetic devices [59] [60]. The exhaustive literature review reveals that there has been no prior attempt of the implementation of a neuromuscular controller in the field of partial assistance to date. This indeed turns to be harder since the user is active in the control loop. Moreover, there have been no novel propositions of models and reflexes different then the one of Geyer and Herr in both full and partial mobilization. The present master project is the first one proposing a modified neuromuscular model based on simplified Hill model and new neural reflexes for selected virtual muscles and a hardware implementation of the later on a robotic device for the hip partial assistance during the gait cycle.

1.3.5 Validation Metrics

An effective controller for any traditional control system is the one that achieves the desired tracking of the set-points by the output of the system, the performance metrics are the conventional errors at the output measurement, transient period characteristics, stability, robustness and sensitivity and other traditional evaluation metrics. This reasoning does not sustain in the realm of gait assistive devices where there is an inner active interaction with the human that changes continuously the set-points. The objectives also differ from the ones of traditional control systems where the main goal is the performance of tracking without further considerations. Whereas, for the assistance, the quest lays in achieving physio-therapeutic objectives with respect to the metabolic effort or the spatio-temporal characteristics of the gait. It means that the effectiveness of the inner hardware controller should be reflected and assessed through its impact on the outer human system. The trending validation approach is to evaluate the reduction of the CoT during the activity. It is in practice quite challenging to demonstrate significance of results because of repeatability and accuracy problems, thus the need to a large experimental sample (subjects). The common methods found in the literature to assess the metabolic effort are the estimation of the energy CoT either through oxygen consumption using respirometers that analyses the exhaled breath or via heart rate monitoring also known as Physiological Cost Index (PCI) [61]. Another method is the monitoring of muscles' activity using EMG signals. Depending on the location of the muscle, the EMG are obtained either through surface electrode or fine wire electrode. In contrast with the first procedure, the second one is invasive and addresses deep muscles [62]. There also exist methods that relies on estimation when biological measures are not possible, in this category is found the study of optimal curves fitting of the kinematics data such as the step length-speed or joint work-speed relationship [58]. Such data, especially the cadence and the step length could be correlated to the energy expenditure of the body during walking as biophysics studies demonstrated that the energy consumption is optimal when subjects were walking with cadence in a close range to their preferred stride frequency (PSF) [63]. Other metrics are found such as the estimation of the positive produced work. For the NMC a method consists in evaluating the synergy of the model by comparing the synchronisation between the controlled stimulation of the virtual muscles and the biological stimulation of the body's muscles during the gait [64][54][37].

Chapter 2

Theoretical Foundations and Controller Design

As hinted in the previous chapter, this thesis proposes a new mid-level controller for the control of a hip orthosis in order to provide partial assistance during the gait cycle. The theoretical work tackles three main aspects; First, an improved model for the muscle coming along the proposition of a new computational approach for hardware implementation. Second, we will propose new simulations and reflexes for the selected virtual muscles at each subphase of the gait. Third, we shall propose new FSMs for a better and sharper sub-division of the gait. The FSM controller enables to introduce hybrid control of the virtual muscles always by varying the simulations and positive feedback as the model remains the same for all subphases.

2.1 The Neuromuscular Controller

2.1.1 Model for the Skeletal Muscle

We will consider as base model the Hill type model to which we will contribute.

The Hill type models mechanically the MTU by an arrangement of three passive non-linear elastic elements and a non-linear active element that is the epicenter of muscular force generation:

— Contractile Element (CE): Center of muscular force generation

— Serial Element (SE): Represents the series elasticity of the tendons

— Parallel Element (PE): En-captures the elasticity of the surrounding tissues and the passive elasticity of the muscle at eccentric contraction

— Buffer Element (BE): Prevents the CE from collapsing if the SE slacks

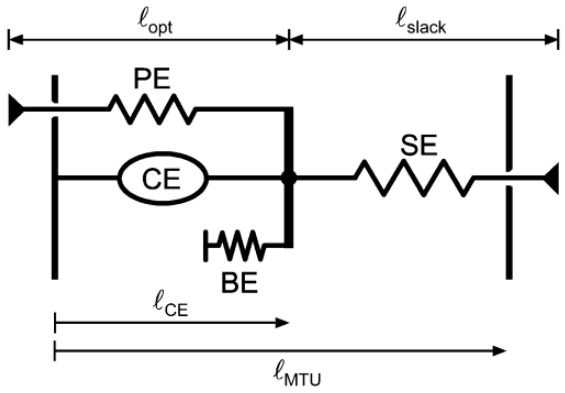

Figure 2.1 – Hill type muscular model [7]

The non-linear passive elastic element's dynamic is given by the length-force relationship:

$$F_{nlp} = F_{max}.\left(\frac{l_{nlp}/l_{slack} - 1}{\epsilon_{nlp}}\right)^2 \tag{2.1}$$

Where l_{nlp} is the length of the non-linear passive (NLP) element, l_{slack} is its slacking length and ϵ_{nlp} the reference strain.

This behaviour is quite particular compared to the linear elasticity of Young for two reasons; First, because the magnitude of the force does not depend on the initial conditions. Second, the force is only in one direction. The graphical representation of each relationship is found in the appendix B.1.

For non-linear active elastic element, its 2^{nd} derivative is coupled with the length of the element but also with its 1^{st} derivative as well as a third state variable that is the muscle's activation; The relationships are given:

$$F_{nla} = Act(t).f_v(v_{nla}).f_l(l_{nla}).F_{max} \tag{2.2}$$

$$f_l(l_{nla}) = e^{\left(\frac{l_{nlp}/l_{slack}-1}{\omega}\right)^2} \tag{2.3}$$

$$f_v(v_{nla}) = \begin{cases} \frac{1-v_{nla}/v_{max}}{1+Kv_{nla}/v_{max}};\ v_{nla} \geq 0 \\ N + (N-1)\frac{1+v_{nla}/v_{max}}{-1+7.56.K.v_{nla}/v_{max}};\ v_{nla} < 0 \end{cases} \tag{2.4}$$

For the third Degree of Freedom (DoF), the muscular Activation, that is purely of biological nature, its dynamic is given by a 1^{st} order low pass filter having the stimulation as command input:

$$\dot{Act}(t) = Stim(t) - \tau.Act(t) \tag{2.5}$$

Where *Stim* is the neural stimulation of the neural system. Dynamically, it is a pure phase delay system regarding the input feedback. The dynamic of the stimulation is given by:

$$Stim(t) = Stim_0 + G.X(t - \delta t) - C \tag{2.6}$$

C captures the inhibition. The term $G.X(t - \delta t)$ represent the state feedback as X could be either the MTU length, velocity or the CE force. One remarkable thing to observe is that the feedback is positive. From the control point of view *Stim* is a pure-delay system. This is the result of a biological phenomenon in muscles called the electromechanical delay roughly explained by the inertia of electro-stimulation

transmitters that are the ions (Calcium Ca^{2+}) inducing propagation delay [65].

The third part of the model links the mechanical state of the joint to the global state of the muscle as well as the muscular force lever. These relationships are specific to each joint and deduced from the mechanical model based on the Free Body Diagram (FBD). We present those of the hip:

For the hip

$$r(t) = r_0 \tag{2.7}$$

$$l_{MTU} = l_{opt} + l_{slack} + r_0.(\theta - \theta_{ref}) \tag{2.8}$$

For the knee and ankle:

$$r(t) = r_0.cos(\theta - \theta_{ref}) \tag{2.9}$$

$$l_{MTU} = l_{opt} + l_{slack} + r_0.(sin(\theta - \theta_{ref}) - sin(\theta_{max} - \theta_{ref})) \tag{2.10}$$

Note that it is relevant to present the equations for the knee in case of considering the hip-knee bi-articular muscles whose states present a coupling of the two joints.

In total, the system is a 3-order non-linear system having 3 mechanical state variables that are the $l_{mtu}(t)$ and $v_{mtu}(t)$ and a biological state variable that is the activation $ACT(t)$. The mechanical variables can be solved directly by knowing the state of the joint, and the activation dynamic can be resolved from the outer input that is the stimulation. Keeping in mind that the objective is to resolve the inner DoF, i.e., finding l_{ce} and v_{ce}

For the bi-articular muscles, the mechanical system becomes coupled and solving it requires knowing the state of the two considered joints (angle and velocity).

The explanation of the parameters is given in table 2.1.

2.1.1.1 Simplification of the Model

One shall bear in mind that the ultimate goal behind determining the state of the CE is to compute the generated muscular force and finally the torque.

Because of the high non-linearity, the high coupling between all the states variable as well as the unpredictability of the neural stimulation (thus ignorance of its function), it is hard to resolve dynamically (regarding time) the state of the muscle.

The other solution is to resolve algebraically the system from the knowledge of the state of the joints. The problem when doing so, is that the system is under-constrained giving infinite number of solutions, the variable to solve being (l_{se}, v_{se}, l_{ce}, v_{ce}) while having only two mechanical equations linking l_{mtu}, v_{mtu} to the joint angle and angular

Parameter	Explanation
l_{slack}	Slack length of the tendon
l_{nlp}	Length of the non linear passive element
v_{nlp}	Velocity of the non linear passive element
ϵ_{nlp}	Reference strain
F_{max}	Maximum force of the muscle
F_{nlp}	Force of the non linear passive element
F_{nla}	Force of the non linear active element
l_{nla}	Length of the non linear active element
v_{nla}	Velocity of the non linear active element
v_{max}	Maximum joint velocity
$Stim$	Neural stimulation
Act	Activation of the muscle
τ	Neural stimulation delay of the muscle
$Stim_0$	Basal stimulation
w	Muscle width
K	Curvature constant [66]
δ_t	Phase delay of the stimulation
C	Muscle inhibition
N	Ratio between the force of the muscle tendon unit and the max force at maximum speed
r_0	Initial lever
l_{MTU}	Length of the muscle tendon unit
θ_{ref}	Initial reference joint angle
θ_{max}	Maximum joint angle
l_{opt}	Muscle optimal length as in [7]
F_{PE}	Force of the parallel element
F_{CE}	Force of the contractile element
F_{BE}	Force of the buffer element
F_{MTU}	Force of the muscle tendon unit

Table 2.1 – Muscle model parameters

velocity.

Based on the contribution of each element, we propose within the scope of this study a simplification of the model. Given the high stiffness of the tendon estimated on average at 150 $KN.m^{-1}$ (taking into account that length variations are in millimeters) [67], under normal working conditions of the muscle (outside hyper-extension) its length will vary poorly around a slacking length, it is then perfectly legitimate to consider it constant given the low relative range of variability as well as the scope of this study that limits to the gait cycle where the muscles are operating under normal lengthening conditions. By making this simplification, the SE element's length is fixed at a constant thus known length inducing a drop out in the DoF, l_{mtu} in this case is function only of the joint position and l_{ce} and by having a feedback on the

state of the joint l_{ce} is obtained in a straightforward manner. We derive the following equations to solve the model.

From the serial configuration we can state that:

$$l_{mtu} = l_{ce} + l_{se} \implies l_{ce} = l_{mtu} - l_{se} \tag{2.11}$$

Given that the tendon is taken to be of constant length and from the equation 2.8 For the hip joint:

$$l_{ce}(t) = l_{opt} + l_{slack} + r_0.(\theta - \theta_{ref}) - l_{se} \tag{2.12}$$

$$v_{ce} = r_0.\dot{\theta} \tag{2.13}$$

for the knee-ankle joint :

$$l_{ce} = l_{opt} + l_{slack} + r_0.(sin(\theta - \theta_{ref}) - sin(\theta_{max} - \theta_{ref})) - l_{se} \tag{2.14}$$

$$v_{ce} = r_0.\dot{\theta}.cos(\theta - \theta_{ref}) \tag{2.15}$$

We call this method the derivative approach, since it relies on the 1^{st} derivative of the joint angle and contrasts fundamentally with the approach of Geyer and Herr.

Originally the MTU force is given by:

$$F_{MTU} = F_{PE} + F_{CE} - F_{BE} \tag{2.16}$$

We also perform the following simplification :

$$F_{MTU} \approx F_{CE} \tag{2.17}$$

Which is also justified given the close expression of F_{PE} and F_{BE} (2.1) and the length equality between the two elements, we consider thus in this simplified model that there is a compensation between the two forces. Bloc diagrams representing each approach can be found in the appendix B.2.

This method requires to have low noise ratio on the velocity sensors otherwise using signal processing. The angular position and velocity of the hip are given by the motors' drive as they are assumed to be the same. This implies that a careful alignment must be achieved between the hip and motor axis.

2.1.2 The Finite State Machine layer

As presented in the literature review, the controller need a first layer in order to synchronize its state with the phase progression of the walker in the gait cycle. During the scope of this thesis, we propose three gait Finite State Machines of varying order ranging from three to five which is more then what it is presented in the literature. FSMs for gait assistance are adequate as the biological responses of the neural system during the gait fits well in a state machine decomposition as its behavior changes according to the gait subphase.

The challenge in conceiving FSMs for the gait is the robustness to the change in the environment (noise) as well as inter-subject profile variability. For instance, the reviewed studies in the literature showed that techniques relying on setting thresholds on the joint position and speed are less robust to inter-subject variability when attempting to sharpen the states. For our FSMs, we rely on robust unequivocal and subject-independent events relying on FSRs input and speed zero-crossing. Our proposed FSMs distinguish also from the ones proposed in the literature with more then 2-states by the fact that the gait is not represented by one single FSM but two independent FSMs, one for each leg, which adds more adaptability and accuracy for leg state estimation.

The used sensors are the Force Sensitive Resistors (FSR) at the level of the foot insole, we also the information on the angular speed of the hip for the 4 and 5- FSM. To measure the later, the angular position and velocity of the hip joint are considered to be the same as the motor, that is why there must be a careful alignment between the motor and the joint axes.

2.1.2.1 3-state Finite State Machine

Our first proposal was a 3-states machine controller having as states: Early Stance (ES), Mid-stance and Pre-swing (MPS) and Swing (S). The events were chosen to be the heel strike, the single support and the ground lift up and were all detected by the estimation of foot loads through FSRs sensors located at the foot insoles. These events are also robust as they are unequivocal.

2.1.2.2 4-state Finite State Machine

Seeking for more precision, our second proposal was a 4-states machine controller having as states: Early Stance (ES), Mid-stance and Pre-swing (MPS), Swing (S) and landing preparation (LP). The events are kept the same as the 3-FSM to which was added the zero-cross detection of the angular velocity of the hip at the late swing.

To increase robustness we set a negative threshold close to zero so as not to take the lead on the intention of the user. This speed threshold is robust in the gait since the tight compulsively needs to revert its speed in order to prepare the HS at the end of the swing otherwise hip continues to flex which is physiologically impossible (impossible to sustain the gait).

2.1.2.3 5-state Finite State Machine

In another attempt to sharpen the decomposition in order to reached the simulated 5-FSM of Ong et al. [5] we proposed an ultimate 5-states FSM having for states: Early Stance (ES), Mid-stance (MS), Pre-swing (PS), Swing (S) and landing preparation (LP). The events are kept the same as the 4-FSM to which was added the recovery of ground contact of the contra-lateral leg for the detection of the pre-swing. Again, this event is highly robust regarding the used sensors.

The Petri network of each FSM is presented in detail in the appendix B.3.

2.1.2.4 Improvement of the Flexibility

A state transition was added between the early stance and the pre-swing in order to allow the switch in hte leading leg that can happen if the user marks a pose at the double support and decides to initiate the toe-off of the last landed leg.

2.1.3 The Neuromuscular Controller

The neuromuscular controller combines two complementary parts, the modeling of the skeletal muscles in a state estimation scheme and the neural command of the latter.

Conceiving such a controller begins first by selecting the right muscles to well represent the physiology of the hip-thigh during the gait cycle always with the implied compromise of model simplicity. Since the motion of the lower limbs during the gait cycle occurs mainly in the sagittal plan, it is fair to consider the hip in such system to be 1 DoF and focus only on the flexion-extension. To fulfill the two previous criteria we opt for one hip flexor and one hip extensor. We perform a different choice of muscles then the one of the commonly known NMC of Geyer's and Herr [7][58] where the hip is represented with three muscles/muscles groups; the Hamstring, the Gluteus and all the HFL (all the hip flexors). In our case, we decide to keep only the mono-articular muscles since the controller addresses hip assistance and because the orthosis is not actuated at the knee level. This excludes the Hamstring and the Rectus

Femoris, leading us to set the choice on the Iliopsoas (ILPS) for the flexion and the Gluteus Maximus (GLU) for extension.

The command part of the controller consists of mimicking the neural response of the nervous system. As a matter of fact, it must capture both the functioning of the central system (the brain) and the reflex arcs (the spinal cord). By doing so, we reproduce the neural stimulation of the biological nervous system to the previously selected muscles during the gait.

The gross change in the central response is induced by the high level FSM. Each state of the FSM represents a continuous behavior and awareness from the central neural system. For instance, biologically, when the brain receives the information of foot contact with the ground via Passini and Meissner contact sensors at the foot soles level, it commands the extension of the hip. Similarly, when the foot sensors of the device detect the heel strike event, the FSM situates the controller in the early stance phase thus ordering the increase of extension by combining the right reflexes. Also, at the late stance, when the extensor is hyper-contracted, the body responds with a stretch reflex inhibiting the later and activating the flexor, thus the neuromuscular controller should perform likewise. We quantify this commanded stimulation via the appropriate reflex which is a positive feedback [3] on the state of the muscles, that could be either l_{ce}, v_{ce} *or* F_{MTU} feedback and that enables the activation or inhibition of the muscle. Note that the system is stable despite a positive (not a negative) feedback, this stability is proved easily via the state variables-force relations. In the conventional neuromuscular controller worked with in the literature [7], they consider only force feedback. The other reflexes have been attempted but only in simulation as presented in the work of Ong et al. [5] where they considered length and velocity feedback as well. In our version of the Neuromuscular controller we choose to base our reflexes only on length feedback. First, because the length variable is more stable and much less jittery then the speed. Second, the influence of length in biological reflexes is well understood through the involuntary mechanism of stretch reflex, for instance at the mid stance and early stance, the extensor is hyper-contracted whereas the flexor is hyper-extended, using a length feedback will induce a higher stimulation of the flexor to revert the hyper-extension thus leading the torque to increase in the pre-swing which is exactly the wanted behavior, whereas if using a force feedback on the same muscle since the extensor is in concentric contraction its force will be higher then the flexor's causing a lower stimulation to the later, which is an unwanted behavior.

After fixing these choices comes the challenge of activating the right reflex with

3. The positive feedback translates into a negative feedback as the direction of force and length increase are in opposite direction

the right magnitude and at the right time to achieving the right behavior of the virtual muscles. This is a real challenge as biologists report that the motion of a limb could be performed in the exact same way by various combinations of muscular simulations [17].

In total, this work presents three selected controllers, animated with different combination of reflexes and FSM s. Each controller offers a different torque profile and thus berrying different effects on the biophysical and spatio-temporal data of the walker. The later are presented as fellow:

Muscle \ Subphase	ES	$MS - PS$	S
Gluteus Max.	$L^+[0.8]$	$L^+[0.8]$, $C^-[0.8]$	*basal*
Iliopsoas	*basal*	$L^+[0.6]$	$L^+[0.6]$

Table 2.2 – 3-FSM positive reflexes

Muscle \ Subphase	ES	$MS - PS$	S	LP
Gluteus Max.	$L^+[0.8]$	$L^+[0.8]$, $C^-[0.08]$	*basal*	$L^+[0.8]$
Iliopsoas	*basal*	$L^+[0.6]$	$L^+[0.6]$	*basal*

Table 2.3 – 4-FSM positive reflexes

Muscle \ Subphase	ES	MS	PS	S	LP
Gluteus Max.	$L^+[0.8]$	$L^+[0.65]$, $C^-[0.03]$	$L^+[0.65]$, $C^-[0.08]$	$L^+[0.65]$, $C^-[0.08]$	$L^+[0.6]$
Iliopsoas	*basal*	$L^+[0.6]$	$L^+[0.6]$	$L^+[0.6]$	$L^+[0.65]$, $C^-[0.04]$

Table 2.4 – 5-FSM positive reflexes

2.1.4 Discrete Computational Approach

A computation approach was proposed by Geyer and Herr [7] to which we refer to by *integral approach*. This method is based on the none simplified model and relies on numerical approximation by iterating on the previous state of the CE to find the current l_{se} and its applied force that is the same as the MTU's given the serial disposition. Then always relying on the previous state of the CE, the BE and PE lengths are approximated with that value. Their associated force is computed and the CE velocity is obtained with force-velocity inverse relationship. Finally a numerical

integration is performed to recover the length from the speed:

$$f_{vk} = \frac{F_{se}(l_{cek-1}) + F_{be}(l_{cek-1}) - F_{pe}(l_{cek-1})}{Act_k.F_{max}.f_l(l_{cek-1})} \tag{2.18}$$

$$v_{cek} = f_{v_k}^{-1} \implies l_{cek} = \int_{num} v_{cek} \tag{2.19}$$

The advantage of this method is the estimation of the speed based only on the joints angle rather then computing it from sensory inputs of the joint which is more robust to noise, the downside is first, the complexity of the model when trying to implement on hardware and second, the approximations used for the computation of $l_{se},\ l_{pe}, l_{be}$ and their forces based on the previous iteration of the l_{ce} which requires small time steps for convergence.

We propose a new computational approach that we name *the derivative approach* in order to contrast with Geyer's. This method has the advantage of being computationally more efficient making it more suitable for hardware implementation. The method relies on discretizing the aforementioned simplified model and computing the CE state based on the measured angular position and velocity of the hip joint and given a mono-articular muscle this gives the following implementation:

$$l_{ce,k} = l_{opt} + l_{slack} + r_0.(\theta_k - \theta_{ref}) - l_{se} v_{ce} = r_0.\dot{\theta} \tag{2.20}$$

for the knee-ankle joint :

$$l_{ce,k} = l_{opt} + l_{slack} + r_0.(sin(\theta_k - \theta_{ref}) - sin(\theta_{max} - \theta_{ref})) - l_{se} \tag{2.21}$$

$$v_{ce,k} = r_0.\dot{\theta}.cos(\theta_k - \theta_{ref}) \tag{2.22}$$

For computing the activation, since the function of the stimulation is not priory known and varies depending on the neural response, we use 1^{st} $order Euler's$ method to numerically solve the 1^{st} ordinary differential equation giving the dynamic of the *Act(t)*:

$$Act_k = (Stim_k - \tau.Act_{k-1})\delta t + Act_{k-1},\ k \leq 1;\ Act(0) = Act_0 = 0 \tag{2.23}$$

$$Stim_k = Stim_0 + G_x.X_{k-\delta} \tag{2.24}$$

Where δ is the electromechanical delay of the stimulation. Finally the muscular torque is found:

$$F_{MTU,k} = Act_k.f_l(l_{ce,k}).f_v(v_{ce,k}).F_{max} \tag{2.25}$$

$$T_{MTU,k} = r_k.F_{MTU,k} \tag{2.26}$$

The end-to-end control scheme is depicted in figure 2.2.

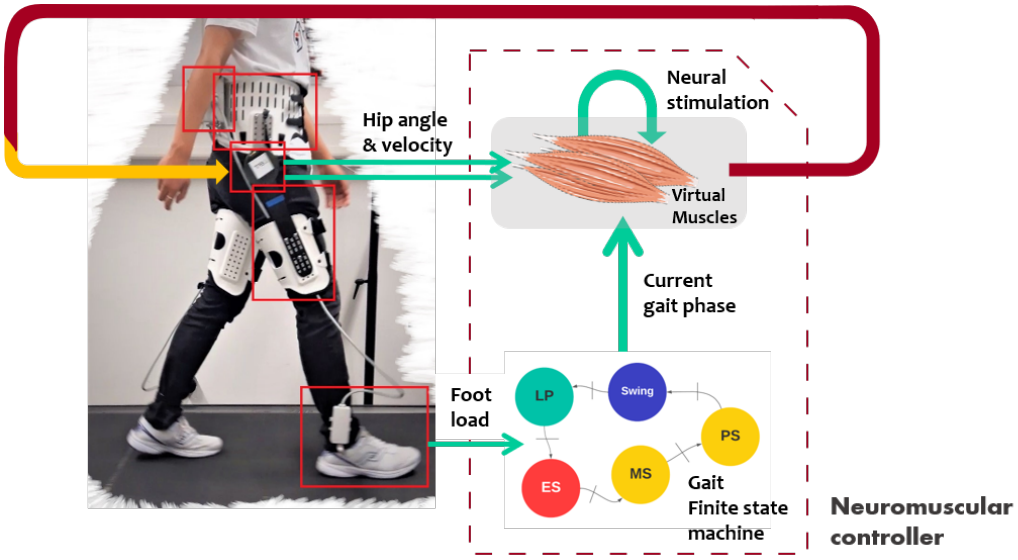

Figure 2.2 – Neuromuscular controller scheme

2.1.5 Torque-Morphology Adaptation

There are several morphological aspects affecting the joint torque magnitude, The dynamic model of the body depends on the limbs length that acts on the lever of forces and thus the torques magnitude, and their biological properties that acts on the generated force. Intuitively, this lead to consider the height and weight of the subject as main factors for determining the torque magnitude. Indeed our model was originally tuned to a person of 75 kg and 1.80 m tall, it is then extrapolated to other morphology by considering the weight and the normalized torque profile per weight unit as it is the main scaling techniques used in the literature.

2.1.6 Walking Condition Adaptation

The independence of FSM between the two legs gives the interesting property of reversibility, which allows assistance for the reverse walking as well. Beside flat and uneven grounds, the controller adapts also to inclined terrains, speed variations, abrupt stopping during walking as well as leading leg switch.

2.2 Parameters Tuning

The model has a total of 18 parameters per muscle, thus 72 parameters to tune for the 4 muscles. Adding to this, there is 6 to 13 gains to tune per muscle (depending on the used FSM) for a total of 96-124 parameters. In order to reduce this number we assume symmetry between the muscles of the two legs, this reduces by half the number of parameters leaving us with a total of 48 to 62 parameters for the entire neuromuscular controller.

2.2.1 Model's Parameters Tuning

Given the high number of parameters, the following methodology was followed: First, the parameters were initially all tuned based on two former contributions: Ong et al. [5] who used optimisation on Scone software [68] and run simulation on OpenSim [69] , the objective functions included minimization of coast of transport and ligament injuries and maximization of the head and step speed stability. The second reference was Geyer and Herr's [7] who used hand-tuning and simulation on Simulink. In order to validate the model tuning, we used Matlab scripting and Simulink to simulate the muscles using real angular positions and velocities recorded and logged using the orthosis. Then, from the analysis of the various state variables (CE length, velocity, torques, stimulation, activation), we restrict a set of plausible parameters that need to be re-tuned. We make sure to vary one parameter per re-tuning for better analysis. Of course, prior to this, a study was carried in order to understand the influence of each parameter on the model:

— Optimal length as well as the reference angle command the Gaussian peak horizontal shift. These are crucial parameters and needed to be re-tuned to provide convenient flexion and extension peaks at the right times of the gait cycle.

— The choice of SE length needed to be tuned to a mean working value since it is assumed constant in the simplified model.

— Maximum speed and K shape constant command the slope of force-velocity relationship, they were also re-tuned so as to attenuate speed fluctuation effect on the torque profile.

— The maximum force needed to be re-tuned as we are using only two muscles, keeping the maximum biological torque would have led to a disequilibrium between flexion and extension. In order to compensate the absence of the other muscles, the maximum force were set equal.

All the other model parameters were left unchanged or had minor modifications.

2.2.2 Gains and Inhibitions Tuning

For the gain tuning, it was not possible to rely on previous works, first because we proposed new sets of length reflexes, second, this controller differs from the traditional controllers in term of approach and objectives, third, the gains influence greatly the magnitudes, thus they needed to be adapted carefully to hardware limitation in term of deliverable peak and nominal torques of the motors. The method used to tune the parameter is in-vivo hardware simulation method with hand tuning. Since there was no prior knowledge of the ranges of gains and to preserve the hardware but still simulating the real-time computation, we programmed a real-time simulation of torques without applying them to the motors, this was performed in 2 ways:

— *Without the orthosis:* Using only the MCU (Beagle Bone Black) by playing in loop previously collected and logged angular positions and velocities of the hip using normal walking with the orthosis.

— *With the orthosis:* The torques were simulated but still not applied on the motor and the angles and speeds of the hip were collected in real time and fed to the model.

The torques were then monitored using a monitoring desktop application of the BBB for quick analysis, then using MATLAB for sharper investigations. The inhibitions and gains were tuned so that to first have a smooth continuous behaviour despite states transitions and second to have a profile close to the biological one in terms of curve tendency, characteristic times and magnitudes.

Chapter 3

Implementation

3.1 Device Presentation

The hardware implementation of the neuromuscular controller is performed on the embedded computer of the E-Walk hip orthosis of the REHAssit research group. The orthosis provides one actuated rotary DoF at the hip joint for each leg, thus a total of 2 actuated rotational joints whose axes are aligned with the hips'. The media-lateral rotation as well as the abduction-adduction are not actuated but remain free with a reduced range because of tight attachment for the former and the side polycarbon torque transmissions for the latter. These two elements remain compliant thus do not lock completely the motion. Mechanical, electronic specifications as well as the low level control are presented in details in the appendix C.1.

Figure 3.1 – E-Walk V1 hardware components: 1) emergency stop button, 2) embedded controller enclosure, 3) torso attachment, 4) motors, 5) thigh segments, 6) thigh attachments, 7) foot sensor amplifier boards, 8) instrumented shoes

3.2 Software Programming

3.2.1 Software Specifications for the E-Walk

The implementation of the controller was performed using low level C^{++} and Linux scripting on *Visual Studio Code (VSC)* Integrated Development Environment (IDE) then on *Qt Creator IDE*, the later was chosen given that it is cross-platforms and enables remote deployment to the embedded system Beagle Bone Black (BBB) board, the cross-compilation was done using the latest version of *Linaro-gcc* tool chain

[70]. The simulations were partially carried out on the device and partially executed using Matlab scripting and Simulink as explained in 2.2.2 and 2.2.1. Data analysis was performed using Matlab.

Using WiFi, a SSH (Secure Shell) session is opened between the Beagle Bone Black and a remote device in a server-client scheme. The only information to provide from the client side is the IP address of the server, the server-client proceed to authentication by exchanging public keys, the server then listen to the client on the Transmission Communication Protocol (TCP) port 22. This allows remote login to and command lines execution on the BBB's Linux system via an external device.

The BBB has a system clock but does not integrate a Real Time Clock module, the time synchronisation between the BBB and the remote device occurs when they are connected via the remote controller application using the Network Time Protocol (NTP) [71]. If the remote device integrates a Real Time Clock (RTC), this allows time synchronisation between the BBB and the real time clock.

The programming paradigm was set to be very modular, readable and sustainable to integrate further peripherals

One very important and extremely useful feature that has been added to the programming paradigm is the introduction of log files to record the successive values of variables of interest. This turned to be a powerful and extremely useful feature in debugging and post data analysing and processing. This is performed via a special objects called the synchvars, whenever a variable with a fixed memory is wanted to be tracked and recorded, it needs to be added to the synchlist as a synchvar object. The values of each variables are written to a local log file at the end of each main loop (update frequency same as the main-loop run frequency)

The code is structured in 3 major types of libraries presented from the lowest to the highest level; The Hardware Abstraction Layer (HAL) (Hardware Abstraction Layer) that encapsulate all the needed libraries for the interaction with the drivers such as the Controller Area Network (CAN), Serial Peripheral Interface (SPI), I2C and motor driver. The Utilities that gather all the utilitarian C^{++} libraries including data structures, synchvars and numerous coded libraries used in the controllers such as filters classes. And finally the Controllers library where all the developed controllers programmed for the orthoses and exoskeletons are grouped. In order to integrate cleanly the code of the NMC controller, this ramification was respected.

The libraries come alongside a desktop graphical application called the *Remote Controller* coded in C^{++} using *Qt creator libraries* that enables online monitoring of the logged variables through streaming and plotting but also make the time synchronisation between the BBB and the remote device at first connection using NTP.

3.2.2 Methodology and Quality Objectives

The long process of screening through the already implemented libraries on the E-Walk's BBB has led to a good understanding of the coding paradigm. **The quality objectives regarding code** implementation were set as follow (with decreasing priority): *Functionality, integrability, modularity, scalability, optimized to embedded system and real time, testability and readability*. The table explaining how each objective was achieved is presented in the appendix C.5.

Speaking of the methodology, after setting the theoretical basis and deriving the computational method, a code architecture was proposed and designed using classes Unified Modeling Language (UML) diagrams (refer to appendix C.4), this step was important to achieve a reusable and none-overlapping code given the complexity and inter-dependencies of the model. The detailed UML diagram is presented in the appendix

The first implementation stage was dedicated to the programming of libraries integrating classes inherent to the controller, this stage was performed on *Visual Code Studio IDE* independently from the device's libraries. There have been gradual debugging at each coding milestone which proved to be very efficient.

After that, a gradual code integration-debugging phase has been performed on *Qt Creator IDE*. This IDE was chosen by former developers because it allows remote deployment to the embedded computer using WiFi provided the knowledge of the BBB's IP address on top of basic functionalities of an IDE. The code was built-debugged then deployed to the BBB to test both integration and functionality. The validation tests are presented more in detail in the next sub-sections.

3.2.3 Validation Tests

The code implementation and integration was submitted to rigorous testing before being validated. The full table of unitary test is presented in the appendix C.6.

3.2.4 Hardware Assessment

As mentioned earlier, the BBB does not run on a Real Time (RT) Linux. Time is a crucial parameter in control system since the model is updated in real time, it was then crucial to determine the maximum acceptable run frequency of the main loop that should fulfill two constraints:

— *Hardware achievable:* The loop must run without timeouts. This depends greatly on the running time of the SPI and CAN threads. Measurement of the run

time and jitter of the two threads have been carried out softwarely. Because of its simplicity, the SPI thread was able to run fast (up to 1.5 KHz) however the CAN that handles two motors was slower because of the motor' drive response delay and it was impossible to exceed a run frequency of 500 Hz because of high jitter. Some solutions were tested to increase the speed such as integrating the program of the SPI thread to the main thread and splitting the CAN thread to two threads one for each motor but the first proposition made the FSM state estimation less accurate and the second increased jittering.

— *Model compatible:* The run frequency of the main loop determines the sampling time of the discretized continuous neuromuscular model. The time step should be small enough to well catch the system's dynamic. This is formalized by Shannon's theorem. In our case, the system is the gait cycle, its period depends on the cadence. The average gait cycle period is the average duration of one stride, thus double the average duration of one step. However for our estimation, we refer to the maximum values reported in the literature 124.77 $step/min$ for slow (average 117.00 $step/min$) and 142.08 $step/min$ (average 128.00 $step/min$) for fast pace [72], this gives a minimum slow period of 0.96 s (average 1.02 s) and a minimum fast period of 0.84 s (average 0.93 s). According to Shannon's theorem, the sampling frequency should then be at least 2.08 Hz (average 1.76 Hz) for slow and 2.38 Hz (average 2.14 Hz) for fast pace.

The first strategy was to implement a separate thread for the SPI and the CAN bus. The SPI handler included reading the value of the FSRs followed by the update of the state of controller's FSM. The CAN handler managed the queued requests to the two motors. The hardware testing results, which are presented in table 3.1, revealed that a 500 Hz frequency was hardwarely reachable with a low time overrun for both the SPI (0.002%) and the CAN (0.06%) relative to the dynamic and it was largely well representing the system variations (250 Shannon's limit frequency) with a 0.002 s sampling time step (minimum number of samples 480 to 420 per cycle). Thus the main loop was set to run at 500 Hz.

Measure	**Threads**	
	SPI	CAN
Average duration (ms)	2.020	2.600
Standard deviation (ms)	12.080	267.030
DRE[4] (%)	0.002	0.06
PRE[5] (%)	1.00	30.00

Table 3.1 – Multithreads run-time measurement for a programmed reference run period of 500 Hz

Among the many solutions that have been attempted to improve the run-time was

to integrate both the SPI and CAN handlers in one thread to verify whether the time latency of the CAN was due to the execution of the SPI thread or to the time response of the motors' driver. The obtained results, shown in table 3.2, were similar to the one with two separate threads which confirms the second hypothesis.

Measure	
Average duration (*ms*)	2.651
Standard deviation (*ms*)	0.096
DRE (%)	0.060
PRE (%)	32.00

Table 3.2 – SPI-CAN joint thread runtime measurement for a programmed reference run-period of 500 *Hz*

To enable threads independence, the first multi-threading solution was kept.

4. Dynamic relative error
5. Period relative error

Chapter 4

Experiments and Validation

4.1 Methodology

4.1.1 Ethical Approval

In Switzerland, research involving humans is permissible only upon prior review and approval by an independent committee that is the Human Research Act (HRA). If the review is positive, a Human Research Ordinance (HRO) is delivered to the research team, allowing him the run of experiments involving human subjects and ultimately the use of their collected data. The ordinance is enforced by the cantonal ethics committee which makes sure that the statutory requirements are complied with all along the project [73].

In the scope of this project, an amendment have been submitted to the Swiss Ethics Committee on July, 23^{rd} in order to proceed with data collection on human subjects. We were tremendously pleased to obtain the approval of the committee on August 11^{th} which enabled scheduling of experiments.

4.1.2 Experimental Setup

Experiments are conducted on healthy subjects with a full walking ability. The prior objective is validation. We target two types of validations; first, we test the control robustness and adaptability in the steady and unsteady conditions including variations in term of speeds and ground inclines. The adopted protocol for this assessment is explained in the intra-lab experiment section. Second, the effectiveness of the assistance is tested. The effectiveness of the control approach is evaluated by measuring the variation of the Cost of Transport (CoT); an effective assistance should induce a reduction of the metabolic rate (Metabolic Rate (MR)) compared to the non-assisted condition and ideally compared to the no-device condition. The latter is harder to reach since tightly correlated to the efficiency of the device' mechatronics. This second objective requires the measure of the oxygen consumption or the heart rate measurement and is thus practically harder to conduct.

For subjects selection, main inclusion criteria are the healthy motor functions and the device fitting. The aim was to compose a sample of high inter-subject variance in terms of body characteristics (height, weight), gait walking profiles and age.

4.1.3 Experimental Protocols

4.1.3.1 Intra-lab Experiments

These experiments are for the first validation objectives and do not include oxygen consumption measurement. They are carried out inside the BioRob laboratory.

The test include ground walking on treadmill with the device in steady and unsteady conditions. Treadmill walking is not a requirement for the controller well-functioning but guarantee inter-subject repeatability of the protocol which is mandatory for significance. For both steady and unsteady conditions, both speed and incline variations robustness and adaptation were tested. The detailed protocol is attached in the appendix D.1.

4.1.3.2 Extra-lab Experiments

Caution: *This type of experiment has not been performed at the time of writing this report.*

These experiments are for the second validation objective and include oxygen consumption measurement. They are carried out in a specialised center outside the BioRob laboratory.

The experiment is a cross-over design and consists of having each subject walk on a treadmill for 8 different settings, 5 minutes in each setting, with a recovery period of 3 minutes in between. We will test walking without the exoskeleton (NO), a transparency condition during which the exoskeleton is worn but does not apply any assistance (TR), and two different control mode conditions (C1 and C2). Each of these conditions will be tested at a normal walking speed fixed at (4 km/h) and two different inclinations (flat level walking at 0% inclination and uphill walking at 10% inclination) on the treadmill. Walking at each condition will last 5 minutes in order to let the metabolic rate reach a steady-state and have reliable measurements. The order of the conditions will be randomized. 5 minutes of walking with each controller will be followed by a 3-minute recovery during which the subjects will also answer a questionnaire. The entire experiment should last about 120 minutes in total. The detailed procedure is outlines in the the appendix.

4.1.4 Measurements

For both the intra and extra-lab experiments, the orthosis provides measurements of the angular positions and velocities of the hips as well as foot loads.

For the extra-lab experiments additional biological measurements are recorded. The participants' metabolic cost of walking is estimated using collected data from a respirometer system (Cosmed Quark CPET, Cosmed, Italy), the power delivered by the robot will be estimated from the integrated sensors and instrumented treadmill data (T150 - FMT-MED, Arsalis, Belgium) [74]. For subjective feedback, the participants will be asked, at the end of each experimental condition, to complete the Borg Scale of Perceived Exertion [75] and answer a separate questionnaire about perceived support by including Likert Scales. The scales are chosen carefully; It contains even number of possibilities if the neutral opinion is not relevant, e.g., when asking about the hindering and an odd number when the neutral response is significant, e.g., when assessing the level of synchronisation. The choices are inserted inside varying color boxes.

These biological measurement are performed in the presence of a biophysicist that ensures the right experimental settings. For instance, the oxygen consumption must respect a specific range since beyond these thresholds, the subject is in the anaerobic condition which must be avoided since it biases the estimation of energy expenditure. The expertise of a physician is also required for the post data processing regarding curve fitting and statistical significance evaluation of the CoT.

4.1.5 Data Processing Pipeline

4.1.5.1 Overall Process

As presented in the previous chapter (3.2.1), at the end of the program execution, a log file is generated containing raw data of all the saved variables including the joint kinematics, the model variables and the software related variables such as the timestamps and the threads duration.

The angular positions and velocities are obtained from a high resolution 18-bit absolute encoder and a fair-resolution driver-embedded estimator, respectively, as explained earlier (C.1). Thus, no further filtering is required. The FSR signals were at first filtered using a 1 kHz simple numerical low pass filter, that was later on removed given the two facts that first, the filter induced unwanted delay and second, the FSM events relied on the gross some of the loads and not the precise value of the cells, thus a simple use of threshold was sufficient to counterbalance the low level noise ratio.

The post-analysis take place on $MATLAB$. The raw data are extracted from the orthosis' log files, a file is either considered alone for intra-subject analysis or aggregated with other log files for inter-subject analysis and controllers comparison. First,

the gait cycles are delimited and broken down, they are then subject to statistical tests for data consistency assessment (as explained more in detail in the next subsection). The next step is the use of the processed data for estimating performance related quantities. Finally, the results are visualised for validation, analyses and conclusions.

Note that, for each stage of the data processing, *MATLAB* functions have been coded.

The process is summarised in the following flow chart:

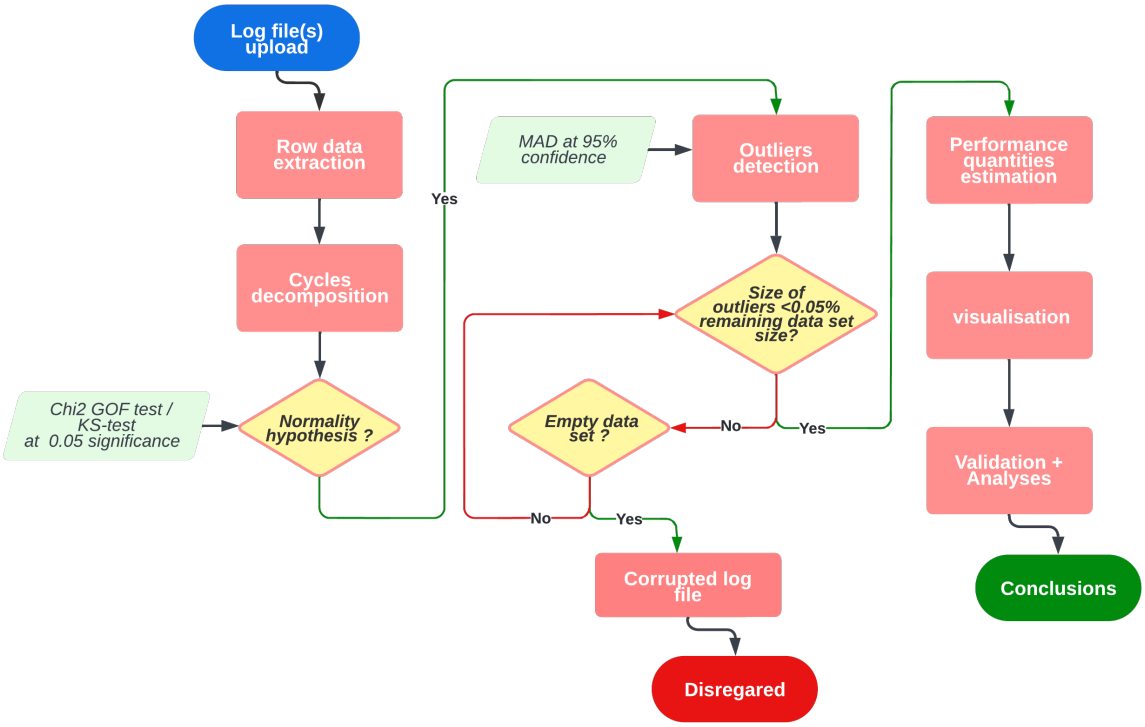

Figure 4.1 – Data processing pipeline

4.1.5.2 Statistical Analysis

The statistical analysis considers two axes:

— The intra-subject analysis: For both intra and extra-lab tests, we collect repeating row data of kinematics and kinetics across all the duration of the experiment. The aggregation of these data follows the law of large numbers (LLN), for instance, for a duration of 1:30 min, an average of 150 cycles are collected with 400 samples on average for each cycle. In order to guarantee the integrity of data, statistical tests are performed to test the normality hypothesis and then detect the outlier cycles, they are then removed and not accounted in the final analysis.

— The cross-subjects analysis: This is employed only for the extra-lab experiments to assess the significance in the MR reduction and is not presented as these experiments were not conducted.

The first test to perform is the normality test of the time series data. A χ^2 $Goodness - of - Fit$ test [76] confirmed with a $Kolmogorov - Smirnov$ test [77] under a significance $\alpha = 0.05$ were performed by considering the measure at each percent of the gait cycle to be an independent stochastic variable. Their results enabled the none rejection of the null hypothesis (normality) with an average $p - value = 50\%$. For the outliers detection, we used the Median Absolute Deviation (MAD) method, this method was preferred over the Inter-quartile Range (IQR) such as χ_2 for its robustness and because it does not rely on the number of DoF which allows samples of varying size, it also relaxes the normality hypothesis to a certain point in case the normality hypothesis was rejected. Note that for a perfectly normal distribution, the variance based IQR are equivalent to the MAD since the mean is the median in that case. Since the data are time-series, each column is considered as a single stochastic variable. The confidence interval using MAD is thus given by [78]:

$$X_{tclean} = \{x_{tk} \mid x_{tk} \in med(X_{tsample}) \pm \ MAD.k\} \tag{4.1}$$

$$MAD = med(|med(X_t) - x_{tk}|) \tag{4.2}$$

When the normality hypothesis is not rejected, and for a chosen confidence of 95% (i.e., the significance level $\alpha = \ 0.05$ the inclusion criterion becomes:

$$X_{tclean} = \{x_{tk} \mid x_{tk} \in med(X_{tsample}) \pm \ MAD.k.\frac{1}{\sqrt{2}}erf^{-1}(3/4),\ k_{0.95} = 1.96\} \tag{4.3}$$

The process of removing outliers was iterative and the stopping criterion was the outliers size being less then 5% (decreased to 1% in some cases) the size of the remaining data set used in the analysis.

Note: The results of outliers detection are presented in the appendix D.3.

4.2 Validation Approach

The validation is done regarding two aspects; First, the assessment of the control strategy from a purely system control point of view and second the contribution to the assistance from a physiological and biological point of view.

4.2.1 Metrics for Model and Controller Validation

The proposed control strategy includes a model of human muscles through a simplified Hill Type model, a state feedback controller via a combination of neural reflexes and 3 FSMs for the gait cycle decomposition.

The validation of the model cannot be achieved by cross-correlating the biological torque profiles to the commanded torque generated from the controller. First, because the biological profiles presented in the literature are averaged profiles inter-subjects, even if the general trend of the torque during gait tends to be similar across subjects, specificity remains regarding the characteristic timings and the magnitudes resulting in high variance compared to the average curve as shown in figure 4.2. This means that unless measuring or estimating the biological hip torque of each subject in vivo the cross-correlation is not possible. This leads us to the second obstacle which is that neither the measure nor the estimation of the biological torque are reachable in this use case given the unavailability of a motion capture system or EMG device as well as the non-monitoring of the remaining leg joints (for inverse dynamics).

Consequently, we propose an alternative approach for the model validation. The assessment takes into account three parameters:

— ***The general trend:*** By a direct comparison with the trend of the biological torque;

— ***The characteristic times:*** Characteristic times correspond to specific events of the gait that are: The extension peak time, extension to flexion zero-cross, the flexion peak and the flexion to extension zero-cross. The biological data reported in the literature present high variance between subjects in the characteristic times, we rely on this data to intake the gross variation range and we compare the model's times to optimal interpolation times regarding minimisation of the energy expenditure obtained from human-in-the-loop optimisation [79];

Charc. time / Source	P_E	EF_{ZC}	P_E	EF_{ZC}
Avg. bio. profile [17]	$6 \mp 4\%$	$6 < 18.27 < 56\%$	$50 < 52 < 60\%$	$70 < 78 < 86\%$
Hum. in the loop opt. [79]	$10.3 \mp 1.2\%$	$36.5 \mp 3.5\%$	66.6%	$88.5 \mp 1.5\%$

Table 4.1 – Reference characteristic times for the gait

— ***The magnitude:*** The ratio of extension to flexion peaks should at least be equal to 1.5, the extension requires biologically more assistance as it corresponds to the phase of body weight bearing by the leg, whereas during flexion, the inertia

around the joint corresponds to the leg's which represents only 17% the body weight on average.

— ***The state transitions timing:*** The state transitions of the controller must be synchronised with the percentage of occurring of their corresponding biological subphases of the gait;

Phase	**Stance**			**Swing**	
Subphase	**ES**	**MS**	**PS**	**S**	**LP**
Gait cycle pct. (%) [21]	0-12%	12-50%	50-62%	60-87%	87-100%

Table 4.2 – Gait cycle subphases timing

— ***Virtual muscles stimulation:*** It should correlate in trend with the biological muscles stimulation [17] [80].

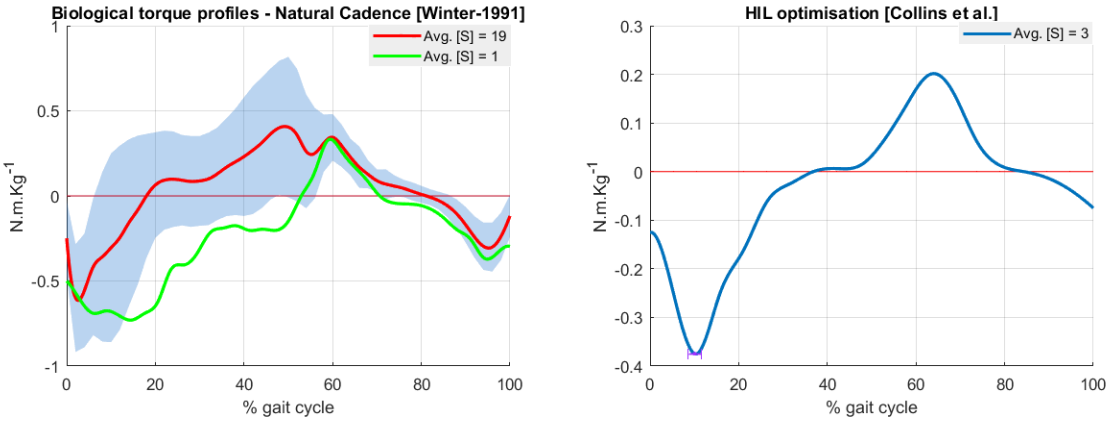

Figure 4.2 – Reference torque profiles as in [17] and [4]

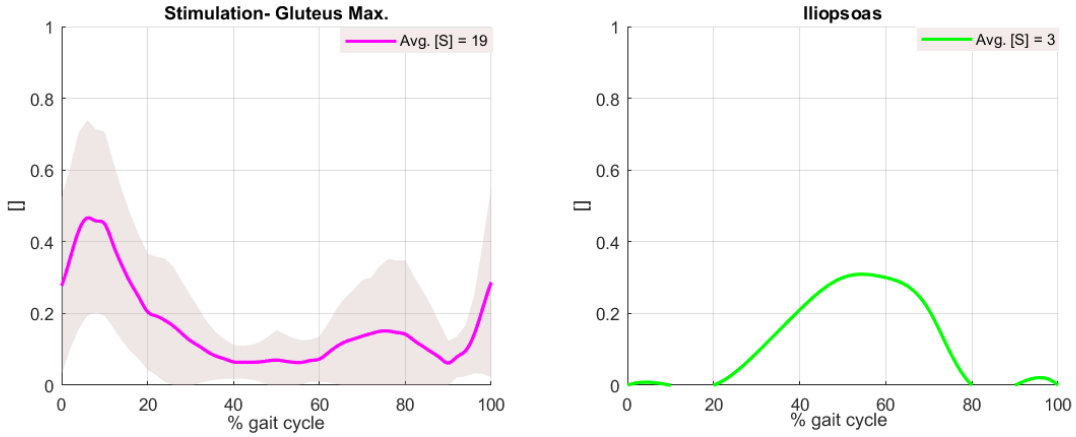

Figure 4.3 – Muscles stimulation during the gait cycle as in [80]

4.2.2 Metrics for the Assistance Effectiveness

This part includes the effectiveness of the assistance in the reduction of the CoT during walking. The direct method is to estimate the energy expenditure by measuring the oxygen consumption as explained previously (4.1.4). However this is possible only for the extra-lab experiences. In absence of the measurement device, the performance was assessed by correlating gait related estimated metrics to the metabolic rate.

— ***The produced work/power:*** The average power delivered to the hip joint or the total work per cycle

$$\bar{P}_{cycle} = E_P[P_k] = E_P[\omega_k.\tau_{cmdk}] \tag{4.4}$$

$$W_{cycle} = \sum_{k=0\%}^{100\%} t_k.\omega_k.\tau_{cmdk} \tag{4.5}$$

The total produced power/work give only an idea of the assistance as authors in the literature suggest that good reduction correlates with high positive power/-work. We push the analysis further by computing the total work for extension and for flexion separately, since the assistance during the extension should be higher then the one during flexion as explained in (4.2.1).

— ***Gait characteristics:*** This includes variations in the range of motion and more importantly the change in cadence and step length. Studies in biophysics demonstrated that the optimal CoT is obtained when subjects walk at their preferred cadence know as the preferred step frequency (PSF). However, these studies have been carried out without assistance

4.3 Results

Important note: *The sign convention for torques is taken to be of positive sign for the flexion and negative for the extension.*

This section presents the results obtained from intra-lab experiments on real subjects of the three proposed controllers as in (2.1.3). The upcoming results were obtained from experiments carried prior to the week of August, 15^{th} and do not necessarily respect the protocol presented in 4.1.3.1.

Note: More comparative graphs are provided in the appendix D.4.

4.3.1 3-States FSM

Analysis The angular positions and velocities of the hip, shown in figure 4.6, are not significantly affected with an increased speed jitter at the mid-stance, The trend of the torque profile at the stance and early swing is similar to the trend of the biological profile, the characteristic times, also depicted in figure 4.5, are also coherent with the reference times advanced earlier. However the profile at landing preparation follows a monotonous positive flexion torque which is the inverse desired behavior. Indeed, at the landing preparation the torque must deceases to initiates extension, whereas the commanded torque here pushes toward more flexion meaning the assistance is resisting the motion. The observation of the muscles stimulation in figure 4.4 at the landing preparation also confirms this claim. During this phase the Iliopsas kept stimulated because of the missing stretch reflex from the Gluteus as the latter is not stimulated while it should be. This is an unwanted behavior that intuited the necessity to reflect upon the landing preparation detection, giving the intuition to the version with 4-FSM.

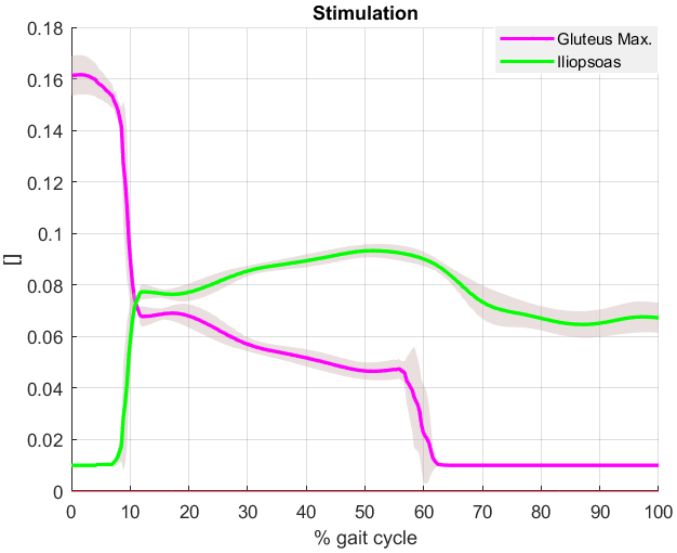

Figure 4.4 – Muscles stimulation - controller V1

The magnitude ratio of extension to flexion is well respected with a peak of flexion at 0.15 $N.m.kg^{-1}$ and 0.225 $N.m.kg^{-1}$ for the extension. The state transitions of the FSM occurs at the right time of the gait percent which validates the detection method.

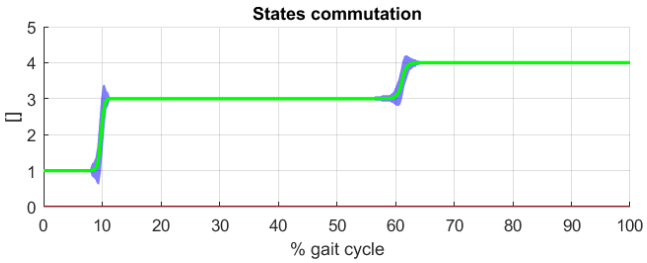

Figure 4.5 – Change in the states of the gait finite state machine - controller V1

Despite the high variance of the inter-subjects profiles in terms of positions and speeds, the torque profile have low variance at the stance and early swing, the variance is higher in the late stage of the swing as the subjects receive resistance from the device, thus different subjects will react differently, some will tend to increase their range of motion and follow up with the controller, others will resist the controller.

This difference in interaction induces different kinematic profiles and thus varying torque.

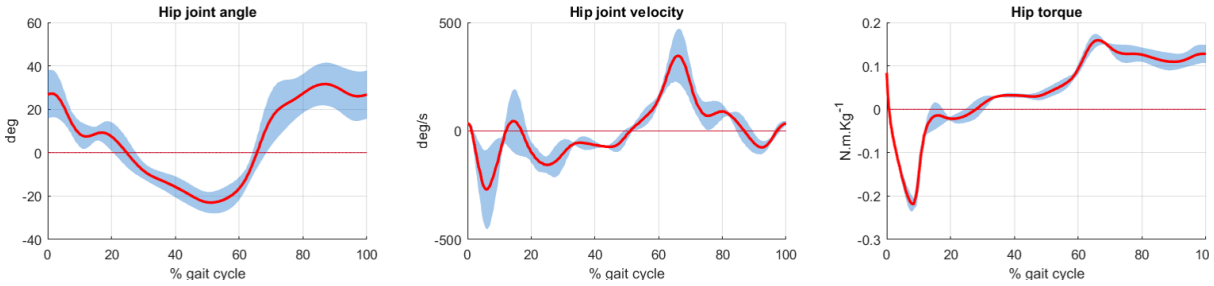

Figure 4.6 – Results of intra-lab experiments averaged on 4 subjects - controller V1

4.3.2 4-States FSM

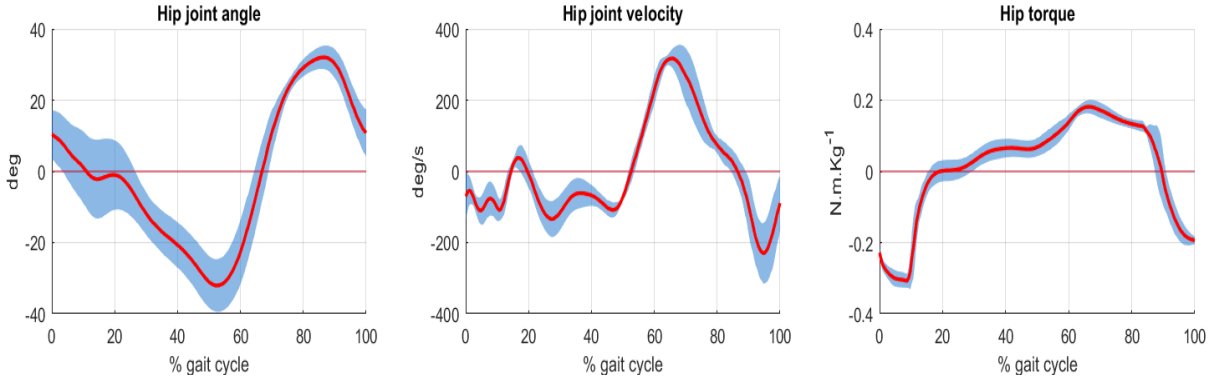

Figure 4.7 – Results of intra-lab experiments averaged on 4 subjects - controller V4

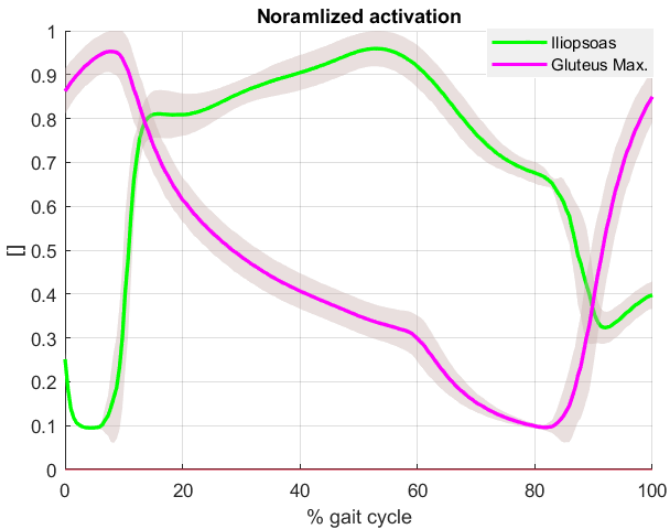

Figure 4.8 – Muscles activation - controller V2

Analysis Figure 4.8 shows the kinematics and dynamic profiles. The angular positions and velocities of the hip are not significantly affected with an increased speed jitter at the mid-stance but lower then the previous version.

The kinetics profiles draw high variance resulting from the differences in gait patterns between subjects which is a desirable finding.

Despite high variance in inter-subjects kinetics, the profile of torque remains steady and shows low variance.

The trend of the muscular stimulation (in figure 4.8) and the torque profile is in accordance with the biological ones, however, the rise from extension to flexion happens quicker then in the the biological trend which leads to an extension duration lower then the flexion one. This is due to the fusion of the mid-stance and pre-swing, the gains consideration for stimulation as well as reflexes are thus kept the same. This observation intuited the necessity to reflect upon the mid-stance and pre-swing separation, which gave birth to the third version with 5-FSM. The characteristic times are fairly close to the biological ones, however the flexion to extension zero cross happens at the limits of the optimal time variance. This observation encourage to consider gain reduction at the landing preparation for the next version of the controller. The magnitude ratio is at 1.5 which meets expectations. The state transitions of the FSM shown in figure 4.9, occurs at the right time of the gait percent which validates the detection method. Note that it is robust to the inter-subjects variance.

The main variance points concern more the magnitude values rather then the characteristic times (apart the zero crossing). The magnitude is tightly related to the range of motion and speeds of the subjects, which justifies the variance.

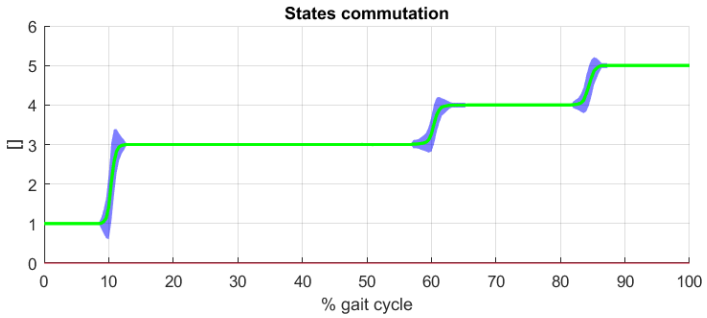

Figure 4.9 – Change in the states of the gait finite state machine - controller V2

4.3.3 5-States FSM

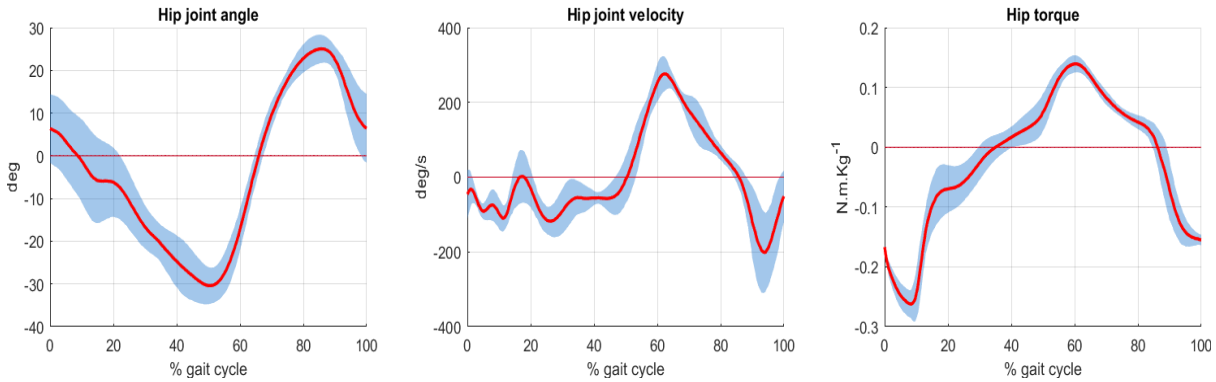

Figure 4.10 – Results of intra-lab experiments averaged on 4 subjects - controller V3

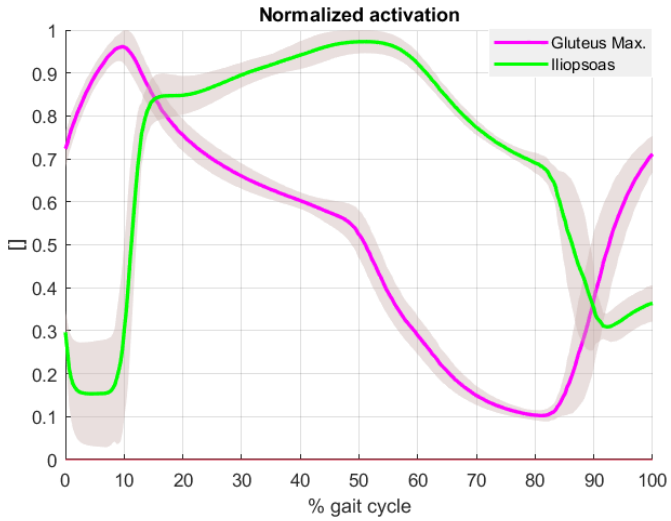

Figure 4.11 – Muscles activation - controller V3

Analysis The angular positions and velocities of the hip are not significantly affected with an increased speed jitter at the mid-stance but lower then the V1 and V2 as reported in figure 4.10. This suggests that the jitter is also related to the slop of the variation in the torque change. The kinetics profiles draw high variance resulting from the differences in gait patterns between subjects which is desirable. Despite high variance in inter-subject kinetics, the profile of torque remains steady and shows least variance.

The trend of the torque profile is in well accordance with the biological profile. Compared to the V2, the slope of the mid-stance is smoother this had two effects; The reduction of the speed jitter in the end of the early stance and a longer duration of extension assistance. The stimulation of the two muscles, as in figure 4.11, are in opposition which means that the antagonism of the muscles is preserved by the model.

The peak of extension is at 2.75 $N.m.kg^{-1}$ and 1.5 $N.m.kg^{-1}$ for the flexion which gives a good ratio of 1.83. The characteristic times are very close to the ones obtained via optimisation. The state transitions of the FSM, presented in figure 4.12, occurs at the right time of the gait percent with low variance except in the transition times where there is discrepancies between subjects to which the model synchronizes well.

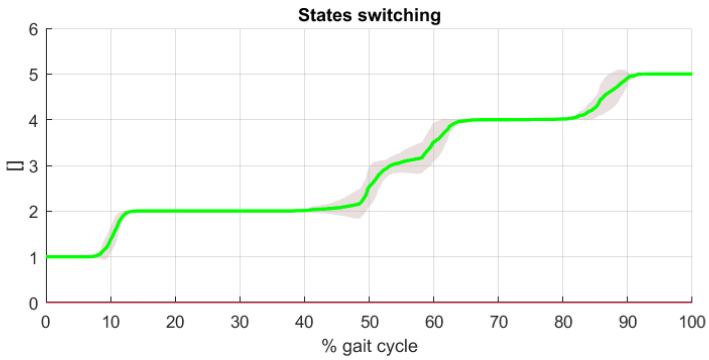

Figure 4.12 – Change in the states of the gait finite state machine - controller V3

The main variance points concern more the magnitude values rather then the

characteristic times (apart the zero crossing). The magnitude is tightly related to the range of motion and speeds of the subjects, which justifies the variance.

4.3.4 Performance Comparison

4.3.4.1 Produced Work

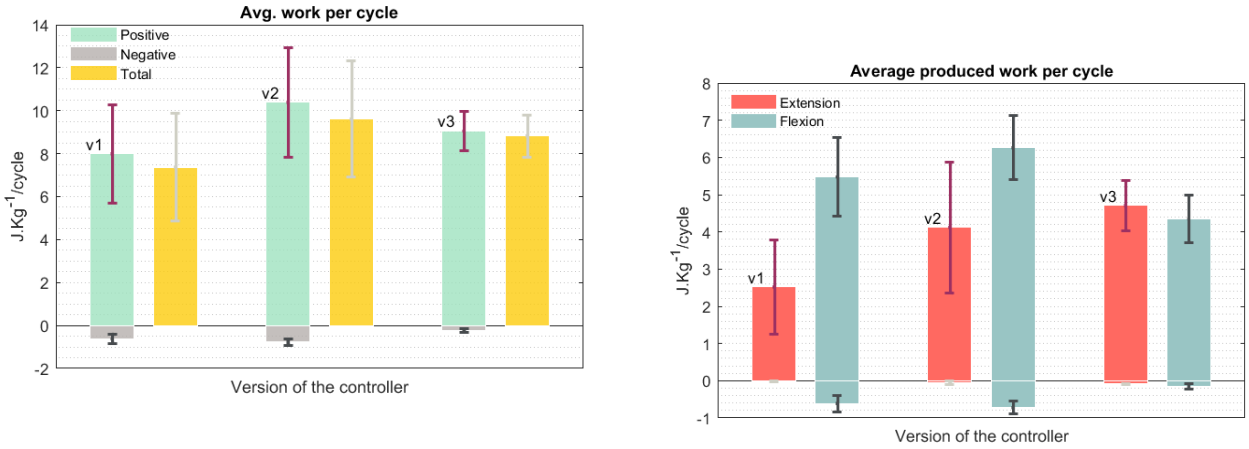

Figure 4.13 – Average produced work across subjects at v = 1.25 $m.s^{-1}$

Analysis As depicted in figure 4.13, on average, the V2 produces the highest amount of positive work but the V3 produces the least negative work. A deeper introspection of the positive work produced in each phase shows that the V3 produces the highest work in extension which place it as favourite since the assistance is mostly sought during extension because of weight bearing. The V1 is the one producing the least positive work in extension which is the result of the extra flexion at the landing preparation besides the fast slope at the mid-stance.

4.3.4.2 Speed Adaptation and Gait Characteristics Change

Analysis Figure 4.15 shows that, compared to the baseline, speed increment induces naturally an expansion of the range of motion. In terms of kinetics changes, the V3 induces the least disturbance on the speed (in terms of jitter in the mid-stance), this is potentially correlated to the smoothness of behavior change (reflected by smoother slopes, closer to the biological ones), it could also be induced by the lower negative work and reaction forces on the upper part as well as the reaction from the contralateral leg motor.

The V1 controller is the only one increasing the range of motion of the flexion in all speed conditions as shown in figure 4.16. This is due to the sustained flexion torque

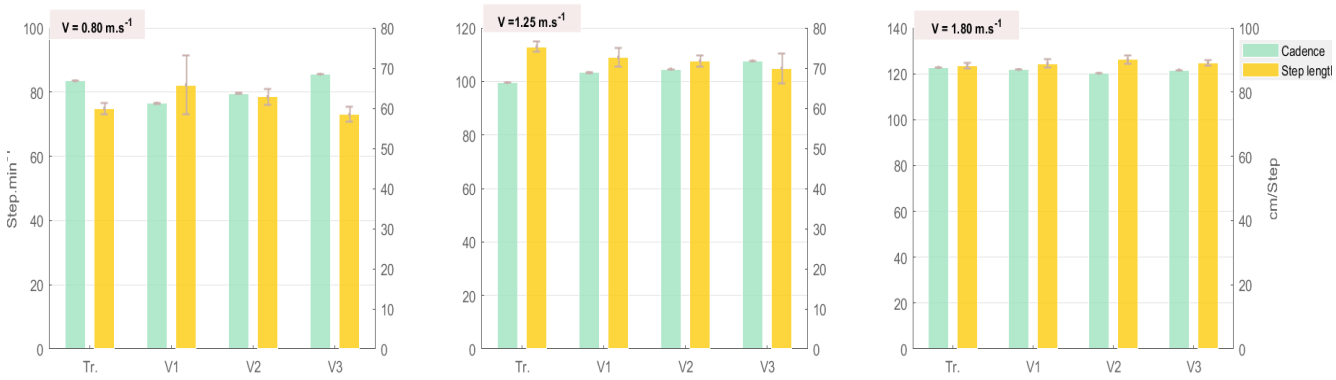

Figure 4.14 – Cadence and step length across different speed conditions

at the landing preparation. Figure 4.17 and 4.18 show that both V2 and V3 decrease the flexion range of motion by 40% on average. Unlike the V2, the V3 increases the range of extension by 16% because of higher extension assistance. These findings correlate with the obtained cadence variations. Indeed, the V1 induces on average lower cadence and longer step lengths, in opposition to the effect of V2 and V3. The cadence and step length are poorly modified for the high pace walking compared to the transparent condition. This could be either because of better synchronisation at high speeds or because the contribution of the assistance torque is blurred next to the high biological torque and ground reaction forces.

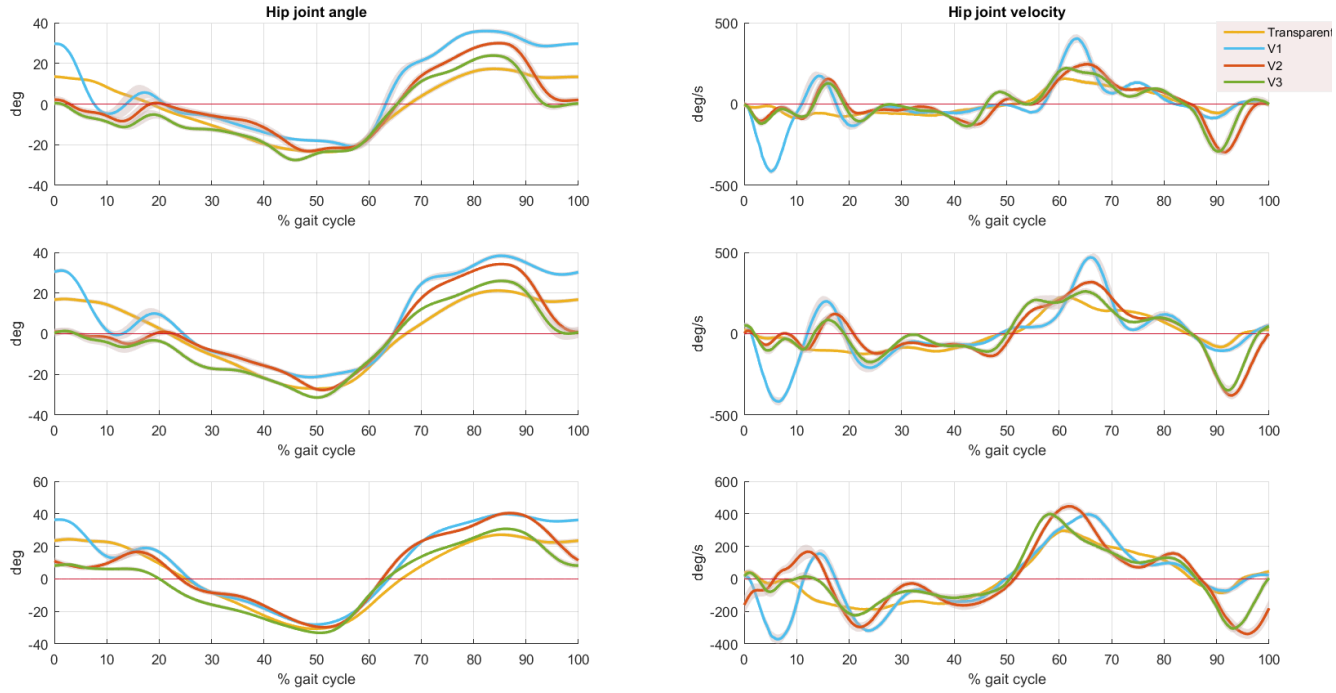

Figure 4.15 – Kinematic profiles adaptation at different speeds. From the top to the bottom; 0.80 $m.s^{-1}$, 1.25 $m.s^{-1}$, 1.80 $m.s^{-1}$

All controllers remained robust in terms of state transition, phase synchronisa-

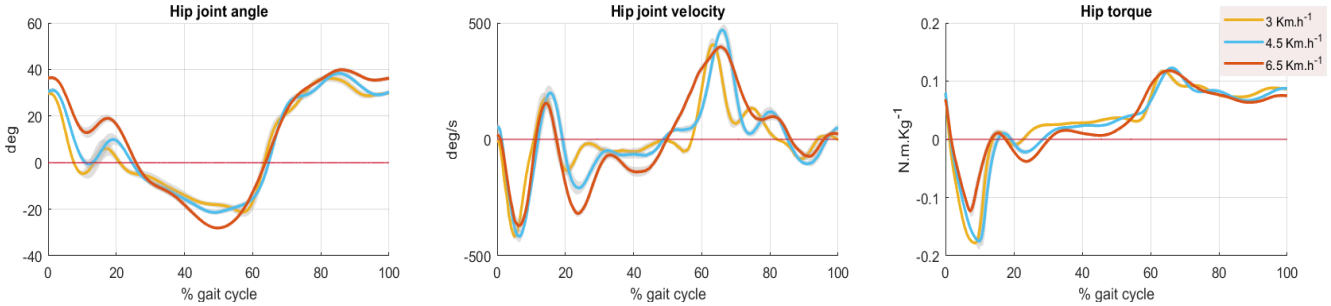

Figure 4.16 – Speed adaptation of the V1

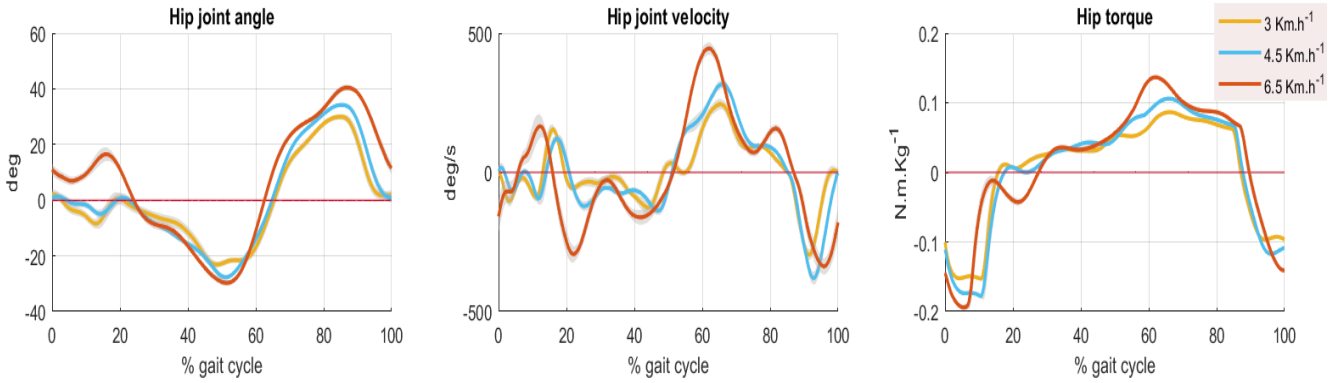

Figure 4.17 – Speed adaptation of the V2

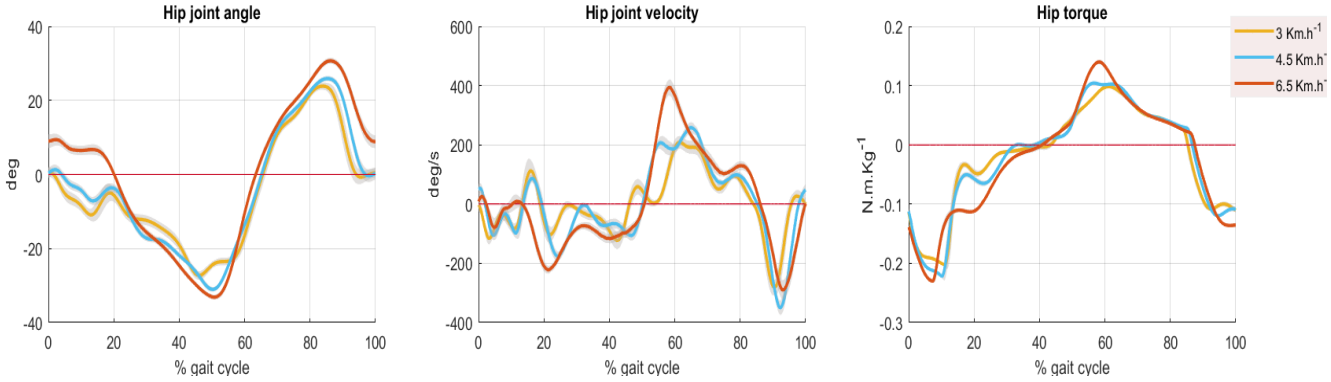

Figure 4.18 – Speed adaptation of the V3

tion and trends against speed variation. The tests includes three speeds belonging to three groups of gait paces. However, the controller was not able to self-adapt the magnitudes to each speed category which requires to add an adaptation factor that was tuned manually depending on the speed category. The adaptation of the magnitudes to the weight of the subject was giving the right magnitudes for a natural walking pace, then the speed factor was linearly computed around 1 for the natural pace assistance, less then 1 for the slow paces and more then 1 for the high speeds, with a value of 90% for the lowest considered speed (3 $km.h^{-1}$) and 110% for the highest considered speed (6.5 $km.h^{-1}$). Even if the trend adaptation was satisfying

in terms of time shifting and flexion augmentation, we believe that the necessity of manually adapting the assistance to the speed is a limitation of this implementation and could be improved more in the future. The way to achieve this objective would be to propose a auto-tuning of the stimulation gain depending on the walking speed.

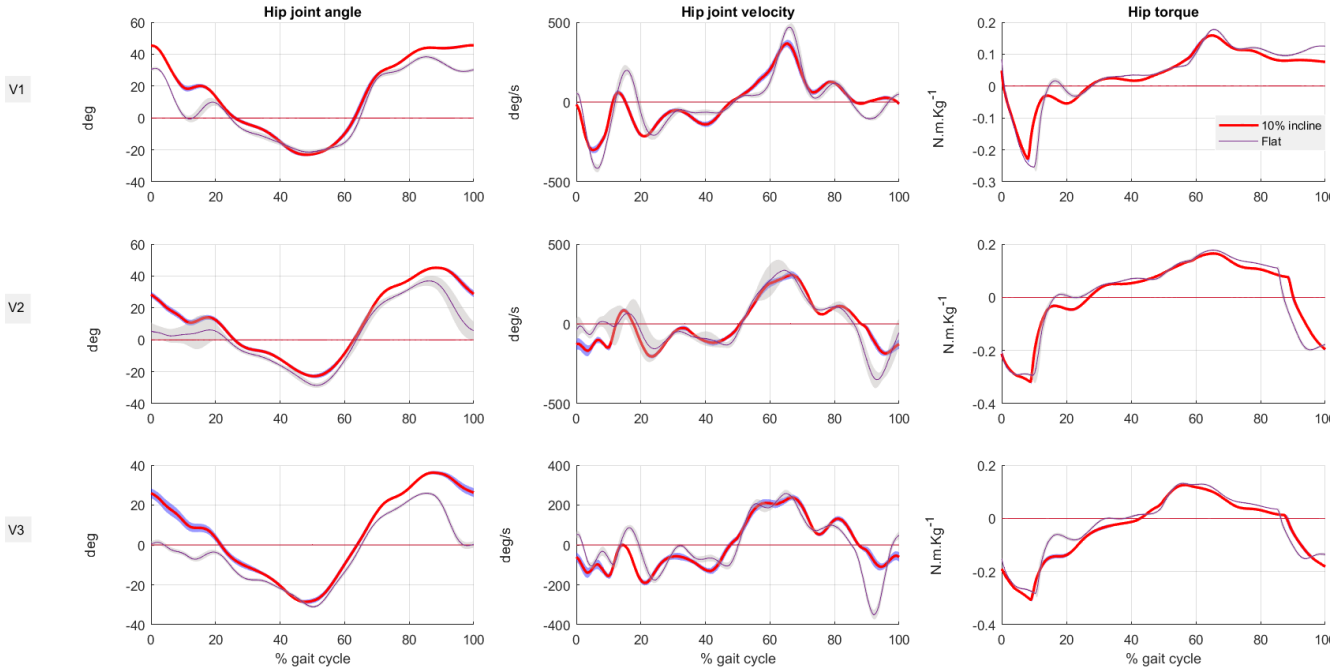

Figure 4.19 – Controllers slope adaptation

4.3.4.3 Slope adaptation

Analysis The performances in slope adaptation off all the controllers are presented in figure 4.19. It appears to match the expectation of the biological recorded profiles. As the ranges of motion are higher then in the flat walking, this induces two effects exposed in the literature; A slight left shift of the peak times and higher torque magnitudes that leads to longer extension and flexion assistance (augmented surface under the curve) [81]. The same behavior is observed in both the V2 and V3 with a better adaptation observed for V3. Note that there was no need to adapt the assistance gains to meet theses behavior which demonstrated the robustness and adaptability of the model to slopes variations.

4.4 Results Discussion and Contributions

Among the three controllers, the V3 is the one achieving the closest behavior to both the biological torque profile and the optimal characteristic times.

In general the V2 and V3 induced a decrement of the flexion range of motion but led to higher extension range for the V3 because of higher extension assistance then the V2. This effect is common between the controllers reviewed in the literature that achieved good metabolic cost reduction, however we do not advance a direct correlation between CoT reduction and such kinematics variation trend.

As exposed in the results section, the controllers demonstrated robustness in terms of trend and synchronization to both speed and incline variation with a preference for V3. For the speed, it has been tested successfully at the three categories of walking paces (slow- 0.8 $m.s^{-1}$, natural- 1.25$m.s^{-1}$, fast- 1.80$m.s^{-1}$). As the trend was self adapting, the torque magnitudes were hand-scaled by using a speed factor. This is a limitation of the model that could be further being investigated and improved. A proposition would be an auto-tuning gain of the stimulation that would depend on the linear speed. For the slope adaptation, the controller succeeded to a range of slopes going from 0 to 15% and demonstrated a satisfying self-adaptation without the need to add slope factors or re-tune parameters. The former results were obtained by testing the controller in steady and unsteady walking conditions, where it demonstrated robustness and adaptability in both. The controller also showed adaptability to varying subject's morphology and range of motion.

Compared to the existing control strategies found in the literature, the developed controller (in its three versions) adds a set of novelties. In terms of gait synchronization, despite the spread of FSM we developed 3 FSMs with three , four and five states, each one coming with propositions of gait events detection. The 5-FSM surpasses the highest number of finite states found in the literature given by four under leg coupling constraints. Unlike the available FSMs, we come with independent FSMs for each leg which decouples the states of the legs and adds more adaptability to gait phase mapping.

Speaking of the control layer, the neuromuscular model is the only known controller relying on the skeletal muscles and neural system state estimation and positive state feedback in achieving online assistive torque commands. Our developed versions are the first upgrade of the traditional 2-states neuromuscular model of Geyer and Herr. Unlike off-line computation techniques, the advantage of this online controller is that it adapts to each subject's gait kinematic profiles and gait characteristics since its computation relies on real time kinematic information. Because of this,

the controller showed robustness and adaptability to varying steady and unsteady walking conditions for speeds and inclines without the need to parameters re-tuning except the speed factor between walking paces. Even if the virtual skeletal muscles were tuned based on a body of 75 kg and 1.80 m tall, it extrapolated well to various morphology by simply adding a weight factor. These morphology and condition adaptation are key strengths of the model compared to the majority of controllers which dedicate to restricted walkers and walking conditions such as the previously cited Human In the Loops Optimisations (HILO) that needs to be tuned to each subject at each speed and at each incline. The controller also brings interesting features such as the reverse walking and the outdoor walking assistance (outside treadmill).

In terms of practical contributions, this project achieved the very first known implementation of a controller in the category of neuromuscular controllers on a partial gait assistance orthosis targeting healthy subjects. It overcame the challenges related to partial assistance resulting from the close interaction with the human as he is an active agent in the control loop. A more detailed comparison and contributions overview can be found in the appendix A.4.

Even if some performance estimation metrics have been computed to intuit the potential effect on the metabolic cost reduction such as the produced work, the consolidation of these findings with further experiments using respirometer for energy expenditure estimation would have been a great input. However this has not been possible because of device unavailability and time and hardware constraints and is left as an open question to future investigations.

In regards with these findings, the implementation of the three version was successful by producing practical results that met the theoretical expectations. The V3 showed excellent results in terms of trend that were correlating the biological ones and in terms of timing that met the ones obtained by optimisation and extrapolation. With this version, we were able to achieve same results as the ones obtained from offline interpolation and optimisation while having an online computation algorithm that adapts to each subject's gait and remains robust to sudden variations in conditions. The obtained results also opens the perspective to a myriad of scientific questions and further model improvement to be carried on later.

4.5 Global Outcomes

On the personal level, this internship has enabled me to build and develop a brand set of skills that have been grouped into 3 major axes (Table 4.3).

The project management of the internship is depicted in the appendix **??** via a

Axes	**Theory**	**Software**	**Methodology**
Skills	Non-linear dynamic systems modeling, state estimation, state feedback controller, bio-inspired controller, biophysics of the neuromuscular system, physiology of the gait, control of wearable devices, sensor data processing, statistic data testing and analysis	Advanced embedded C^{++}, Linux, MATLAB scripting and Simulink, multithreading, real time programming, communication protocols (NTP, CAN, SPI)	Research project conducting, efficient software development, scientific experimentation and protocols, Scrum managing method

Table 4.3 – Skills outcome

Gantt chart.

For the REHAssist group, my work adds a third controller on the list of the E-Walk assistive strategies, the first one using FSM and the first one relying on an online neuromuscular model. It is also the first implementation of such controller in a partial assistance device ever in the literature. The work proposed novelties on the two mid-level control layers, it also contributed to better understand muscles' compliance, reflexes during gait and the challenges of gait assistance. It paved this way a bridge between biophysics and assistive robotics.

Chapter 5

Recommendations for Future Work

5.1 Improving the Hill Type Model

The force-length relationship in Hill type model is a Gaussian centered at the optimal length. This representation takes into account only the active working region of the muscle and could be sufficient for normal motor task, when the later does not lay in a hyper-extension configuration. When this scenario occurs, the muscle enters a reactive working region where its impedance changes to become stiffer thus exerting a higher force to counter balance the hyper-contraction of the antagonist muscle, in a stretch reflex pattern. If representing the $f_l(l_{ce})$ with only a Gaussian, the hyper-extension of the muscle will shift the length of the contractile element away from the optimal length thus leading to a null force which is the inverse outcome of the desired biological behavior.

A proposition would be to improve the force-length relationship so as to consider the reactive behavior of the muscle at the hyper-extension. A way could be to determine a length threshold of hyper-extension and to shift to an exponential curve starting from it rather then keeping on the Gaussian, this will add at least 3 parameters to the model (the length threshold, the exponential time constant and a factor for the continuity between the two curves. Another alternative is to make curve fitting using interpolation or approximation based on literature and simulated values of the force-length relation. As this method is numerical it removes the biological interpretation of parameters and might be less robust yet simpler.

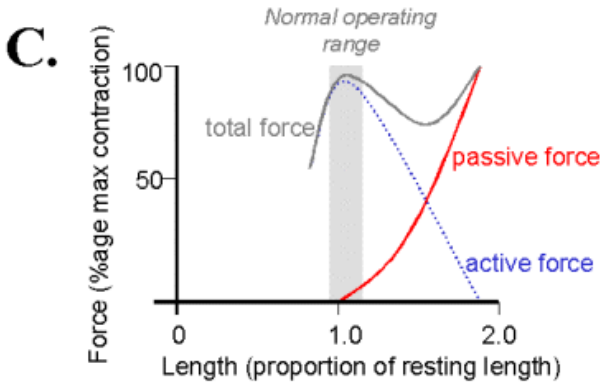

Figure 5.1 – Real force-length relationship [82]

5.2 Dynamic Approach for LP Detection

As presented earlier, in the scope of this thesis we proposed a method for detecting the landing preparation phase (LP) based on the detection of the zero crossing of the joint angular velocity. As the speed remains jittery, we set a constant negative threshold speed value but close to zero so as not to detect prematurely the transition.

Based on the observations from the experiments, depending on the speed, the subjective impression of the wearer sometimes placed the transition to occur at the

right moment for medium walking speeds, a little bit late for fast speeds and a little bit early for the slow speeds. This findings is quite logic and led to the conclusion that the threshold should be a function of the linear speed of the walker. From here we open the window to a new improvement possibility that is to replace the constant detection threshold by a threshold function that varies according to the speed. The value of the threshold must increase with respect to angular speed. A simple suggestion would be a none normalised saturation function whose parameters are only the ranges and the slope.

5.3 Auto-tuning of the Assistance Rate and Gains

The advantage of this model implementation is that the state variables and torque profiles estimation are cross-subjects and there is no parameter re-tuning except the weight and the speed factor adaptation. The magnitudes are estimated based on the normalised per weight torque magnitude multiplied with the weight of the wearer.

Another direction worth exploring is to study the contribution of other parameters such as the person's height, leg weight, lower limbs size and other morphological factors that influence the leg dynamic. It is also relevant to explore non-measurable data such as the user's experience with wearable robotic devices as studies show that it influences the amount of torque the user is ready to intake and thus its feeling of comfort with the assistance. Another key factor is also the physical condition. Indeed, while conducting testing of the assistance with sportive subjects, their feeling of exert did not vary for the proposed conditions they also reported that they tended to prefer the condition without exoskeleton. The usefulness of the assistance for this category of users during the Activities of Daily Living (ADLs) is questionable given their excellent physical condition. For this category, the effectiveness of the assistance should rather be experimented during extreme activities where a higher effort is required from them. This also pushes to reflect upon the experimental protocol regarding subjects selectivity and conditions.

5.4 Orthosis Improvement

E-Walk V1 does not provide an optimal fitting and user experience for two reasons; First, The fitting is not ideal, the waist attachment does not fit perfectly the trunk leaving a space between the back and the attachment, this space induces lost of transmitted power to the lower limb for the profit of torsion applied on the trunk

causing discomfort, hindering oscillations and of course lost in the assistance efficiency. Second, it is heavier compared to other devices in the same category, for instance Samsung GEMS hip orthosis [56] weights 2.4 Kg for a maximum assistance magnitude of 15 $N.m$ that is nearly the same provided by E-Walk. The exosuits having deported actuators such as the emulator of Collins et al. [4] and the one of Walsh et al. [3] with its 625 g have demonstrated incredible CoT reduction up to 24% for the hip, the control strategy is also praised but can not be decorrelated from the contribution of the device mechanics. Note that for portable devices the maximum CoT reduction achieved up to date does not exceed 14% on average on treadmill contributed by Samsung [56]. This explains by the fact that exosuits and emulators add nearly zero hindering which is not the case for portable devices where the weight of the actuators and the structure add inertia on the wearer. For E-Walk the hindering added only by the device is estimated to 13% in average. The review of the mechanical structure is now being performed as a version 2 is being designed at the REHAssist and should lead to a net improvement of the assistance.

5.5 Toward a Continuous Controller

The good understanding of the muscle compliant behavior as well as the functioning of the neural reflexes have led to the conviction that there is a possibility to establish a continuous estimator independent of FSM and thus that does not require the use of the FSR sensors at the foot insoles. When observing the profiles kinematic and the kinetic profiles of the hip during the gait and comparing it to the ones of a mass-spring system, there are irrevocable similarities in the shapes, the discrepancies occurs on the phase shifts as presented earlier, the ones of the neuromuscular gait system has a variable phase shift, providing an estimation of the phase, an online computation of torque is possible using the same model at the co-contraction of the two antagonist muscles. Preliminary tests have been performed and suffered from a weakness of phase shift estimation but gave promising results. This opens the door to a new thrilling research quest, that will lead to the design of a continuous controller independent from FSMs and thus suppressing the FSR sensors. As presented, the neuromuscular system has three state variables, the estimation of the phase shift will compensate the third state variable that is the reflex, relying only on one state that is the co-contraction of the two muscles.

5.6 Improving the Software Implementation

The scalability could has been improved if more time was given. A proposition is to replace the parameters tuning in the controller class by an import of the parameters from a text file combined to a configuration file, this could also be performed for the choice of the state machines (FSMs) and the neural reflexes for the controller. There are several propositions for the normalised text file, a way could be to use YAML or JSON files which provide parser and could be integrated easily to the implemented C^{++} code.

Final Conclusion

The initial objective fixed at the start of this internship was the investigation of a neuromuscular controller and the inspection of its potential implementation on the e-Walk hip assistive orthosis. The outcome of this internship did not only achieve the former objective but enabled to go even further to assess sharper scientific questions and propose improvement to the initial model resulting in a total of three implemented versions of the new neuromuscular controller. The theoretical work proposed in a first step an improvement of the Hill type model for skeletal muscles and derived a lightweight computational approach that made its implementation possible on the available hardware. To model the gait cycle system, the choice was set on one pair of antagonist mono-articular muscles; The Iliopsoas as a hip flexor and the Gluteus Maximus as a hip extensor. In a second step, a new set of reflexes control based on positive state feedback has been proposed for controlling the modeled virtual muscles. The third contribution concerns the gait synchronisation layer, where three finite state machines of increasing order from three to five have been proposed for gait decomposition. The combination of the skeletal muscles modeling, the synchronising FSM as well as the positive neural reflexes enabled the capture of the physiology and dynamics of the gait cycle in a fair manner. The computed torque from the virtual muscles presented a trend similar to the biological profiles found in the literature and met the optimal assistance timing obtained from Human in The Loop Optimization studies.

This work add valuable contributions to the literature. It is the first real upgrade of the 2-states neuromuscular controller of Geyer and Herr coming with an appealing concept of high modularity in the behavioral control that was drawn from justified simplifications conjugated to modular state machine decomposition of the gait. The obtained results of profiles are close to the ones obtained from offline torque computation with a real time online model. The present work is also the first implementation of a neuromuscular controller on a partial assistance hip orthosis ever. The outcomes also open the perspective to a myriad of scientific questions and further model improvement to be carried on later.

Bibliography

[1] J. R. Montgomery and A. M. Grabowski, « The contributions of ankle, knee and hip joint work to individual leg work change during uphill and downhill walking over a range of speeds », *R Soc Open Sci*, vol. 5, no. 8, p. 180 550, Aug. 2018, ISSN: 2054-5703. DOI: 10.1098/rsos.180550. [Online]. Available: https://www.ncbi.nlm.nih.gov/pmc/articles/PMC6124028/.

[2] K. Seo, J. Lee, and Y. J. Park, « Autonomous hip exoskeleton saves metabolic cost of walking uphill », in *2017 International Conference on Rehabilitation Robotics (ICORR)*, 2017, pp. 246–251. DOI: 10.1109/ICORR.2017.8009254.

[3] Y. Ding, F. A. Panizzolo, C. Siviy, *et al.*, « Effect of timing of hip extension assistance during loaded walking with a soft exosuit », en, *J NeuroEngineering Rehabil*, vol. 13, no. 1, p. 87, Dec. 2016, ISSN: 1743-0003. DOI: 10.1186/s12984-016-0196-8. [Online]. Available: http://jneuroengrehab.biomedcentral.com/articles/10.1186/s12984-016-0196-8.

[4] J. Zhang, P. Fiers, K. A. Witte, *et al.*, « Human-in-the-loop optimization of exoskeleton assistance during walking », *Science*, vol. 356, no. 6344, pp. 1280–1284, Jun. 2017, Publisher: American Association for the Advancement of Science. DOI: 10.1126/science.aal5054. [Online]. Available: https://www.science.org/doi/10.1126/science.aal5054.

[5] C. F. Ong, T. Geijtenbeek, J. L. Hicks, and S. L. Delp, « Predicting gait adaptations due to ankle plantarflexor muscle weakness and contracture using physics-based musculoskeletal simulations », en, *PLoS Comput Biol*, vol. 15, no. 10, M. Srinivasan, Ed., e1006993, Oct. 2019, ISSN: 1553-7358. DOI: 10.1371/journal.pcbi.1006993. [Online]. Available: https://dx.plos.org/10.1371/journal.pcbi.1006993.

[6] G. M. Bryan, P. W. Franks, S. C. Klein, R. J. Peuchen, and S. H. Collins, « A hip–knee–ankle exoskeleton emulator for studying gait assistance », *The International Journal of Robotics Research*, vol. 40, no. 4-5, pp. 722–746, 2021. DOI: 10.

1177/0278364920961452. eprint: https://doi.org/10.1177/0278364920961452. [Online]. Available: https://doi.org/10.1177/0278364920961452.

[7] H. Geyer and H. Herr, « A Muscle-Reflex Model That Encodes Principles of Legged Mechanics Produces Human Walking Dynamics and Muscle Activities », *IEEE Transactions on Neural Systems and Rehabilitation Engineering*, vol. 18, no. 3, pp. 263–273, Jun. 2010, Conference Name: IEEE Transactions on Neural Systems and Rehabilitation Engineering, ISSN: 1558-0210. DOI: 10.1109/TNSRE.2010.2047592.

[8] Y. Z. Arslan, D. Karabulut, F. Ortes, and M. B. Popovic, « Neuromuscular control models of human locomotion », en, in *Humanoid Robotics*, P. V. Ambarish Goswami, Ed., Academic Press, 2019, pp. 980–1005, ISBN: 978-94-007-6047-9. DOI: https://doi.org/10.1007/978-94-007-6046-2.

[9] G. A. Lichtwark and C. J. Barclay, « The influence of tendon compliance on muscle power output and efficiency during cyclic contractions », *Journal of Experimental Biology*, vol. 213, no. 5, pp. 707–714, Mar. 2010, ISSN: 0022-0949. DOI: 10.1242/jeb.038026. eprint: https://journals.biologists.com/jeb/article-pdf/213/5/707/1434215/707.pdf. [Online]. Available: https://doi.org/10.1242/jeb.038026.

[10] T. A. McMahon, *Muscles, Reflexes, and Locomotion*. Princeton University Press, 1984, ISBN: 9780691083223. [Online]. Available: http://www.jstor.org/stable/j.ctv173f1sp.

[11] Y. Ugawa, « Voluntary and involuntary movements: A proposal from a clinician », *Neuroscience Research*, vol. 156, pp. 80–87, 2020, ISSN: 0168-0102. DOI: https://doi.org/10.1016/j.neures.2019.10.001. [Online]. Available: https://www.sciencedirect.com/science/article/pii/S0168010219304341.

[12] D. L. Smith and S. A. Plowman, « Chapter 2 - Understanding Muscle Contraction**Based on Plowman SA, Smith DL: Exercise physiology for health, fitness, and performance, ed 2, San Francisco, 2003, Benjamin Cummings. », in *Sports-Specific Rehabilitation*, R. Donatelli, Ed., Saint Louis: Churchill Livingstone, 2007, pp. 15–38, ISBN: 978-0-443-06642-9. DOI: https://doi.org/10.1016/B978-044306642-9.50005-8. [Online]. Available: https://www.sciencedirect.com/science/article/pii/B9780443066429500058.

[13] Physiopedia. « Muscle ». (), [Online]. Available: https://www.physio-pedia.com/Muscle#:~:text=Muscles%20in%20Humans-,Skeletal,Sarcomere%2C%20found%20within%20the%20Myofibrils..

[14] Ekeberg, « A combined neuronal and mechanical model of fish swimming », en, *Biol. Cybern.*, vol. 69, no. 5, pp. 363–374, Oct. 1993, ISSN: 1432-0770. DOI: 10.1007/BF00199436. [Online]. Available: https://doi.org/10.1007/BF00199436.

[15] A. J. Ijspeert, « A connectionist central pattern generator for the aquatic and terrestrial gaits of a simulated salamander », *Biological cybernetics*, vol. 84, no. 5, pp. 331–348, 2001.

[16] J. F. Veneman, R. Kruidhof, E. E. G. Hekman, R. Ekkelenkamp, E. H. F. Van Asseldonk, and H. van der Kooij, « Design and evaluation of the lopes exoskeleton robot for interactive gait rehabilitation », *IEEE Transactions on Neural Systems and Rehabilitation Engineering*, vol. 15, no. 3, pp. 379–386, 2007. DOI: 10.1109/TNSRE.2007.903919.

[17] D. Winter, *The Biomechanics and Motor Control of Human Gait: Normal, Elderly and Pathological*. University of Waterloo Press, 1991, ISBN: 978-0-88898-105-9. [Online]. Available: https://books.google.ch/books?id=q_EHAQAAMAAJ.

[18] L. M. Biga, S. Dawson, A. Harwell, *et al.*, « 9.5 Types of Body Movements », en, Sep. 2019, Book Title: Anatomy & Physiology Publisher: OpenStax/Oregon State University. [Online]. Available: https://open.oregonstate.education/aandp/chapter/9-5-types-of-body-movements/.

[19] C. L. Brockett and G. J. Chapman, « Biomechanics of the ankle », *Orthopaedics and trauma*, vol. 30, no. 3, pp. 232–238, 2016.

[20] J. Richards, A. Chohan, and R. Erande, « Chapter 15 - Biomechanics », in *Tidy's Physiotherapy (Fifteenth Edition)*, S. B. Porter, Ed., Fifteenth Edition, Churchill Livingstone, 2013, pp. 331–368, ISBN: 978-0-7020-4344-4. DOI: https://doi.org/10.1016/B978-0-7020-4344-4.00015-8. [Online]. Available: https://www.sciencedirect.com/science/article/pii/B9780702043444000158.

[21] *The Gait Cycle*, en. [Online]. Available: https://www.physio-pedia.com/The_Gait_Cycle.

[22] *Hip Anatomy*, en. [Online]. Available: https://www.physio-pedia.com/Hip_Anatomy.

[23] J. L. Pons, Ed., *Wearable robots: Biomechatronic exoskeletons*. Chichester: John Wiley & Sons, 2008, ISBN: 978-0-470-51294-4 (HB).

[24] J. Pons, R. Ceres, and L. Calderón, « Introduction to wearable robotics », in Mar. 2008, pp. 1 –16, ISBN: 9780470987667. DOI: 10.1002/9780470987667.ch1.

[25] A. M. Dollar and H. Herr, « Lower Extremity Exoskeletons and Active Orthoses: Challenges and State-of-the-Art », en, *IEEE Trans. Robot.*, vol. 24, no. 1, pp. 144–158, Feb. 2008, ISSN: 1552-3098. DOI: 10.1109/TRO.2008.915453. [Online]. Available: http://ieeexplore.ieee.org/document/4456745/.

[26] H. Kazerooni and R. Steger, « The Berkeley Lower Extremity Exoskeleton », *Journal of Dynamic Systems, Measurement, and Control*, vol. 128, no. 1, pp. 14–25, Sep. 2005, ISSN: 0022-0434. DOI: 10.1115/1.2168164. eprint: https://asmedigitalcollection.asme.org/dynamicsystems/article-pdf/128/1/14/5490077/14_1.pdf. [Online]. Available: https://doi.org/10.1115/1.2168164.

[27] E. Guizzo and H. Goldstein, « The rise of the body bots [robotic exoskeletons] », *IEEE Spectrum*, vol. 42, no. 10, pp. 50–56, 2005. DOI: 10.1109/MSPEC.2005.1515961.

[28] K. Yamamoto, K. Hyodo, M. Ishii, and T. Matsuo, « Development of power assisting suit for assisting nurse labor », *JSME International Journal Series C Mechanical Systems, Machine Elements and Manufacturing*, vol. 45, no. 3, pp. 703–711, 2002.

[29] G. Bionic. « Cray x power suit ». (), [Online]. Available: https://www.germanbionic.com/en/.

[30] M. Vukobratovic, D. Hristic, and Z. Stojiljkovic, « Development of active anthropomorphic exoskeletons », *Medical and biological engineering*, vol. 12, no. 1, pp. 66–80, Jan. 1974, ISSN: 1741-0444. DOI: 10.1007/BF02629836. [Online]. Available: https://doi.org/10.1007/BF02629836.

[31] K. N. Winfree, P. Stegall, and S. K. Agrawal, « Design of a minimally constraining, passively supported gait training exoskeleton: alex ii », in *2011 IEEE International Conference on Rehabilitation Robotics*, 2011, pp. 1–6. DOI: 10.1109/ICORR.2011.5975499.

[32] C. Meijneke, G. van Oort, V. Sluiter, *et al.*, « Symbitron exoskeleton: design, control, and evaluation of a modular exoskeleton for incomplete and complete spinal cord injured individuals », *IEEE Transactions on Neural Systems and Rehabilitation Engineering*, vol. 29, pp. 330–339, 2021. DOI: 10.1109/TNSRE.2021.3049960.

[33] D. Sanz-Merodio, M. Cestari, J. C. Arevalo, X. Carrillo, and E. Garcia, « Development of a Lower-Limb Active Orthosis and a Walker for Gait Assistance », en, in *ROBOT2013: First Iberian Robotics Conference: Advances in Robotics, Vol. 1*,

ser. Advances in Intelligent Systems and Computing, M. A. Armada, A. Sanfeliu, and M. Ferre, Eds., Cham: Springer International Publishing, 2014, pp. 219–233, ISBN: 978-3-319-03413-3. DOI: 10.1007/978-3-319-03413-3_16. [Online]. Available: https://doi.org/10.1007/978-3-319-03413-3_16.

[34] A. J. Young and D. P. Ferris, « State of the art and future directions for lower limb robotic exoskeletons », *IEEE Transactions on Neural Systems and Rehabilitation Engineering*, vol. 25, no. 2, pp. 171–182, 2017. DOI: 10.1109/TNSRE.2016.2521160.

[35] A. P. M. S. Alberto Esquenazi 1 Mukul Talaty, « The rewalk powered exoskeleton to restore ambulatory function to individuals with thoracic-level motor-complete spinal cord injury », *American journal of physical medicine rehabilitation*, vol. 91, no. 11, pp. 911–921, 2005. DOI: 10.1097/PHM.0b013e318269d9a3.

[36] N. Karavas, A. Ajoudani, N. Tsagarakis, J. Saglia, A. Bicchi, and D. Caldwell, « Tele-impedance based stiffness and motion augmentation for a knee exoskeleton device », in *2013 IEEE International Conference on Robotics and Automation*, 2013, pp. 2194–2200. DOI: 10.1109/ICRA.2013.6630872.

[37] R. Baud, A. R. Manzoori, A. Ijspeert, and M. Bouri, « Review of control strategies for lower-limb exoskeletons to assist gait », *Journal of NeuroEngineering and Rehabilitation*, vol. 18, no. 1, p. 119, Jul. 2021, ISSN: 1743-0003. DOI: 10.1186/s12984-021-00906-3. [Online]. Available: https://doi.org/10.1186/s12984-021-00906-3.

[38] B. T. Quinlivan, S. Lee, P. Malcolm, *et al.*, « Assistance magnitude versus metabolic cost reductions for a tethered multiarticular soft exosuit », *Science Robotics*, vol. 2, no. 2, eaah4416, 2017. DOI: 10.1126/scirobotics.aah4416. eprint: https://www.science.org/doi/pdf/10.1126/scirobotics.aah4416. [Online]. Available: https://www.science.org/doi/abs/10.1126/scirobotics.aah4416.

[39] Y. He, D. Eguren, J. M. Azorín, R. G. Grossman, T. P. Luu, and J. L. Contreras-Vidal, « Brain–machine interfaces for controlling lower-limb powered robotic systems », *Journal of Neural Engineering*, vol. 15, no. 2, p. 021 004, 2018. DOI: 10.1088/1741-2552/aaa8c0. [Online]. Available: https://doi.org/10.1088/1741-2552/aaa8c0.

[40] T. Yan, A. Parri, M. Fantozzi, *et al.*, « A novel adaptive oscillators-based control for a powered multi-joint lower-limb orthosis », in *2015 IEEE International Conference on Rehabilitation Robotics (ICORR)*, ISSN: 1945-7901, Aug. 2015, pp. 386–391. DOI: 10.1109/ICORR.2015.7281230.

[41] T. Vouga, R. Baud, J. Fasola, M. Bouri, and H. Bleuler, « Twiice — a lightweight lower-limb exoskeleton for complete paraplegics », in *2017 International Conference on Rehabilitation Robotics (ICORR)*, 2017, pp. 1639–1645. DOI: 10.1109/ICORR.2017.8009483.

[42] P. Beyl, M. Van Damme, P. Cherelle, and D. Lefeber, « Safe and compliant guidance in robot-assisted gait rehabilitation using proxy-based sliding mode control », in *2009 IEEE International Conference on Rehabilitation Robotics*, 2009, pp. 277–282. DOI: 10.1109/ICORR.2009.5209505.

[43] C. L. Lewis and D. P. Ferris, « Invariant hip moment pattern while walking with a robotic hip exoskeleton », *Journal of Biomechanics*, vol. 44, no. 5, pp. 789–793, 2011, ISSN: 0021-9290. DOI: https://doi.org/10.1016/j.jbiomech.2011.01.030. [Online]. Available: https://www.sciencedirect.com/science/article/pii/S0021929011000728.

[44] R. Ronsse, T. Lenzi, N. Vitiello, *et al.*, « Oscillator-based assistance of cyclical movements: model-based and model-free approaches », en, *Med Biol Eng Comput*, vol. 49, no. 10, p. 1173, Sep. 2011, ISSN: 1741-0444. DOI: 10.1007/s11517-011-0816-1. [Online]. Available: https://doi.org/10.1007/s11517-011-0816-1.

[45] S. Sridar, Z. Qiao, A. Rascon, *et al.*, « Evaluating immediate benefits of assisting knee extension with a soft inflatable exosuit », *IEEE Transactions on Medical Robotics and Bionics*, vol. 2, no. 2, pp. 216–225, 2020. DOI: 10.1109/TMRB.2020.2988305.

[46] F. Dzeladini, A. R. Wu, D. Renjewski, *et al.*, « Effects of a neuromuscular controller on a powered ankle exoskeleton during human walking », in *2016 6th IEEE International Conference on Biomedical Robotics and Biomechatronics (BioRob)*, ISSN: 2155-1782, Jun. 2016, pp. 617–622. DOI: 10.1109/BIOROB.2016.7523694.

[47] B. Lim, J. Lee, J. Jang, *et al.*, « Delayed Output Feedback Control for Gait Assistance With a Robotic Hip Exoskeleton », *Trans. Rob.*, vol. 35, no. 4, pp. 1055–1062, Aug. 2019, ISSN: 1552-3098. DOI: 10.1109/TRO.2019.2913318. [Online]. Available: https://doi.org/10.1109/TRO.2019.2913318.

[48] R. Kobetic, C. S. To, J. R. Schnellenberger, *et al.*, « Development of hybrid orthosis for standing, walking, and stair climbing after spinal cord injury », eng, *J Rehabil Res Dev*, vol. 46, no. 3, pp. 447–462, 2009, ISSN: 1938-1352.

[49] A. Martínez, C. Durrough, and M. Goldfarb, « A single-joint implementation of flow control: knee joint walking assistance for individuals with mobility impairment », *IEEE Transactions on Neural Systems and Rehabilitation Engineering*, vol. 28, no. 4, pp. 934–942, 2020. DOI: 10.1109/TNSRE.2020.2977339.

[50] J. Kim, S.-J. Kim, and J. Choi, « Real-time gait phase detection and estimation of gait speed and ground slope for a robotic knee orthosis », in *2015 IEEE International Conference on Rehabilitation Robotics (ICORR)*, 2015, pp. 392–397. DOI: 10.1109/ICORR.2015.7281231.

[51] D. D. Molinaro, I. Kang, J. Camargo, and A. J. Young, « Biological Hip Torque Estimation using a Robotic Hip Exoskeleton », en, in *2020 8th IEEE RAS/EMBS International Conference for Biomedical Robotics and Biomechatronics (BioRob)*, New York City, NY, USA: IEEE, Nov. 2020, pp. 791–796, ISBN: 978-1-72815-907-2. DOI: 10.1109/BioRob49111.2020.9224334. [Online]. Available: https://ieeexplore.ieee.org/document/9224334/.

[52] S. Kyeong, W. Shin, M. Yang, U. Heo, J.-r. Feng, and J. Kim, « Recognition of walking environments and gait period by surface electromyography », *Frontiers of Information Technology & Electronic Engineering*, vol. 20, no. 3, pp. 342–352, Mar. 2019, ISSN: 2095-9230. DOI: 10.1631/FITEE.1800601. [Online]. Available: https://doi.org/10.1631/FITEE.1800601.

[53] O. Unluhisarcikli, M. Pietrusinski, B. Weinberg, P. Bonato, and C. Mavroidis, « Design and control of a robotic lower extremity exoskeleton for gait rehabilitation », in *2011 IEEE/RSJ International Conference on Intelligent Robots and Systems*, 2011, pp. 4893–4898. DOI: 10.1109/IROS.2011.6094973.

[54] M. R. Tucker, J. Olivier, A. Pagel, *et al.*, « Control strategies for active lower extremity prosthetics and orthotics: a review », en, *J NeuroEngineering Rehabil*, vol. 12, no. 1, p. 1, 2015, ISSN: 1743-0003. DOI: 10.1186/1743-0003-12-1. [Online]. Available: http://www.jneuroengrehab.com/content/12/1/1.

[55] J. Olivier, A. Ortlieb, M. Bouri, and H. Bleuler, « Influence of an assistive hip orthosis on gait », ser. Advances in Intelligent Systems and Computing, vol. 540, Cham: Springer International Publishing Ag, 2017, pp. 10. 531–540. DOI: 10.1007/978-3-319-49058-8_58. [Online]. Available: http://infoscience.epfl.ch/record/232133.

[56] K. Seo, J. Lee, and Y. J. Park, « Autonomous hip exoskeleton saves metabolic cost of walking uphill », in *2017 International Conference on Rehabilitation Robotics (ICORR)*, ISSN: 1945-7901, Jul. 2017, pp. 246–251. DOI: 10.1109/ICORR.2017.8009254.

[57] J. R. Koller, C. David Remy, and D. P. Ferris, « Comparing neural control and mechanically intrinsic control of powered ankle exoskeletons », in *2017 International Conference on Rehabilitation Robotics (ICORR)*, 2017, pp. 294–299. DOI: 10.1109/ICORR.2017.8009262.

[58] A. R. Wu, F. Dzeladini, T. J. H. Brug, *et al.*, « An Adaptive Neuromuscular Controller for Assistive Lower-Limb Exoskeletons: A Preliminary Study on Subjects with Spinal Cord Injury », *Front Neurorobot*, vol. 11, p. 30, Jun. 2017, ISSN: 1662-5218. DOI: 10.3389/fnbot.2017.00030. [Online]. Available: https://www.ncbi.nlm.nih.gov/pmc/articles/PMC5476695/.

[59] M. F. Eilenberg, H. Geyer, and H. Herr, « Control of a Powered Ankle–Foot Prosthesis Based on a Neuromuscular Model », *IEEE Transactions on Neural Systems and Rehabilitation Engineering*, vol. 18, no. 2, pp. 164–173, Apr. 2010, Conference Name: IEEE Transactions on Neural Systems and Rehabilitation Engineering, ISSN: 1558-0210. DOI: 10.1109/TNSRE.2009.2039620.

[60] J. Markowitz, P. Krishnaswamy, M. F. Eilenberg, K. Endo, C. Barnhart, and H. Herr, « Speed adaptation in a powered transtibial prosthesis controlled with a neuromuscular model », *Philos Trans R Soc Lond B Biol Sci*, vol. 366, no. 1570, pp. 1621–1631, May 2011, ISSN: 0962-8436. DOI: 10.1098/rstb.2010.0347. [Online]. Available: https://www.ncbi.nlm.nih.gov/pmc/articles/PMC3130448/.

[61] H. S. d. Silva, F. Y. Nakamura, M. Papoti, A. S. da Silva, and J. W. Dos-Santos, « Relationship between heart rate, oxygen consumption, and energy expenditure in futsal », *Frontiers in Psychology*, vol. 12, 2021, ISSN: 1664-1078. DOI: 10.3389/fpsyg.2021.698622. [Online]. Available: https://www.frontiersin.org/articles/10.3389/fpsyg.2021.698622.

[62] M. W. Whittle, *Gait analysis: an introduction*. Butterworth-Heinemann, 2014.

[63] K. G. HOLT, J. HAMILL, and R. O. ANDRES, « Predicting the minimal energy costs of human walking », *Medicine & Science in Sports & Exercise*, vol. 23, no. 4, 1991, ISSN: 0195-9131. [Online]. Available: https://journals.lww.com/acsm-msse/Fulltext/1991/04000/Predicting_the_minimal_energy_costs_of_human.16.aspx.

[64] D. Torricelli, J. Gonzalez-Vargas, J. F. Veneman, *et al.*, « Benchmarking bipedal locomotion: a unified scheme for humanoids, wearable robots, and humans », *IEEE Robotics Automation Magazine*, vol. 22, no. 3, pp. 103–115, 2015. DOI: 10.1109/MRA.2015.2448278.

[65] P. R. Cavanagh and P. V. Komi, « Electromechanical delay in human skeletal muscle under concentric and eccentric contractions », *European journal of applied physiology and occupational physiology*, vol. 42, no. 3, pp. 159–163, 1979.

[66] H. Geyer, A. Seyfarth, and R. Blickhan, « Positive force feedback in bouncing gaits? », *Proc Biol Sci*, vol. 270, no. 1529, pp. 2173–2183, Oct. 2003, ISSN: 0962-8452. DOI: 10.1098/rspb.2003.2454. [Online]. Available: https://www.ncbi.nlm.nih.gov/pmc/articles/PMC1691493/ (visited on 12/27/2021).

[67] C. N. Maganaris and J. P. Paul, *In vivo human tendon mechanical properties*, 1999.

[68] T. A. McMahon, *Muscles, Reflexes, and Locomotion*. Princeton University Press, 1984, ISBN: 9780691083223. [Online]. Available: http://www.jstor.org/stable/j.ctv173f1sp.

[69] S. L. Delp, F. C. Anderson, A. S. Arnold, *et al.*, « Opensim: open-source software to create and analyze dynamic simulations of movement », *IEEE Transactions on Biomedical Engineering*, vol. 54, no. 11, pp. 1940–1950, 2007. DOI: 10.1109/TBME.2007.901024.

[70] *Linaro Releases*. [Online]. Available: https://releases.linaro.org/components/toolchain/binaries/latest-7/.

[71] D. L. Mills, *Computer network time synchronization: the network time protocol*. CRC press, 2006.

[72] E. M. Murtagh, J. L. Mair, E. Aguiar, C. Tudor-Locke, and M. H. Murphy, « Outdoor walking speeds of apparently healthy adults: a systematic review and meta-analysis », *Sports Medicine*, vol. 51, no. 1, pp. 125–141, 2021.

[73] *SR 810.301 - Ordinance of 20 September 2013 on Human Research with the Exception of Clinical Trials (Human Research Ordinance, HRO)*. [Online]. Available: https://www.fedlex.admin.ch/eli/cc/2013/642/en.

[74] S. Das Gupta, M. F. Bobbert, and D. A. Kistemaker, « The metabolic cost of walking in healthy young and older adults–a systematic review and meta analysis », *Scientific reports*, vol. 9, no. 1, pp. 1–10, 2019.

[75] G. A. Borg, « Psychophysical bases of perceived exertion. », *Medicine & science in sports & exercise*, 1982.

[76] K. Pearson, « X. on the criterion that a given system of deviations from the probable in the case of a correlated system of variables is such that it can be reasonably supposed to have arisen from random sampling », *The London, Edinburgh, and Dublin Philosophical Magazine and Journal of Science*, vol. 50, no. 302, pp. 157–175, 1900.

[77] M. A. Stephens, « Edf statistics for goodness of fit and some comparisons », *Journal of the American statistical Association*, vol. 69, no. 347, pp. 730–737, 1974.

[78] P. J. Rousseeuw and C. Croux, « Alternatives to the median absolute deviation », *Journal of the American Statistical association*, vol. 88, no. 424, pp. 1273–1283, 1993.

[79] P. W. Franks, G. M. Bryan, R. Reyes, M. P. O'Donovan, K. N. Gregorczyk, and S. H. Collins, « The Effects of Incline Level on Optimized Lower-Limb Exoskeleton Assistance », en, Bioengineering, preprint, Sep. 2021. DOI: 10.1101/2021.09.13.460170. [Online]. Available: http://biorxiv.org/lookup/doi/10.1101/2021.09.13.460170.

[80] M Burnfield, « Gait analysis: normal and pathological function », *Journal of Sports Science and Medicine*, vol. 9, no. 2, p. 353, 2010.

[81] E. Reznick, K. R. Embry, R. Neuman, E. Bolívar-Nieto, N. P. Fey, and R. D. Gregg, « Lower-limb kinematics and kinetics during continuously varying human locomotion », en, *Sci Data*, vol. 8, no. 1, p. 282, Dec. 2021, ISSN: 2052-4463. DOI: 10.1038/s41597-021-01057-9. [Online]. Available: https://www.nature.com/articles/s41597-021-01057-9.

[82] *Lab lt: frog sartorius muscle length-tension curve*, en. [Online]. Available: https://www.brown.edu/Departments/Engineering/Courses/En123/MuscleExp/Length_Tension.htm.

[83] *Bi-articular muscles in running*, en. [Online]. Available: https://www.alexandertechnique-running.com/bi-articular-muscles/#:~:text=Stated\%20otherwise\%2C\%20the\%20gluteus\%20maximus,of\%20the\%20bi\%2Darticular\%20muscles.

[84] J. C. Moreno, J. Masood, U. Schneider, C. Maufroy, and J. L. Pons, Eds., *Wearable Robotics: Challenges and Trends: Proceedings of the 5th International Symposium on Wearable Robotics, WeRob2020, and of WearRAcon Europe 2020, October 13–16, 2020* (Biosystems & Biorobotics), en. Cham: Springer International Publishing, 2022, vol. 27, ISBN: 978-3-030-69546-0 978-3-030-69547-7. DOI: 10.1007/978-3-030-69547-7. [Online]. Available: https://link.springer.com/10.1007/978-3-030-69547-7.

[85] J. Pons, A. F. Ruiz, and E. Racon, « Wearable upper limb robots », in Mar. 2008, pp. 235 –278, ISBN: 9780470987667. DOI: 10.1002/9780470987667.ch1.

[86] J. Pons, J. C. Moreno, and E. Turowska, « Wearable lower limb and full-body robots », in Mar. 2008, pp. 283 –319, ISBN: 9780470987667. DOI: 10.1002/9780470987667.ch1.

[87] D. Chiaradia, M. Xiloyannis, M. Solazzi, L. Masia, and A. Frisoli, « Comparison of a soft exosuit and a rigid exoskeleton in an assistive task », in *Wearable Robotics: Challenges and Trends*, M. C. Carrozza, S. Micera, and J. L. Pons, Eds., Cham: Springer International Publishing, 2019, pp. 415–419, ISBN: 978-3-030-01887-0.

[88] Y. Ding, I. Galiana, C. Siviy, F. A. Panizzolo, and C. Walsh, « IMU-based iterative control for hip extension assistance with a soft exosuit », in *2016 IEEE International Conference on Robotics and Automation (ICRA)*, May 2016, pp. 3501–3508. DOI: 10.1109/ICRA.2016.7487530.

[89] Y. Stauffer, Y. Allemand, M. Bouri, *et al.*, « The walktrainer—a new generation of walking reeducation device combining orthoses and muscle stimulation », *IEEE Transactions on Neural Systems and Rehabilitation Engineering*, vol. 17, no. 1, pp. 38–45, 2009. DOI: 10.1109/TNSRE.2008.2008288.

[90] F. Dzeladini, A. R. Wu, D. Renjewski, *et al.*, « Effects of a neuromuscular controller on a powered ankle exoskeleton during human walking », in *2016 6th IEEE International Conference on Biomedical Robotics and Biomechatronics (BioRob)*, 2016, pp. 617–622. DOI: 10.1109/BIOROB.2016.7523694.

Appendix A

A.1 Articulated Muscles

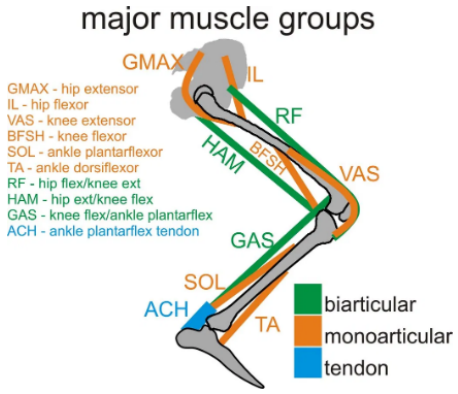

Figure A.1 – Mono-articular and Bi-articular muscles [83]

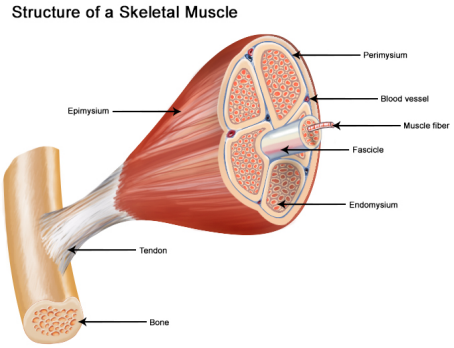

Figure A.2 – Muscles composition [13]

A.2 Gait Cycle Phases

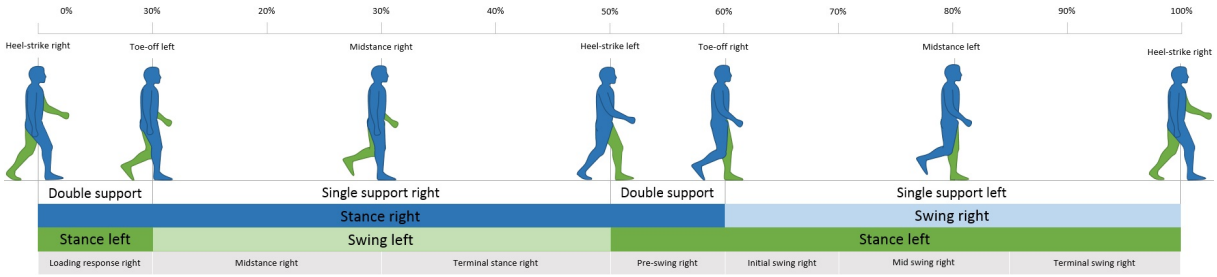

Figure A.3 – Gait cycle phases [21]

A.3 Taxonomy of Wearable Robotic Devices

Classification paradigm and criterion diverge greatly between authors. In the above a summary of the reviewed classes is presented:

— Function: The most recurrent classification criterion found in the literature which also determines the terminology of the device is the level of augmentation. On this basis there are three groups to be enumerated as presented in [84]:

— Exoskeleton: From the Greek exõ meaning external and skeletons. In biology, exoskeleton refers to the outer hardened skeletal envelop that covers the body of some animals, especially insects and crustaceans and that

plays a major role in protecting them against external elements. Analogically, robotic exoskeleton are devices that are mounted in parallel with the human body for the purpose of augmenting its capacities, also known as human enhancement. This implies reaching performance and strength levels that exceed its normal abilities. Such tasks includes, e.g., high load lifting, endurance and ambulatory activities augmentation such as jumping and running.

- — Prosthesis: Robotic prosthesis are active devices meant to replace a damaged or imputed part of the human body. They come generally in series with the limbs and compensate the lost motor function.
- — Orthosis: In the use case of assistance, rehabilitation or full mobilization, the device is called orthosis. Unlike the previous subset, orthosis work collaboratively with the limbs. Full mobilization is specific to subjects with complete and irreversible motor neuron diseases (e.g., paraplegia). Their inherent motion patterns are most often pre-computed offline based on healthy subjects' profiles. Rehabilitation orthosis targets therapeutic training of partially impaired subjects to recover damaged motor activities. Whereas, assistive devices tend to have broader target users ranging from elderly to young and from healthy to people with motor weaknesses in the intent of physical effort reduction at a specific task.

— Motor activity: The classification is sometimes also done according to the addressed motor activity, e.g., gait assistance, lifting enhancement, endurance augmentation, sit-to-stand and stand-to-sit assistance, arm and hand positioning, stairs assent

— Scope: The scope refers to the percent of human body covered by the device. A rough decomposition could be the full body *versus* multiple joint *versus* single joint. Some devices have a narrower breakdown, this is the case for leg orthoses labeled according to the assisted joint(s); Thus different combinations is found, e.g., TH orthosis for thunk-hip, HK for hip-knee, HKA for hip-knee-ankle, HKAF hip-knee-ankle-foot [23].

— Body part: Some authors base their classification on the working region of the device. They are thus coarsely decomposed into upper body and lower body devices. Upper limb orthoses address mainly arm weaknesses and hand positioning [85], while most lower body orthoses address the gait assistance and rehabilitation given the fact that walking is on of the most important activity of daily living (ADL) [86].

— Mechanics: Despite high discrepancies in mechanical designs, they all fall under two rubrics; Soft devices and rigid devices. Soft devices or exo-suits are made of compliant materials (e.g., fabric and elastomers) and resemble greatly wearable clothes. Reversely, rigid structures relies on traditional materials and actuators which makes them stiffer and bulkier. While the former provide great comfort and high fitting to the user they are prone to weaker forces and torques then the later [87].

— Portability: A caution have been made earlier regarding the common confusion between wearable and portable robots. Portability in this context refers to ground detached devices fulfilling power autonomy, lightweight mechatronics and anthropomorphism. Treadmill based orthosis [25] such as the LOPES [16] and ALEX II [31] as well as architectures with deported actuators such as the exoskeleton emulator of Collins et al. [79] [6] and the exo-suit of Walsh et al. [88] are examples of wearable non-portable devices. On the other hand, the Samsung's GEMS gait assistive orthosis is a good example of a portable orthosis. In practice, non portable devices are restricted to therapeutic or experimental environments, they cannot be extended to outdoor environments, they obey to less constraints then the portable ones which brings them to show better performances by having bulkier actuators and more complex but more efficient control paradigms. An example of non-wearable robotic device is the WalkTrainer [89].

A.4 Studies Comparison and Contributions

Ref.	Authors	Classification	Device	Scope	Synch. layer	Model	Control layer	Findings
[7]	Geyer, Herr	Gait Simulation	/	Fixed medium speed $1m/s$ Flat ground	2-states FSM	Hill type model with 3 muscular groups at the hip	Force feedback	Good kinematics and kinetics correlations
[5]	Ong *etal.*	Gait Simulation	/	Slow to fast speeds $0.5-2m/s$ Flat ground	2-states FSM	Geyer's model	Lenght and velocity feedback	Good kinematics and kinetics correlations
[58]	Dzeladini *etal.*	Full mobilization exoskeleton	Lopes 3 joints actuation	Slow and medium speeds $0.6-1.5m/s$ (problems with lower speeds) Flat ground	2-states FSM	Geyer's model	Force feedback	Discrepancies in the torque profile
[90]	Dzeladini *etal.*	Partial ankle assistance orthosis Portable	Achilles orthosis	Slow and medium speeds $0.58-1.08m/s$ Uneven terrains	2-states FSM	Geyer's model And CPG controller	Force feedback	Good kinematics and kinetics correlations
[59]	Eilenberg *etal.*	Full mobilization ankle prosthesis	Ankle prosthesis	Medium speed $1m/s$	2-states FSM	Geyer's model	Force feedback	Good kinematics and kinetics correlations
	Messara *etal.*	Partial hip assistance Portable ADL adapted	e-walk orthosis	Slow to fast $0.8-2.08m/s$ Reverse walking Leading leg switching Uneven terrains	3-states FSM 4-states FSM 5-states FSM	Simplified Hill type with 2 muscles at the hip	Lenght feedback	Good kinematics and kinetics correlations

Table A.1 – Highlight of the major NMC related works in the literature and the present work contributions

A.5 Project Provisional Gantt Chart

Master internship - Neuromuscular controller

Ecole Polytechnique Fédérale de Lausanne - BioRob/REHAssist

Sara Messara

TASK		DURATION	START	END
Phase 1 *Design*	**26%**	**35**	**4/18**	**5/22**
Softaware setup and installation		8	4/18	4/25
Literature review		14	4/18	5/1
Model theorical foundations - 1st controller proposition		24	4/22	5/15
Hands on the Beagle Bone HAL and e-Walk libraries		9	5/7	5/15
Code structuring and UML diagramming		8	5/15	5/22
Phase 2 *Implementation and testing*	**24%**	**32**	**5/15**	**6/15**
Model simulation and muscles behavior investigation on MATLAB		19	5/15	6/1
C++ Implementation and integration of the models		17	5/22	6/7
Implementation of the V1		9	6/7	6/15
Main loop rain time assessment and multithreading strategies		5	6/1	6/5
Phase 3 *Validation*	**61%**	**82**	**5/26**	**8/15**
Code validation		29	5/26	6/23
Intra-lab experiences and protocol		16	6/24	7/24
Analysis and conclusions		22	7/25	8/15
Phase 4 *Project closure*	**43%**	**58**	**6/30**	**8/26**
Report writing		46	6/30	8/14
Gantt Chart design		1	8/10	8/10
Final presentation preparation		7	8/15	8/21

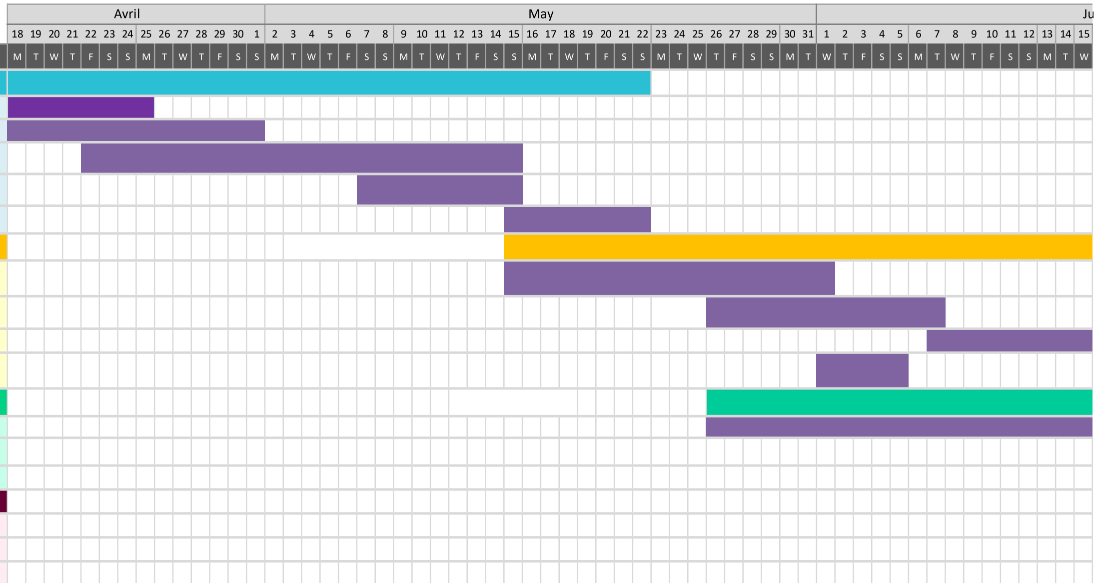

Sara Messara - Master Internship - e-Walk Neuromuscular Controller -

Table A.2 – Provisional Gantt chart - first part

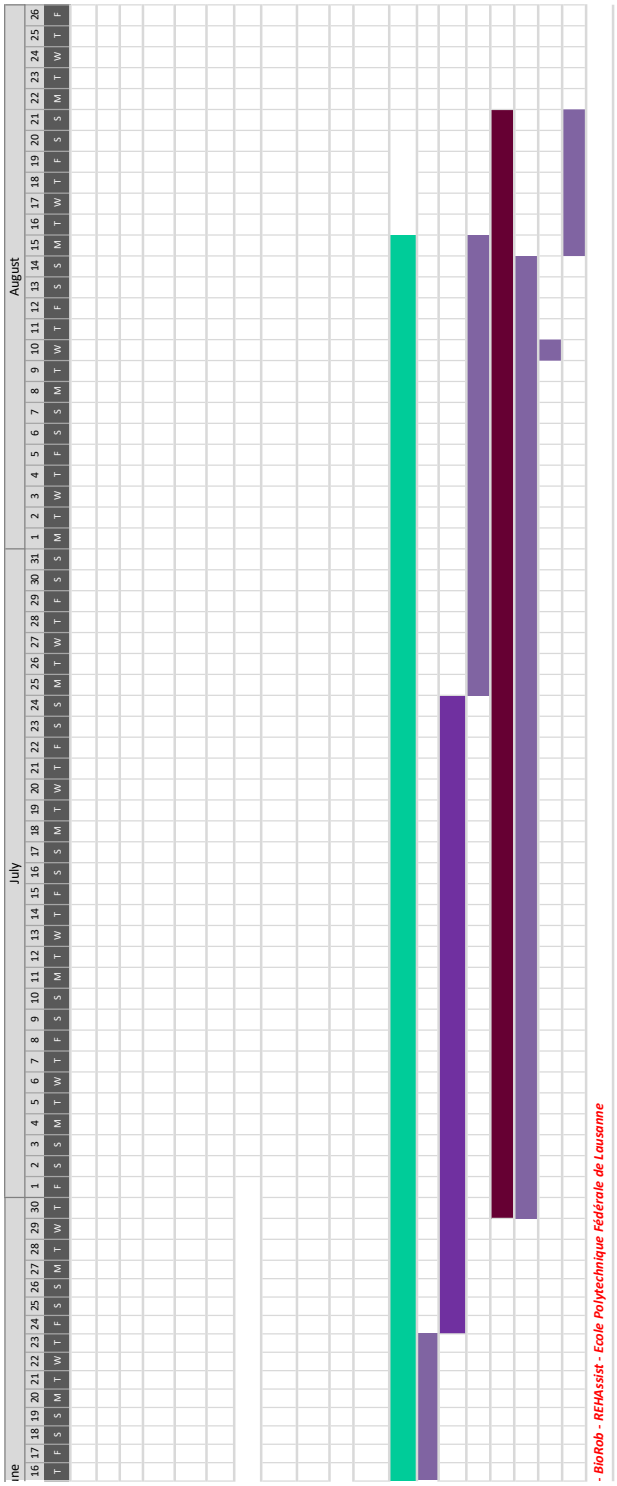

Table A.3 – Provisional Gantt chart - second part

A.6 Project Effective Gantt Chart

Master internship - Neuromuscular controller

Ecole Polytechnique Fédérale de Lausanne - BioRob/REHAssist

Sara Messara

TASK		DURATION	START	END
Phase 1 ***Design***	**20%**	**19**	**4/18**	**5/6**
Softaware setup and installation		1	4/18	4/18
Literature review		9	4/18	4/26
Model theorical foundations - 1st controller proposition		5	4/22	4/26
Hands on the Beagle Bone HAL and e-Walk libraries		6	4/26	5/1
Code structuring and UML diagramming		3	5/2	5/4
Phase 2 ***Implementation and testing***	**50%**	**59**	**5/4**	**7/1**
Model simulation and muscles behavior investigation on MATLAB		19	5/4	6/2
C++ Implementation and integration of the models		7	5/6	5/12
Implementation of the V1		8	5/12	5/19
Main loop rain time assessment and multithreading strategies		1	5/17	5/17
Implementation of the V2		8	6/6	6/13
Implementation of the V3		9	6/18	6/26
Parameters and gains tuning		25	5/16	7/1
Phase 3 ***Validation***	**30%**	**31**	**5/12**	**8/19**
Code validation		6	5/12	5/17
Intra-lab experiences and protocol		16	6/10	8/9
Ethical amendement preparation		9	7/13	7/21
Extra-lab experiments		5	8/15	8/19
Data processing - Gait metrics estimation		10	8/1	8/10
Analysis and conclusions		6	8/10	8/15
Phase 4 ***Project closure***		**58**	**6/30**	**8/26**
Report writing		46	6/30	8/14
Gantt Chart design		1	8/10	8/10
Final presentation preparation		7	8/15	8/21

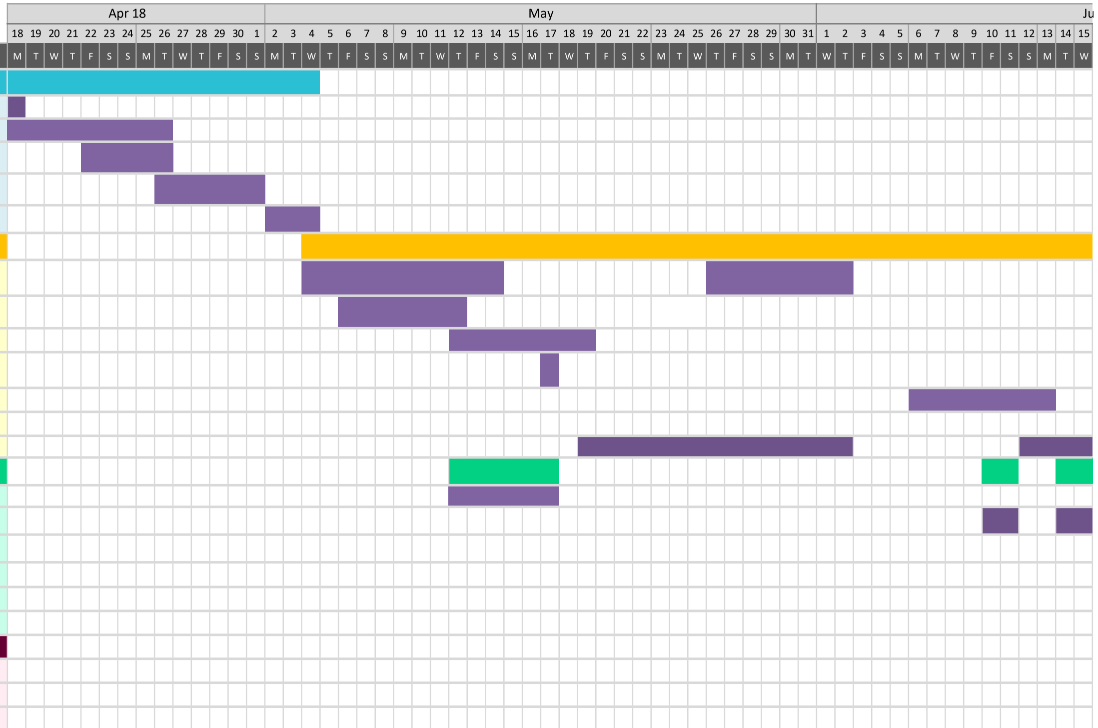

Sara Messara - Master Internship - e-Walk Neuromuscular Controller -

Table A.4 – Effective Gantt chart - first part

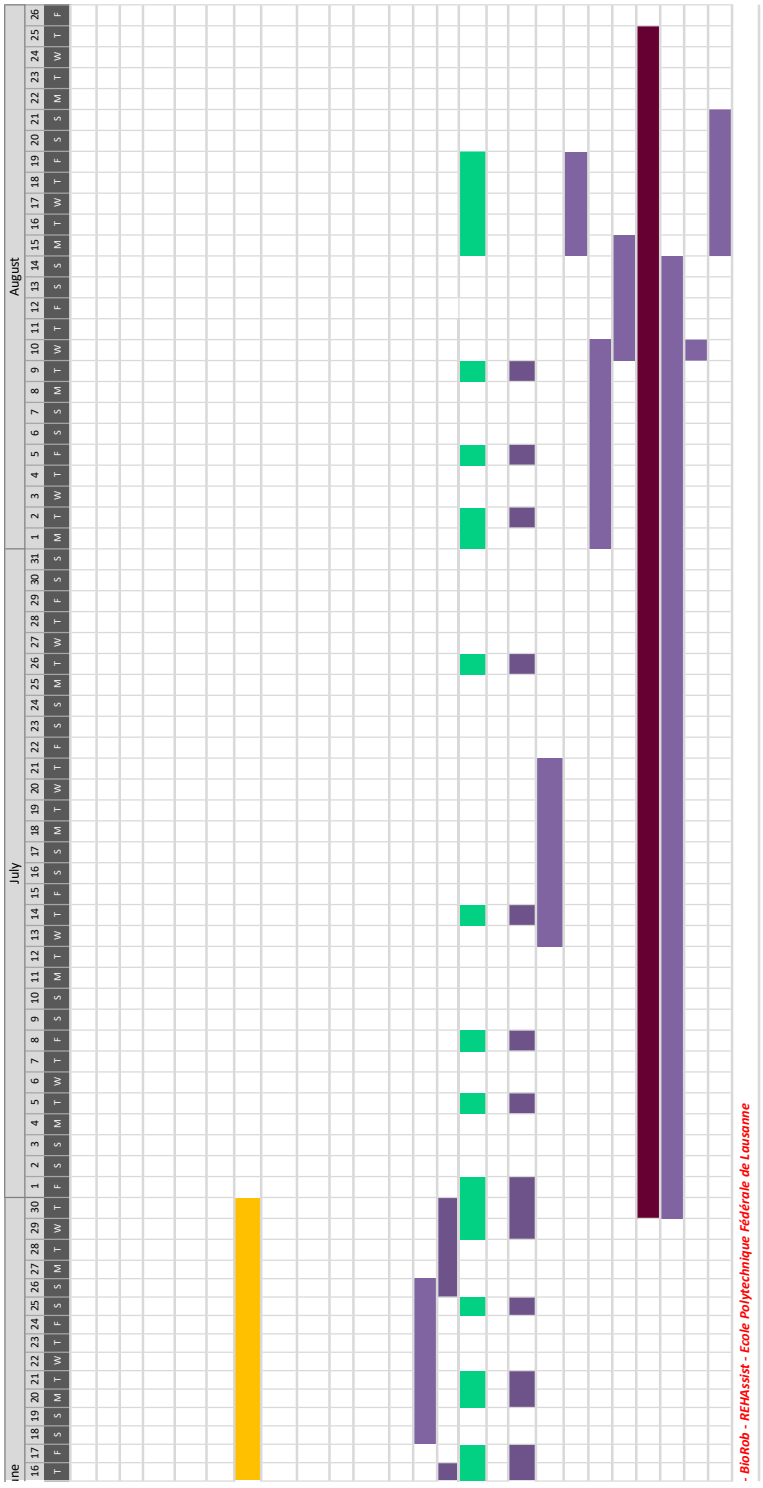

Table A.5 – Effective Gantt chart - second part

Appendix B

B.1 Model's Relationships

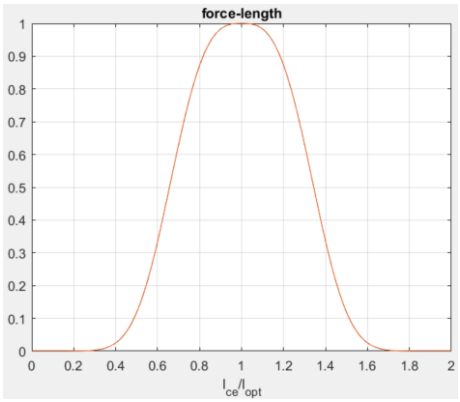

Figure B.1 – $force - l_{ce}$ relationship

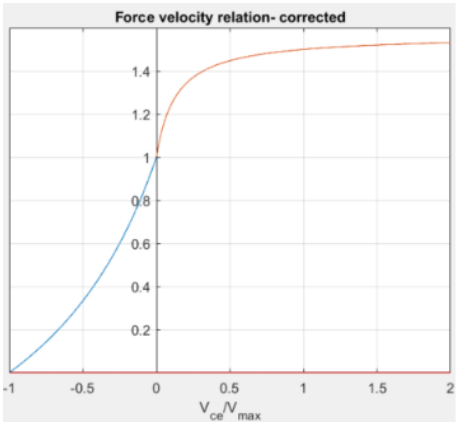

Figure B.2 – $force - v_{ce}$ relationship

B.2 Hill Type Computational Approaches

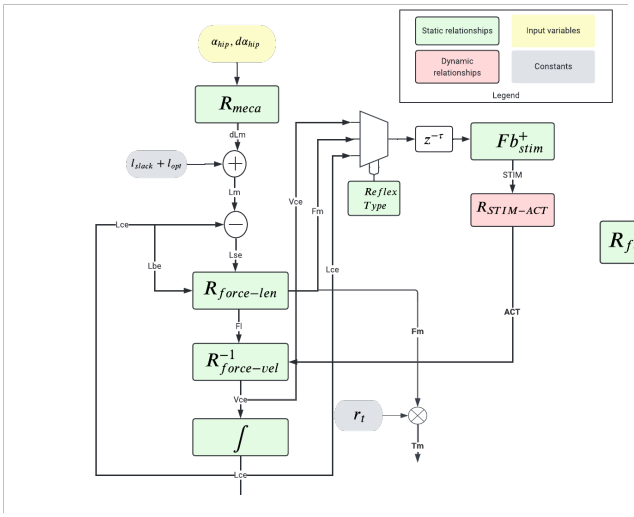

Figure B.3 – Geyer's Integral computational approach

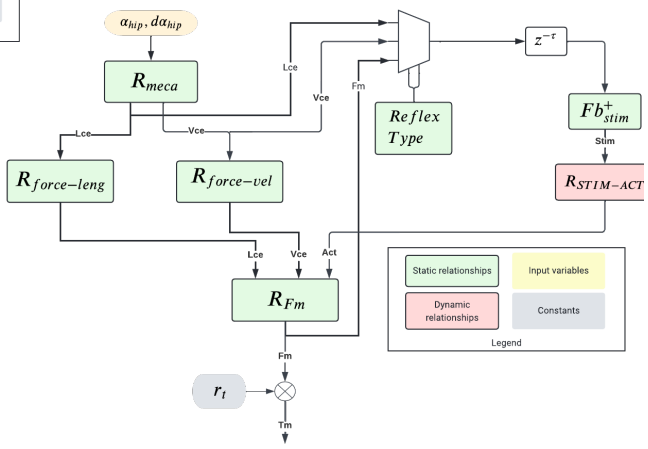

Figure B.4 – Derivative approach and simplified model

B.3 FSMs Petri Networks

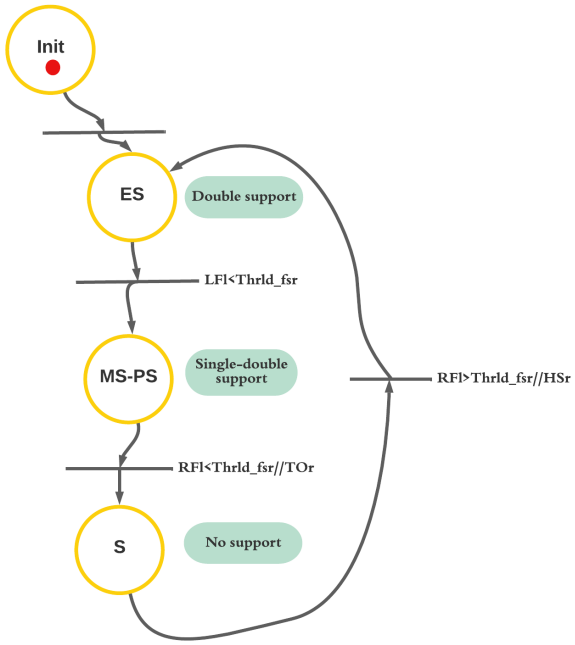

Figure B.5 – 3-FSM Petri network

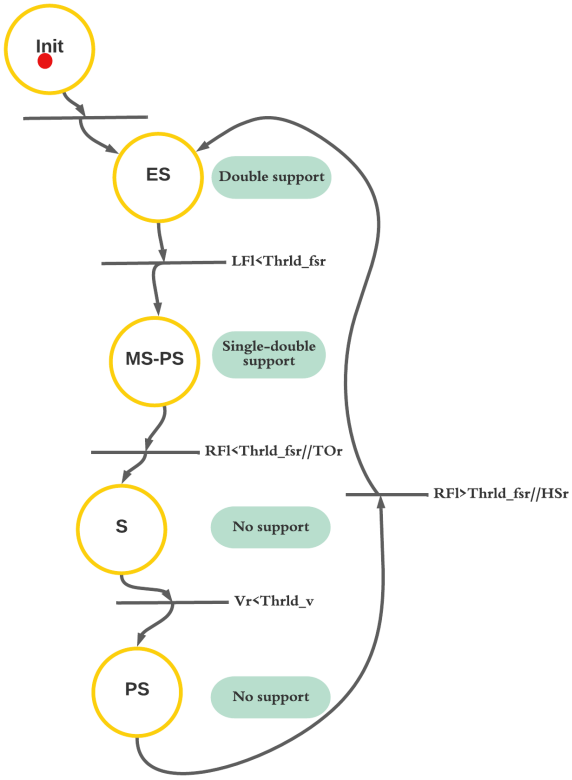

Figure B.6 – 4-FSM Petri network

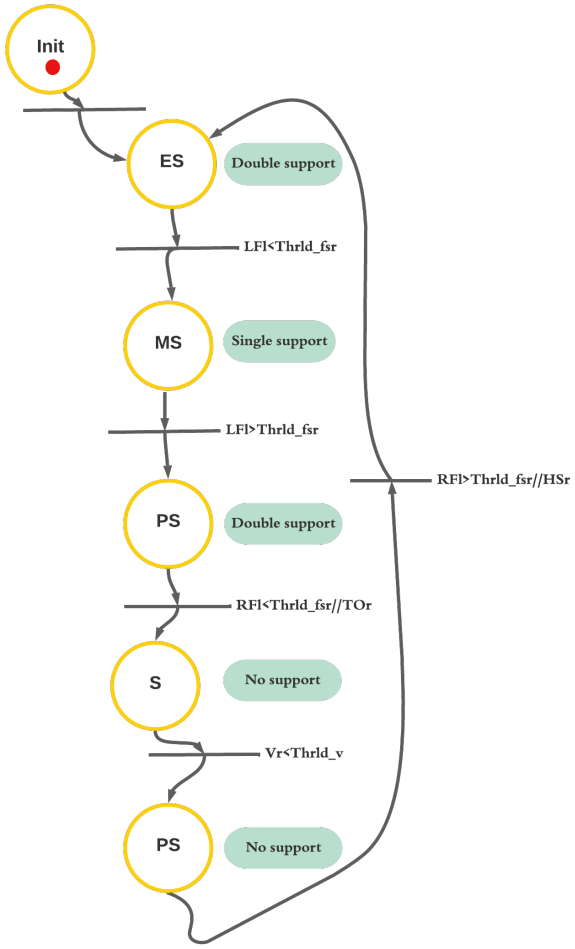

Figure B.7 – 5-FSM Petri network

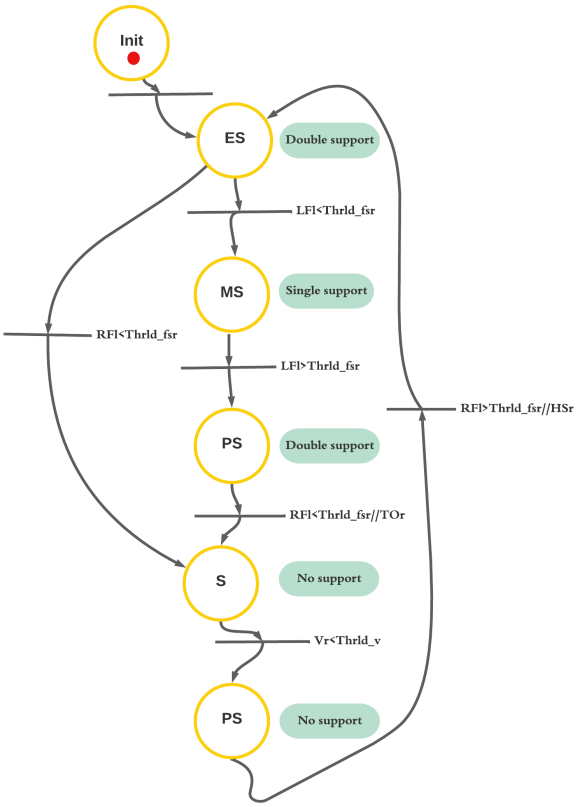

Figure B.8 – Improved 5-FSM Petri network

Appendix C

C.1 Mechanical Specifications

The orthosis weights 4.5 Kg and is composed of 3 distinguishable parts; The trunk-waist attachment, the hip actuators and the instrumented shoes.

The first part consists of an outer flexible plastic structure and an inner fiber cover that is adjustable to the waist size of the wearer and that is fastened to the trunk using two sliding ratchet straps. The back of this structure supports the electronics box that contains the batteries, the PCB circuits and the Black Beagle Bone microcontroller. The device is able to fit wearers weighting between 45 Kg to 120 Kg with 1.5 m to 2.10 m tall.

The actuators consists of two busheless DC motors Gyems RMD X8 Pro whose rotation axes are aligned with the two hip joints. Each motor integrate an embedded driver and is able to deliver 35 N.m and 13 N.m peak and nominal torques, respectively. It is provided with a high resolution 18-bits absolute encoder for the angular position and a gear box with a ratio of 6:1. It does not include a velocity sensor and the speed delivered from the driver is estimated from the position. The motors are fixed rigidly to the waist attachment and via two adjustable polycarbon segments to the tight attachment which enables power transmission between the actuators and the end effectors. The tight attachment has the same composition as the trunk's and is fastened using double-sided Velcro belts.

The instrumented shoes integrates Force Sensitive Resistances (FSR) placed under the shoe insole. The resistance values varies depending on the amount of applied load on each foot. The sensor deliver a resistance value that is converted to its proportional equivalent ground reaction force (GRF) value. The FSRs board are removable and could be placed in any pairs of shoes which means that it is cross-users.

C.2 Electronic Specifications

The main electronic is the microcontroller that is a Beagle Bone Black running a Stretch Debian Linux distribution and a having a 4.9.51-bone7 kernel with an Arm7l processor. The BBB is booted from the SD card as it does not have a ROM. The drivers count a CAN interface to communicate with the motors driver for setting the commands and reading the values of angular position and velocity from the encoder, an SPI channel for the foot load sensors on top of WiFi, Bluetooth, Universal Asynchronous Receiver Transmitter (UART) and Inter-Integrated Circuit (I2C) ports. It also integrates a 6-DoF Inertial Measurement Unit (IMU). The electronics counts also a PCB for the power distribution from the two 12 V batteries to the peripheral

components and a switch for the powering on/off. The BBB is powered with 5 V and the motors with 11.1 V each.

C.3 The Low Level Control Layer

As presented earlier, the motors of the e-Walk are not torque back-drivable given the absence of torque sensor at the output. The manufacturer offers many low level control modes for the motors among which the current control. When working in the nominal region of the DC-motors it is known that the current is proportional to the generated torque. A characterization of the motors have been performed previously in order to determine the torque-current gain. Given this information, it is finally possible to torque-command the motors through the current control. The current regulation is performed at 10 KHz frequency. The set-points of the mid-level controller are torque references. They are then mapped to the current to command the motors.

The torque/current tracking of the motors have been carefully assessed and the error was poor.

The manufacture provides no further details about this low level control.

C.4 UML Diagram of the Software Implementation

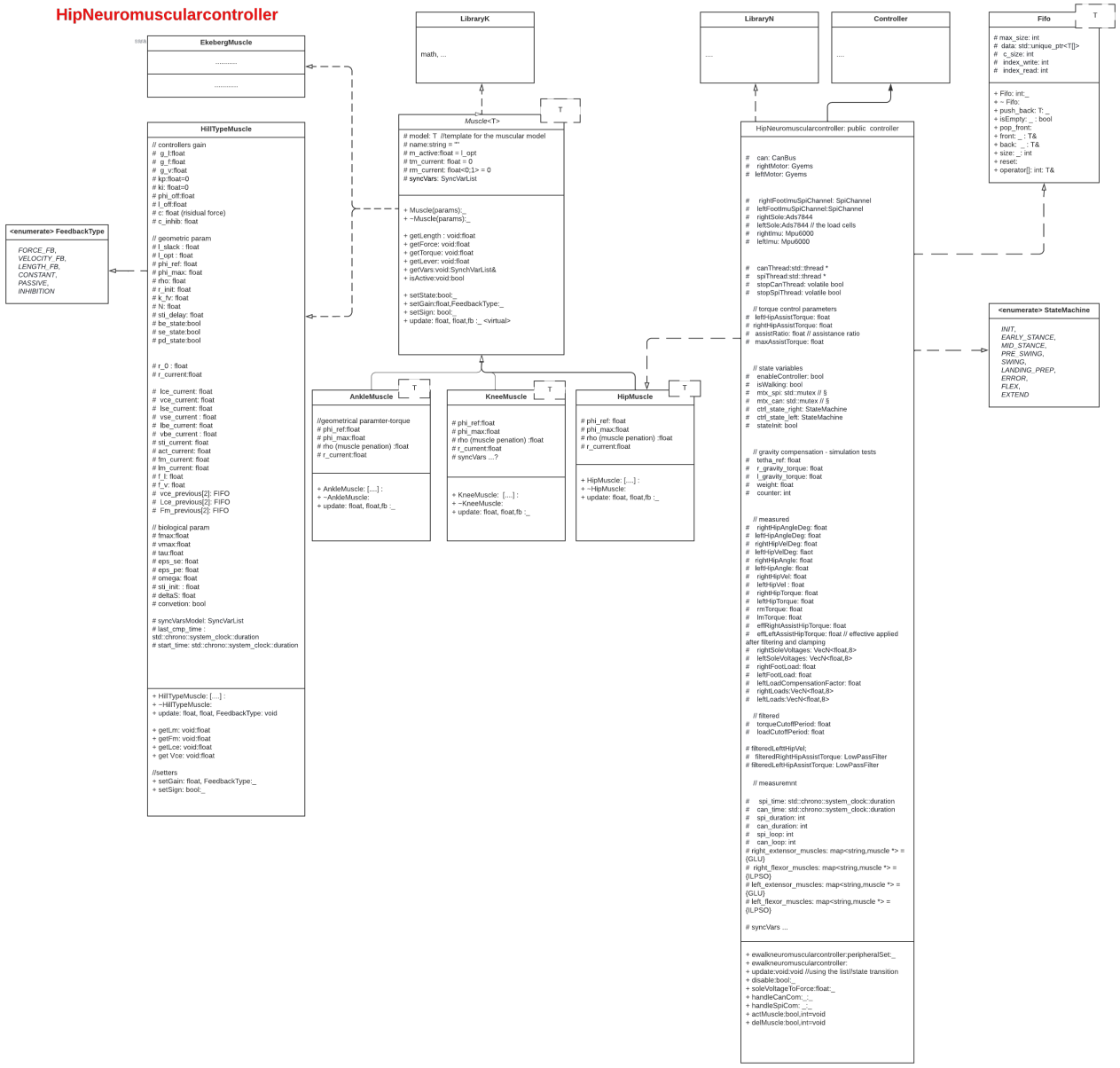

Figure C.1 – UML diagram

C.5 Coding Quality Objectives

Quality objectives	How achieved?
Functionality	The model was tested and its results in terms of model state variables values and torque were compared to the simulated model on Simulink and MATLAB for the same angle and angular velocities before validating the implementation (refer the in-vivo simulation)
Integration/Conforming to the existing coding pattern	Respecting the file hierarchy Respecting the controller programming scheme Good use of the HAL
Modularity	None-overlapping UML diagramming Use of template functions and classes and interfaces, for instance the muscle class is a template classe of muscular model class, this allow changing the choice of the model without changing the muscle interface Use of pre-compilation directive in order to use various combination of controllers, FSMs and muscles' parameters tuning
Scalability	Use of C++ maps to make the number of selected muscles scalable Using heritage and polymorphism for muscles in forecast of future uses for other joints, e.g., the hip joint muscles are polymorphic and inherit from the muscle class
Embedded optimization	Coding of a dynamic fixed size FIFO data structure class that was used instead of C++ original stacks and double queued structures which were not of fixed size and could have caused stack overflow and memory jam (available on github) Using elementary instruction and avoid including libraries as much as possible (e.g., torque saturation using simple if-else clause instead of using std::clamp that requires the ¡algorithm¿ library include)
Testability / Traceability / debuggability	Tracking key variables using synchvars allowing the variables values to be logged in a log file
Readability	Logical classes architecture depicted suing UML diagramming Commenting and documenting

Table C.1 – Coding Quality Objectives

C.6 Software Unitary Tests

Task	Test	Expected result
Implementation and integration validation tests		
Implementation of the neuromuscular model, the muscle and hip muscle classes	Simple C++ compilation using on VSC IDE	Successful compilation and intended functionalities
Equations validation	Comparing the obtained logged values on the microcontroller from the online simulation to the simulated model in Simulink using post-processing on MATLAB	Matching values of torque and state variables between simulation and online computation for the same angles and angular velocities variables
Integration to the device HAL	Building and deployment on Qt Creator IDE using the Linaro-gcc cross-compilation toolchain	Successful building and deployment
Integration of SPI/FSRs	Readability from the sensor monitored using remote control application	Coherence in load plot variations
Integration of the CAN bus	Monitoring angles and velocity change using the remote controller Writing torque commands to the motors	Coherence in angle-speed plot variations Match between the commanded torque and estimated torque at the output
Main loop run period	Measuring the SPI thread runtime and jitter	Dynamic relative error < 5% Period relative error < 50%
	Measuring the CAN thread runtime and jitter	
Numerical convergence of the activation	MATLAB post-analysis using the in-vivo logged values of the activation and stimulation	Convergence under a time limit of $3\tau<t<5\tau$
FSM implementation and integration	States transitions occurring and robustness using post-processing on MATLAB	Match between state transitions and the percentage of occurring in the gait cycle
Adaptation of torques magnitudes to motor capacities	Monitoring the computed but non-applied torque via the remote controller	Torques must remain under 30 N.m for peak values and under 15 N.m for nominal values
Low level controller torque tracking	Evaluating the tracking between the commanded torque and estimated torque at the output from the current using logged values	Convergence and error should be bellow
Logging the interest variables by attaching each to synchvars	Monitoring variables update on the remote controller of the device – checking logging to log files and non-corruption of data using data analysis from log file on MATLAB	Matching load variation-plot on the monitor
Routine tests before using the device		
Available and sufficient power supply	Voltameter measurement	12V output at each battery
Waist adjustment to user's size	Visual verification	The waist should be tightly enclosed in the device without leaving space at the back level, otherwise feeling torsion at the higher limbs and discomfort
Motor – Hip axes alignment	Visual verification	Right height, concurrent centers and parallel axes
Board and motors power supply	Visual verification and remote device WiFi detection	Blue light detection on the board and green for the motors
Board WiFi detection	Visual verification	Blue light on the WiFi dingle Detected by the remote device
Motor position initializing	Testing error offset on the angles using the remote controller	Near 70 deg at the initialization position
CAN bus socket availability	Running a test executable from the command line	No error message in the terminal otherwise getting a streaming of "CAN socket unavailable" warning message
FSR functioning	Running a test executable from the command line and monitoring the load values on the remote application by applying variable loads with the hand	Variation in the plots of each resistance, the peak values must be close

Table C.2 – Implementation and integration validation tests and device testing

Appendix D

D.1 Experimental Protocol Intra-lab

Objective	Label	Conditions	Duration [min]	Resting duration [min]
Steady state validation	C1.1	Flat -Slow pace v = 0.8 m/s	2.5	1
	C1.2	Flat - Natural pace v = 1.25 m/s	2.5	1
	C1.3	Flat - Fast pace v = 1.8 m/s	2.5	1
	C1.4	10% incline v = 1.25 m/s	3	2
Unsteady state validation	C2.1	Flat - Varying speed (shuffled step profile 0.8-1.8 m/s)	4.5	2
	C2.2	Various incline (linear increasing 0%-15% with steps at 5%, 10%, 15%) - v = 1.25 m/s	4	_
		Total duration [min]	26	

Table D.1 – Experimental protocol

D.2 Subjects information

Subject	**Gender**	**Age** (year)	**Height** (m)	**Weight** (Kg)
S1/Ali	M	30	1.73	65.0
S2/Chenghao	M	22	1.74	63.0
S3/Ozge	F	24	1.71	63.0
S4/Olivier	M	26	1.75	65.0
S5/Amalric	M	33	2.03	100.0
S6/Ekrem	M	25	1.70	60.0
S7/Larbi	M	23	1.80	65

Table D.2 – Intra-lab experiments' subjects information table

D.3 Outliers Detection

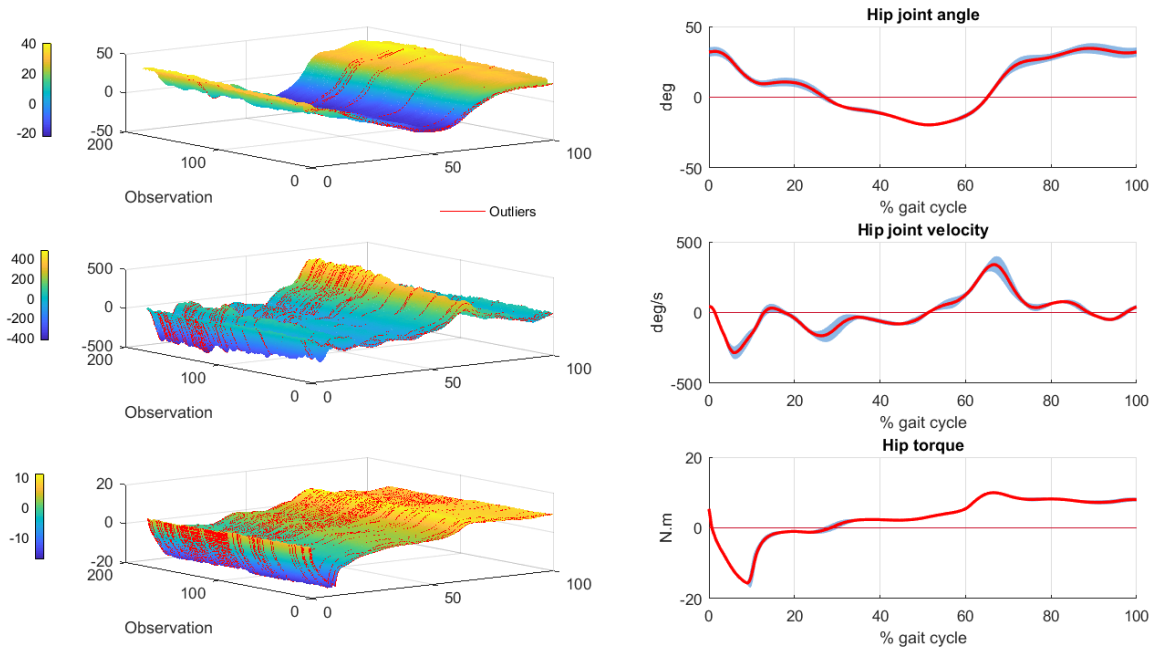

Figure D.1 – Results on the subject S1 with outliers detection - V1

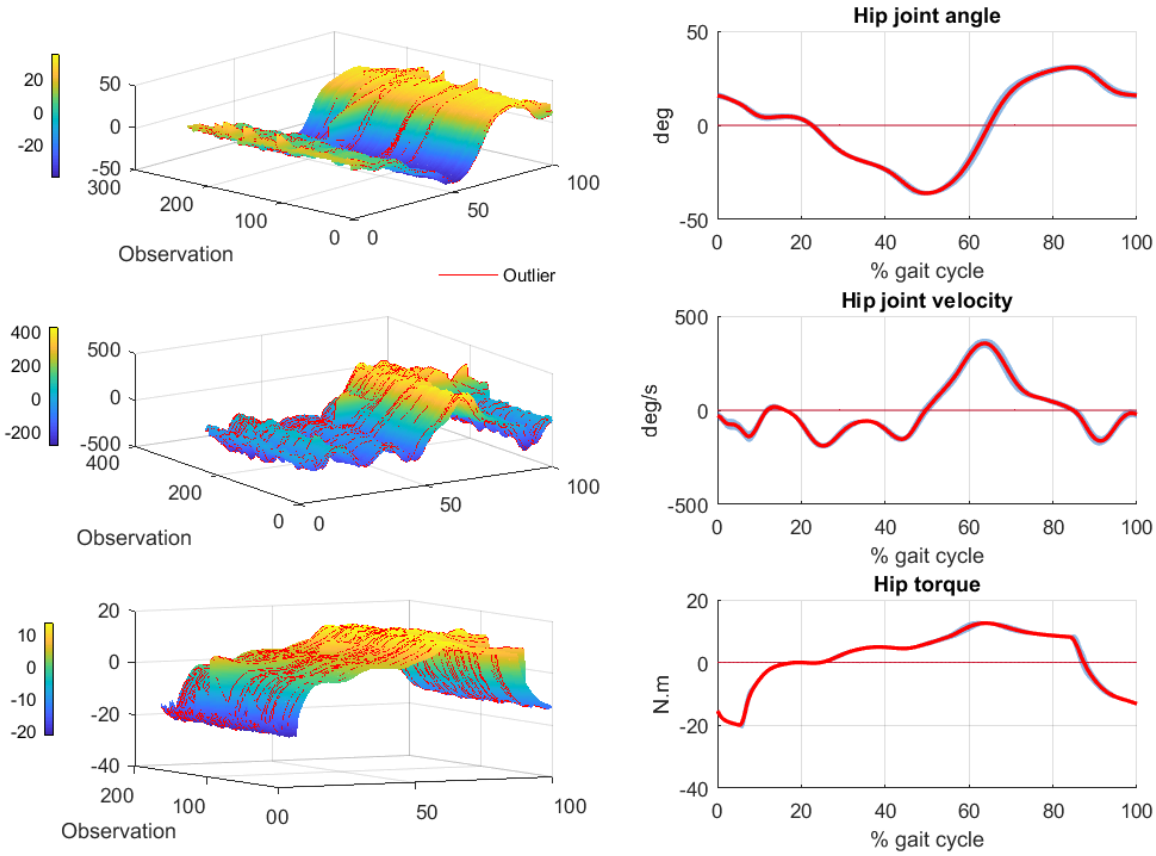

Figure D.2 – Results on the subject S7 with outliers detection - V2

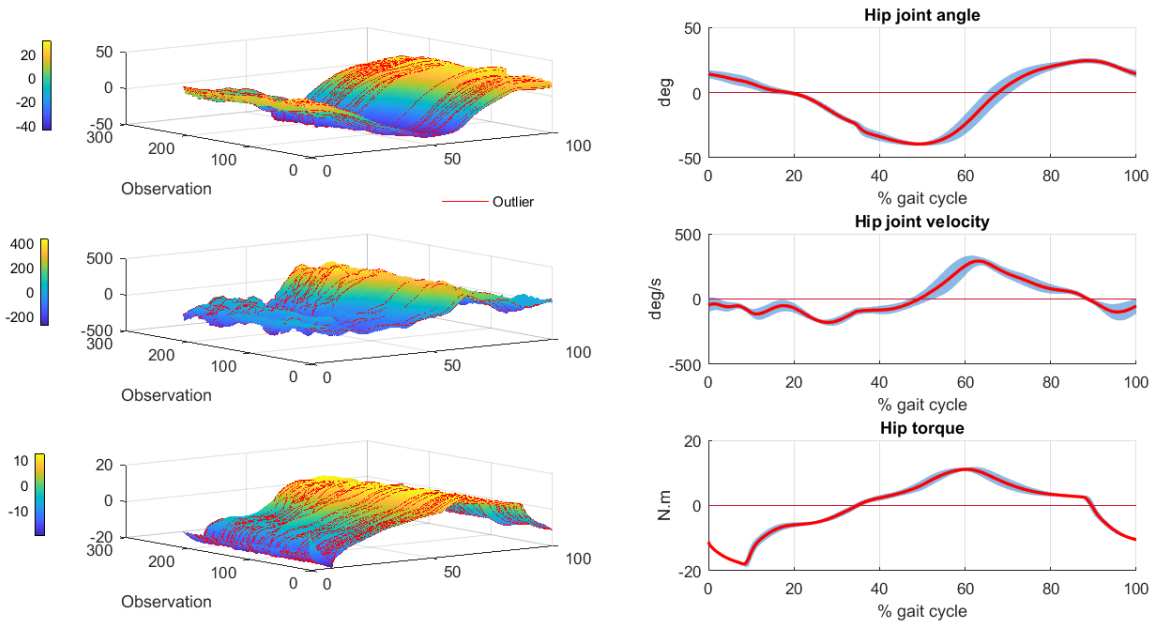

Figure D.3 – Results on the subject S7 with outliers detection - V3

D.4 Torque Comparison

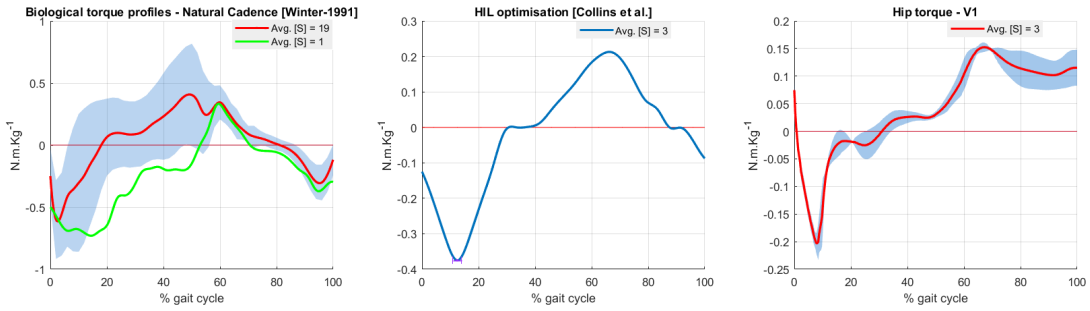

Figure D.4 – Torque profiles comparison

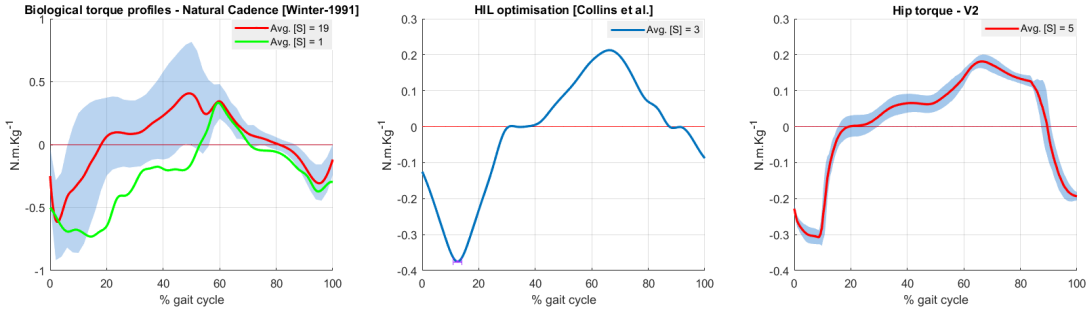

Figure D.5 – Comparison of V2 to reference torques

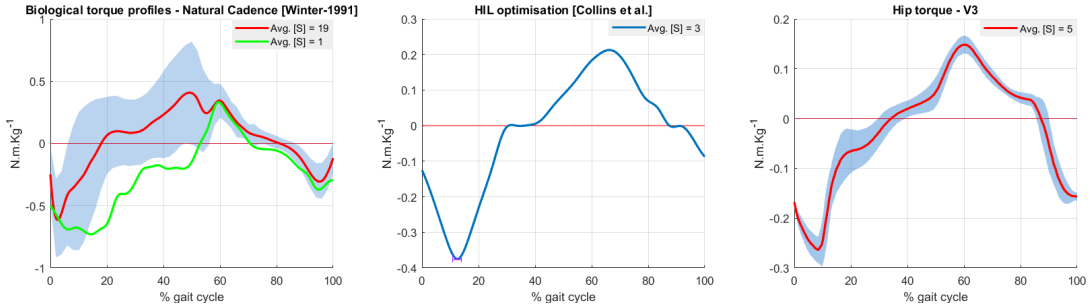

Figure D.6 – Comparison to reference torques